PhD-Thesis

The Function of Adipose Triglyceride Lipase as a Tumor Suppressor

Submitted by

Wael Al-Zoughbi

for the Academic Degree of

Doctor of Philosophy

(Ph.D.)

at the

Medical University of Graz

Institute of Pathology

under the Supervision of

Univ. Prof. Dr. Gerald Hoefler, M.D.

(2016)

Declaration

I hereby declare that this thesis is my own original work and that I have fully acknowledged by name all of those individuals and organizations that have contributed to the research for this thesis. Due acknowledgement has been made in the text to all other material used. Throughout this thesis and in all related publications I followed the “Standards of Good Scientific Practice and Ombuds Committee at the Medical University of Graz“.

Parts of this thesis have been accepted for publication in *Seminars in Oncology* and in *Oncotarget*. Permissions to reuse relevant data from these two journals have been granted and can be found in the appendix section.

Acknowledgements

The completion of this work would not have been possible without the assistance and guidance of several individuals. Writing this section provides me a great opportunity to express my gratitude to all those who offered support throughout the project. In particular, my heartfelt gratitude is due to my advisor *Professor Gerald Hoefler*, director of the Institute of Pathology.

At first, I would like to thank the core team of the DK-MCD program for establishing an admirable PhD program in Graz. I consider myself lucky to be a candidate in this program and will be proud to receive my PhD degree from Graz under the supervision of *Professor Gerald Hoefler*. I am thankful to him for accepting me in his research group and for providing consistent support over the years. I very much appreciate his wisdom, understanding, and of course his encouragement and friendship. I remember his motivation in several instances and how his engorgement could make these experiences productive and joyful. First was before my presentation during the "*94. Jahrestagung der Deutschen Gesellschaft für Pathologie e.V*." in Berlin 2010, but certainly it was not the last. *Professor Hoefler* not only supervised this project and guided me to achieve my goal, but also supports me to develop my academic career—his advices and guidance are invaluable. Beside my advisor, I would like to thank *Professor Dagmar Kratky* and *Mag. Karin Osibow* for their professional and friendly support; I appreciate your time and all efforts to make my PhD study a wonderful experience. Again, congratulations for this excellent doctoral program.

I would like to thank my thesis committee members: *Professor Michael Speicher* and *Professor Robert Zimmermann*, as well as *Professor Barbara Guertl-Lackner*. I am grateful for their constructive discussions and suggestions that helped to improve this project. I would also like to thank *Professor Rudolf Zechner* for his continued guidance and valuable discussions during the publication process.

I am especially grateful to all past and present lab members who I have been fortunate to meet and to work with. Your friendship and support were, and are, very important; thank you so much to all of you.

This project required relatively enormous amount of laboratory work. I would like to express my gratitude to each personnel who provided assistance in the work or introduced me to a new method. Parts of this project were published in peer reviewed journals: “reference #1” and “reference #30”. I am very thankful for the authors who contributed to these two articles. Similarly, and because a considerable part of this work is unpublished, I would like to seize this unique opportunity to thank everyone provided assistance and guidance for the unpublished part—all efforts were made to acknowledge each and every researcher and research assistant and to clearly indicate their names and contributions in the relevant parts of this thesis. Besides, I am also thankful to our colleagues and collaborators who gave me the opportunity to participate in their scientific projects and to be a coauthor in the relevant published articles.

I am thankful to those who made me feel welcome during my research stay: *Professor Paul Waring* and *Professor Jonathan Cebon* at the University of Melbourne, and *Professor Veronika Sexl* in Vienna. I would also like to extend my thanks to all members of their research teams.

This project was supported by the Austrian Science Fund (FWF) projects, SFB LIPOTOX F30 and W1226 DK “Metabolic and cardiovascular disease”. The author is also supported by the Austrian Research Promotion Agency (FFG) funded CBmed project: MR-PDX models for the evaluation of cancer treatment.

To my family and friends: You continue to make my life more beautiful.

This work is dedicated to my former supervisors at the Pathology Department, Damascus University: *Professor Eyad Chatty* and *Professor Charif El Salem*

1 TABLE OF CONTENTET

2 Abbreviations and Definitions

ATP	Adenosine triphosphate
ACACA	Acetyl-CoA carboxylase alpha
ACLY	ATP citrate lyase
AKT	A serine/threonine kinase
ALL	Acute lymphocytic leukemia
ATGL	Adipose triglyceride lipase
BCR	Breakpoint cluster region
BrdU	Bromo-deoxyuridine
DG	Diacylglycerol
ECAR	Extra cellular acidification rate
FAs	Fatty acids
FASN	Fatty acid synthase
FH	Fumarate hydratase
GLDC	Glycine dehydrogenase
H&E	Haematoxylin and eosin stain
HSL	Hormone-sensitive lipase
IHC	Immunohistochemistry
IDH	Isocitrate dehydrogenase
L-Gln	L-glutamine
MG	Monoacylglycerol
MGL	Mono-acyl-glycerol lipase
mTOR	Mammalian target of rapamycin
NNK	Nitrosamine 4-(methyl-nitrosamino)-1-(3-pyridyl)-1-butanone
OCR	Oxygen consumption rate
Paraganglioma	Neuroendocrine neoplasm
PBS	Phosphate buffered saline
Pheochromocytoma	Tumor of the adrenal gland
PHL	Phospholipids
PI	Propidium iodide
PI3K	Phosphatidylinositol 3-kinase (PI3K)
qPCR	Quantitative real-time polymerase chain reaction
RHEB	Ras homolog enriched in brain
SB	Sodium Benzoate
SDH	Succinate dehydrogenase
Sirtuin-6	A stress responsive protein
SREBP	Sterol regulatory element-binding protein
TCA	Tricarboxylic acid
TG	Triglyceride
TLC	Thin-layer chromatography
TPBC	Transformed B-cells precursors
WAT	White adipose tissue

3 Abstract in German

Ein veränderter Zellstoffwechsel ist eines der Kennzeichen von Tumorzellen und rückt immer mehr in den Fokus der Therapie. Ein klares Verständnis der Unterschiede zwischen normalen und Krebszellen, ist der Schlüssel zum Erfolg bei der Nutzung metabolischer Ziele im Kampf gegen den Krebs. Anders als differenzierte Zellen, weisen Krebszellen kontinuierlich eine anabole Form des Stoffwechsels auf, einschließlich der Induktion von lipogenschen Enzymen. Von allen lipolytischen Enzymen wurde bisher ausschließlich Monoglyceridlipase (MGL) eindeutig mit humanem Krebs in Verbindung gebracht. Hier berichten wir über eine neuartige Tumorsuppressorfunktion des in der Trigliycerid-Hydrolyse-Kaskade relevanten Enzyms, adipose Triglycerid-Lipase (ATGL).

ATGL mRNA und ATGL Proteinspiegel sind in mehreren humanen malignen Tumoren, verglichen mit den entsprechenden normalen Geweben, deutlich herabgesenkt. Eine reduzierte ATGL mRNA-Expression korreliert mit einer sinkenden Gesamtüberlebenszeit von Patienten bei mindestens vier Arten von Malignitäten. Der Verlust des ATGL-Protein in Fällen von Bauchspeicheldrüsenkrebs ereignet sich in einem frühen Stadium der Tumorgenese und lässt darauf schließen, dass sich dadurch ein selektiver Vorteil für die Tumorzelle ergibt. Diese Hypothese stützt sich auf Untersuchungsergebnisse, die zeigen, dass der Verlust von ATGL das Tumorwachstum und die Progression in Mausmodellen fördert.

Tumorzellen in denen ATGL fehlt, weisen eine höhere Proliferationsrate *in vitro* und *in vivo* auf, sowie eine verstärkte Fähigkeit in umgebendes Gewebe einzudringen und sich auszubreiten. Es ist möglich, dass ATGL, als ein entscheidendes Enzym im Fettkatabolismus, anabole Vorgänge, die die Zellproliferation beeinflussen – zumindest zum Teil – reguliert und kontrolliert. Die Tumorzellenerkennung durch das Immunsystem des Wirts ist durch das Fehlen von ATGL stark beeinträchtigt wodurch sich neben dem Wachstumsvorteil noch ein weiterer Nutzen für das Überleben der Zellen in immun-kompetenten C57BL6 Mäusen verglichen mit immungeschwächten Mäusen ergibt. Der Verlust von ATGL führt nicht nur zu Wachstums- und Überlebensvorteilen für Tumorzellen,

sondern löst auch spontane bronchoepitheliale Neoplasien und Tumore in Lungen von C57BL6 Mäusen aus. Das zeigt, dass ATGL möglicherweise eine Rolle in der Kontrolle und der Tumorinitiierung und –entwicklung zuteil wird. Da das humane ATGL-Gen, das sich in der Tumor-Suppressor-Region 11p15.5 befindet, eine hohe Frequenz von Gen-Kopienzahlverluste in mehreren Krebsarten aufweist, könnte der Verlust des humanen ATGL-Gens einen Einfluss auf die Entwicklung von menschlichen Krebserkrankungen ausüben, die mit einer Veränderung in der 11p15.5 chromosomalen Region einhergehen. Die Beeinträchtigung der antitumoralen Immunantwort durch das Fehlen von ATGL verweist auf eine einzigartige mechanistische Verbindung zwischen dem zellulären Katabolismus-Vorgang und der adaptiven Immunantwort auf Tumore.

Zusätzlich zu der bereits bekannten Rolle von MGL in der Entwicklung und Progression von Krebs, zeigen wir, dass die Deregulierung des ATGL ebenso eine Rolle in der Tumorgenese spielt. Unsere Ergebnisse identifizieren eine neuartige Diskrepanz im Fettstoffwechsel von normalen und Krebszellen und deuten darauf hin, dass das wichtigste Enzym in der TG Lipolyse, ATGL eine wichtige Funktion in der Kontrolle von Tumorentwicklung, -wachstum und –aggressivität innehat. Diese Studie etabliert eine Tumorsuppressorfunktion von ATGL und trägt zu einem besseren Verständnis des Krebsstoffwechsels bei.

4 Abstract in English

Altered cellular metabolism has been recognized as one of the hallmarks of tumor cells and is emerging as a therapeutic target. Certainly, understanding the metabolic differences between normal and cancer cells is the key for success in utilizing metabolic targets to combat cancer. Unlike specialized cells, cancer cells constitutively exhibit an anabolic form of metabolism including the induction of lipogenic enzymes. Of lipolytic enzymes, only monoglyceride lipase (MGL) has been clearly implicated in human cancer. Here, we report a novel tumor suppressor function for the rate limiting enzyme in the triglyceride hydrolysis cascade, adipose triglyceride lipase (ATGL).

ATGL mRNA and ATGL protein levels are significantly downregulated in several human malignant tumors compared to the corresponding normal tissues and reduced *ATGL* mRNA expression correlates with decreased patients overall survival in at least four types of malignancies. Remarkably, loss of ATGL protein in pancreatic cancers is an early event during tumorigenesis suggesting that there is a selective advantage conferred by losing ATGL. This hypothesis is supported by the finding that loss of ATGL enhances tumor growth and progression in mouse models.

Tumor cells in which ATGL is absent exhibit higher proliferation rate *in vitro* and *in vivo*, and increased ability to invade and spread. It is possible that ATGL, as a critical enzyme in fat catabolism, regulates and controls –at least in part— anabolic pathways that influence cell proliferation. Besides the growth advantage, tumor cell recognition by the host immune system is severely impaired upon the loss of ATGL. As a result, these cells have additional survival advantage in immune-competent *C57BL6* mice compared to immune compromised mice that exhibit severe combined immune deficient phenotype. In fact, escaping the antitumor immune response upon the loss of ATGL might reveal a unique mechanistic link between the cellular triglyceride (TG) catabolism pathway and the adaptive immune response against tumors.

Loss of ATGL not only confers growth and survival advantages for tumor cells, but also is sufficient to induce spontaneous bronchoepithelial neoplasias and tumors

in lungs of *C57BL6* mice, thus revealing a possible role for ATGL in controlling tumor initiation and development. Given that the human *ATGL* gene – located in the tumor suppressor region 11p15.5 — exhibits high frequency of gene copy number loss in multiple cancer types, the loss of human *ATGL* gene may be instrumental for the development of human cancers that are associated with alteration in the 11p15.5 chromosomal region.

In addition to the reported role of MGL in cancer development and progression, we show that deregulation of the rate limiting enzyme in the catabolic arm of the TG/Fatty acids cycle plays a role in tumorigenesis. Our results identify a novel discrepancy in lipid metabolism between normal and cancer cells, and indicate that the principal enzyme in TG lipolysis, ATGL, is implicated in controlling tumor development, growth and aggressiveness. This study establishes a tumor suppressor function for ATGL and contributes to a better understanding of cancer metabolism.

5 Introduction

Cellular homeostasis is one of the main characteristics of living organisms. Cells need to maintain their homeostasis in order to survive changes in the environment. For unicellular organisms, which are in direct contact with the environment, this process is regulated through intra- and extra-cellular adaptations. Regulation of homeostasis is more complicated in multicellular organisms. In addition to the adaptation to changes within the local environment (microenvironment), cells require to interact and adapt to changes and signals from the macro-environment. Failure of adaptation or defects in the interaction may result in diseases. Cancer is one of the chronic diseases where these physiological and regulatory processes between diseased cells and their environment are not only lost but rather result in pathological interactions. The cartoon schematic in **figure.1** shows a simplified illustration of the two main steps in forming this abnormal interaction in cancer; tumor micro- and macro-environment (1). The following introduction chapter briefly discuses cellular energy homeostasis in normal and cancer cells, with an emphasis on lipid metabolism.

Early stage of tumor development

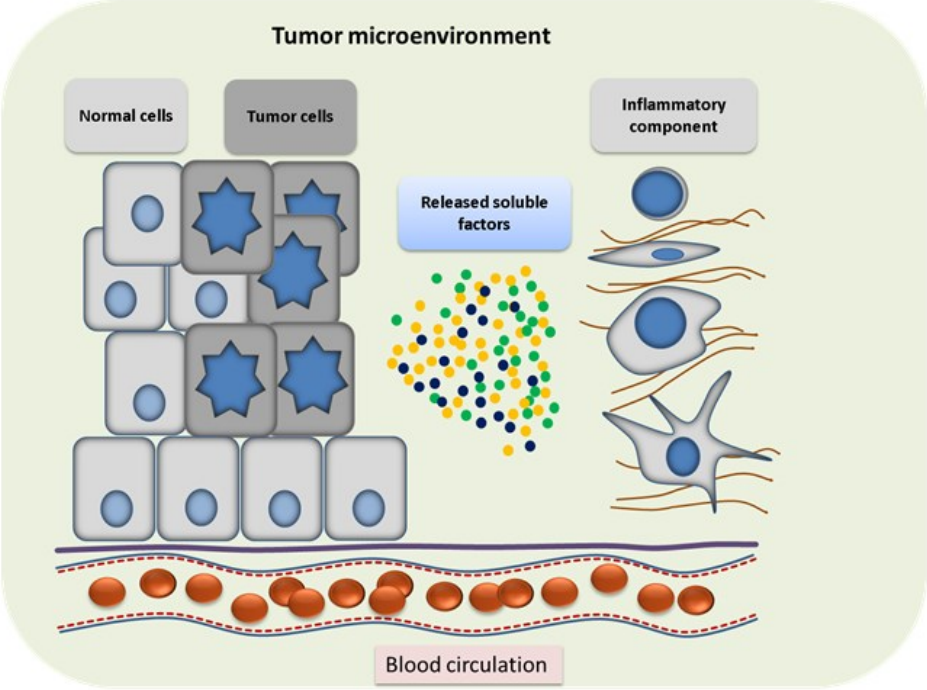

Late stage of tumor development

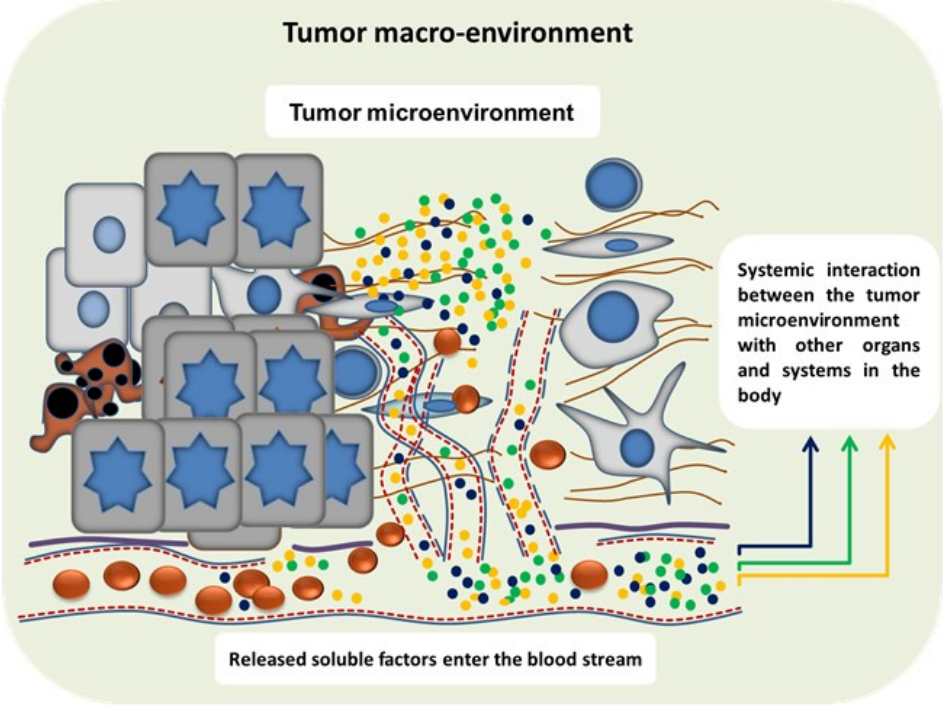

Figure .1 Tumor developments. *A cartoon schematic shows the main two stages of tumor development. Tumor development is a multi-step process which can be classified into two stages. The early stage (upper panel) is characterized by the transition from normal cells to genetically abnormal cells. This transition is a relatively slow process and often clinically silent. Transformed cells are generally dedifferentiated cells – not functionally active — and have the potential for rapid proliferation. When the cells start dividing and invading the neighboring tissues, the tumor microenvironment evolves. In this stage of tumor development, the reciprocal, but abnormal, interactions between cancer cells and the surrounding tissue are mainly localized and limited to the microenvironment. Tumor-induced angiogenesis is a critical process in tumor development, since it not only supplies the tumor with required nutrients, but allows the released soluble molecules to enter the blood and/or lymph circulation; thus resulting in a complex systemic interaction between the tumor and other systems in the body (lower panel). In contrast to the tumor microenvironment, where the localized auto and paracrine types of interaction are dominating, the systemic and pathological endocrine types of interactions explain fundamental mechanism of the tumor macro-environment in late stages of cancer progression. This figure is reproduced with modifications with permission from Elsevier (see Appendix).*

5.1 Cellular Energy Homeostasis

Energy homeostasis is a tightly controlled process provides differentiated cells with the energy required to carry out their physiological functions (1-5). Adenosine triphosphate (ATP) production is essential for many, if not all, pathways involved in maintaining this homeostasis. To perform a defined function, differentiated cells require a large number of ATP molecules which are mainly generated by cellular respiration. Pyruvate, the end product of glycolysis, and acetyl-CoA that generated from fatty acids (FAs) breakdown, are oxidized in the tricarboxylic acid (TCA) cycle. When cellular respiration is impaired, for example under limited oxygen concentration or because of mitochondrial disorders, cells stop oxidizing glucose and convert pyruvate to lactate. In contrast to differentiated cells, biosynthesis is the most prominent feature of proliferating cells. In order to divide into two cells, proliferating cells duplicate the biomass to build up sufficient macromolecules including nucleotides, amino acids, protein and lipids.

5.1.1 Lipid Metabolism: The TGs/FAs Cycle

Our knowledge on how lipid hemostasis is regulated was amended in 2004 upon the discovery of a new enzyme named by *Zimmermann et al*. as adipose triglyceride lipase (ATGL) (also referred to as patatin-like phospholipase domain containing 2, *PNPLA2*) (2). This discovery highlighted the importance of the triglyceride (TG)/ FAs cycle in cellular metabolism. Under conditions where increased nutrients are available, several cell types are able to store FAs in TGs pools; excess nutrients are converted into FAs which are stored as intracellular TGs (3). This pathway is regulated via several enzymes including, but not limited to, ATP citrate lyase (ACLY); acetyl-CoA carboxylase alpha (ACACA); and fatty acid synthase (FASN) (3). Mobilizing these highly energetic stores in a lipolytic cascade is an essential biological process that provides normal cells not only with substrates in the form of FAs, but also with signaling molecules and intermediate nutrients (4). Upon demand, stored FAs can be cleaved and utilized for energy production. The principle enzymes are ATGL, hormone-sensitive lipase (HSL) and mono-acyl-glycerol lipase (MGL). ATGL, which is the rate limiting enzyme in this

pathway, initiates lipolysis by cleaving one FA converting TG to diacylglycerol (DG) 1,2; DG1,3; or DG2,3. Subsequently, HSL cleaves the second FA generating monoacylglycerol (MG) which is the substrate for the third enzyme in the lipolytic pathway. MGL cleaves the last FA converting MG to FA and glycerol. Released FAs are substrates for beta oxidation either in mitochondria or in peroxisomes. The regulation “balance” between anabolic and catabolic pathways in TGs/FAs cycling is crucial for cellular metabolism (3, 4).

As mentioned above, the discovery of the new lipase, ATGL has had an important impact on the field of lipid metabolism. Because the work presented in this thesis is focused on this particular enzyme, I provide a short summery about the discovery of ATGL in the following paragraph.

5.1.2 Identification of ATGL

The observation that the amount of white adipose tissue (WAT) found in hormone-sensitive lipase deficient (*Hsl-/-*) mice is less than WAT stored in control mice led to an important discovery in the catabolic arm of the TGs/FAs cycle; the identification of ATGL as the rate limiting enzyme in TGs hydrolysis. HSL was the enzyme known to catalyze FAs from TG and DG stores. Accordingly, it was expected that *Hsl*-/- mice have increased WAT stores. Remarkably *Hsl-/-* mice have reduced WAT compared to control mice (5, 6). Investigating possible mechanisms, the laboratory of *R. Zechner* in Graz, showed that not only TGs synthesis is reduced in *Hsl-/-* mice, but also that TGs in these mice are hydrolyzed to DGs, by an unknown enzyme, which in turn are accumulated due to the lack of HSL (7). Based on these findings the authors hypothesized that there must be a lipase, yet an unidentified, capable of catalyzing FAs from the TG stores. One year later, the “unidentified lipase” was reported to be ATGL by three independent groups, including the team from the Institute of Molecular Biosciences, Graz (2, 8, 9). Indeed, it was shown that ATGL is the rate limiting enzyme in the TGs hydrolysis pathway in WAT as well as in almost all mouse tissues (10).

5.2 Metabolism of Cancer Cells

Unlike specialized cells, cancer cells – having no apparent physiological function – constitutively exhibit an anabolic form of metabolism (1, 11, 12). This supplies proliferating tumor cells with building blocks necessary for generating nucleic acids, proteins and lipids (12, 13). Importantly, deregulating cellular metabolism has been recently considered as an emerging hallmark of cancer and as a possible targeted therapy (11, 13, 14). Although the metabolic reprograming of many cancer cells is known as an adaptation process to the activation of several growth pathways, recent evidences show that these metabolic alterations are indeed sufficient to induce tumorigenesis (12, 15).

5.2.1 Metabolic Reprogramming to Provide Energy for Cancer Cells

Tumor cells are capable to reprogram the metabolic machinery to provide for the energetic needs for increased replication (12, 14). In several cancer types, this neoplastic proliferation is associated with abnormal metabolism of glucose, well known as “Warburg effect” (11, 16). In contrast to normal cells, malignant cells have high rates of glucose consumption and lactate production under aerobic conditions. The assumption that this alteration is due to mitochondrial defect was not widely supported (17, 18). Recently, several studies revealed an important role for a well-known metabolic pathway. This pathway –which is formed mainly by phosphatidylinositol 3-kinase (PI3K); a serine/threonine kinase (Akt), also known as protein kinase B; and mammalian target of rapamycin (mTOR), PI3K/Akt/ mTORC1 pathway– is frequently activated in cancer cells (19). Indeed it was shown that it is the key regulatory pathway for aerobic glycolysis and for increased glucose uptake in tumors. Although the proposed therapy to target the increased glucose uptake failed, the observation that tumor cells uptake glucose at high magnitude helped to establish essential diagnostic and prognostic applications. For example the application of 2-[(18)F] Fluoro-2-deoxyglucose positron emission tomography (FDG-PET) in cancer imaging (20).

Altered tumor metabolism involves not only glucose but also lipid metabolism (21-23). In addition to regulating aerobic glycolysis, the PI3K/Akt/ mTORC1 pathway supports lipid biosynthesis of rapidly proliferating cells. Independent of the levels of exogenous lipids, cancer cells are characterized by high rates of *de novo* lipogenesis (24, 25). Cancer cells rely on *de novo* synthesis of FAs to generate precursor molecules for macromolecular biosynthesis. The induced lipogenesis in tumor cells is mainly driven by Akt activation which enhances sterol regulatory element-binding protein (SREBP) transcription factor. Accordingly, the induction of lipogenic enzymes, such as ACLY, ACACA, and FASN, is a critical adaptation during malignant transformation.

5.2.2 Altered Metabolism Drives Carcinogenesis

The changes in cancer metabolism are not only an adaptation to the requirements of proliferation, but several metabolic enzymes have been recently shown to play a direct role in driving tumorigenesis "*metabolism in the driver's seat*" (15). Two mitochondrial enzymes, succinate dehydrogenase (SDH) subunits and fumarate hydratase (FH), play role as tumor suppresser proteins in rare types of tumor: paraganglioma and pheochromocytoma (26). An additional example for the importance of metabolic enzymes in tumor growth is the role of isocitrate dehydrogenase (IDH). Both, the cytoplasmic (IDH1) and the mitochondrial (IDH2) enzymes are reported to be mutated in approximately 70 % of brain tumors; gliomas grade II & III, and secondary glioblastomas. Patients who have tumors with gain-of-function mutation have better prognosis (27). Mutations in this enzyme were also reported in several other cancers including hematopoietic tumors; 10% of acute myeloid leukemia (AML) (27, 28). Importantly, the identification of Sirtuin **6** enzyme as metabolic tumor suppressor protein provided additional evidence that a number of the deregulated metabolic enzymes can drive tumorigenesis (15, 29).

6 Material and Methods

The majority of the experiments were carried out at the “Institut für Pathologie” and at the “Zentrum für Medizinische Grundlagenforschung” (ZMF) at the Medical University of Graz. Unless otherwise stated, the work was performed by the author according to instructions and guidance provided by the researchers responsible. For experiments were the lab work was performed in other labs or the author has received guidance during the work, names and affiliations of researchers involved and research assistants are provided. Names and affiliations of researchers and research assistants who performed work and analyses –where the author did not participate—or who have provided samples used for this project are clearly stated. Part of the material and methods in this section are reproduced with modifications from the published article (30) with the permission of the *Oncotarget* journal.

6.1 Histopathology Techniques

6.1.1 Tissue Processing and Staining

The analysis of human tissues was approved by the ethics committee of the Medical University of Graz (Number: 21-244 ex 09/10; 23-279 ex 10/11). Approved applications were written by *Prof. Gerlad Hoefler, Dr. Barbara Guertl-Lackner*, and *Dr. Martin Pichler*. Tissue blocks contains formalin-fixed, paraffin-embedded (FFPE) samples were obtained from the Biobank of the Medical University of Graz. These blocks were sectioned, and stained with H&E according to standard protocols at the Institute of Pathology. *Silvia Schauer*, *Mohamed Al-Effah* and *Marianne Brence* have performed tissues sectioning.

ATGL IHC was performed by *Silvia Schauer*. Sections were incubated with anti-human ATGL antibody (Cat#3814-100, Biovision, Milpitas, CA, USA, 1:50 dilution). Antibody binding was visualized using aminoethyl carbazole (AEC) substrate chromogen (cat#3464, Dako, Glostrup, Denmark). *Prof. Gerald Hoefler* and *Prof. Gregor Gorkiewicz* helped to establish the ATGL IHC methods by evaluating the sensitivity and specificity of the staining on control samples. ATGL/Glut1 IHC

double staining was performed by *Mag. Elisa Nusshold* and the author. For Glut1 IHC, sections were incubated with anti-human Glut1 antibody (Cat#MS-10637-R7, Thermo scientific, Fermont, CA, USA, 1:400 dilutions). Antibody binding was visualized using EnVision+ System-HRP (DAB) (code K4006, Dako, CA, USA). For ATGL/Glut1 IHC double staining, sections were incubated with anti-human Glut1 antibody and with anti-human ATGL antibody. Antibody binding was visualized using MACH 2 Double Stain 2 (cat# MRCT525 G, H, L, Biocare Medical, concord, CA, USA) according to the manufacturer's instructions.

CD3 and CD31 (Thermo scientific, USA), IHC on mouse tumors were established by the author and the help of *Silvia Schauer* who performed all technical work. Tissue samples were counter stained with haematoxylin according to standard methods. For Oil Red O staining, lung tissues were collected and stored in liquid nitrogen. Frozen sections were stained with Oil Red O according to standard protocols by *Silvia Schauer*. For electron microscopic studies lung samples were collected by the author. Samples were prepared for cutting by the investigator with the help of *Andrea Koschell* who sectioned the samples.

6.1.2 Evaluation of ATGL Immunohistochemistry

Specificity of the ATGL IHC on each tumor type was first documented by *Prof. Gerald Hoefler* and by the author. Next, it was confirmed by an expert pathologist at the Institute of Pathology for each tumor entity: *Prof. Helmut Popper* reviewed samples from non-small cell lung cancers; *Prof. Carolin Lackner* reviewed samples from pancreatic preneoplastic lesions and cancers; and *Dr. Bernadette Liegl-Atzwanger* reviewed samples from smooth muscle cell tumors. The signal intensity of ATGL IHC and the percentage of labeled cells from tumors and healthy adjacent tissues were evaluated by the author according to the (H-Score) scoring system (31). Briefly, the intensity (I) of ATGL granular and cytoplasmic staining signal was graded into four grades (0, 1, 2, and 3). The percentage (P) of cells within each grade was estimated and the H-score for each grade was calculated according to the formula: H-score= I x P. Cells in normal and tumor tissue were evaluated and the final H-score value was calculated by summing up the individual

H-score values specific for each grade. The final H-score formula can be summarized as the flowing: H-score = [(I(0)xP(0))+(I(1)xP(1))+(I(2)xP(2))+(I(3)xP(3))].

6.2 Microarray-based Comparative Genomic Hybridization

DNA was extracted from formalin-fixed, paraffin-embedded (FFPE) samples using a commercially available kit (QIAamp®DNA mini kit). FFPE blocks were cut into 9 µm thick tissue sections. Tumor tissues were dissected manually from 4 sections per sample into 1.5 ml Eppendorf tubes and incubated overnight in lysis buffer. Next, DNA extraction and purification was performed according to a standard protocol from the manufacturer. Subsequent steps, for testing DNA quality by multiplex PCR and for analyzing copy number variations using the microarray-based Comparative Genomic Hybridization (array CGH) method were performed at the "Institut für Humangenetik, MUG". This work has been performed during a PhD course in molecular cytogenetics and array technologies, February 2010, with the help of *Dr. Anna Obenauf* and under the supervision of *Prof. Michael Speicher*.

6.3 Patients and Clinical Data

Clinico-pathological correlation analysis and evaluation of the prognostic relevance of ATGL expression in pancreatic cancer tissue was performed by *Dr. Martin Pichler* and the author. These analysis included data from 51 randomly selected patients with confirmed pancreatic adenocarcinoma, who were treated at the Division of Clinical Oncology, Medical University of Graz between 2004 and 2010. All clinico-pathological data were retrieved from medical records at the Division of Clinical Oncology, as well as from pathology records from the Institute of Pathology. The study was approved by the local ethical committee of the Medical University of Graz (No. 23-279 ex 10/11). Cytoplasmic ATGL staining in tumour cells was considered positive, and immunoreactivity was semi-quantitatively categorized as either negative (0% of tumour cells) or positive (>1% of tumour

cells) by the author. The relationship between ATGL expression and other clinico-pathological parameters including age, gender, tumour grade and tumour stage was studied by non-parametric tests by *Dr. Martin Pichler*.

6.4 Data Mining

The work listed in this paragraph was performed in part by *Dr. Alida Kindt* and *Prof. Zlatko Trajanoski* at the Division of Bioinformatics, Medical University of Innsbruck; by *Dr. Martin Pichler*; and by the author.

Analysis of The Cancer Genome Atlas (TCGA) datasets for *ATGL* mRNA expression was performed with the R (version 3.02) package DESeq version 14.1. The *P*-values were corrected for multiple testing using the Benjamini-Hochberg False Discovery Rate (Adjusted *P*-values). Data on the *ATGL* gene methylation status were downloaded from the TCGA atlas (accessed on 13 Feb 2014) and analyzed. A two-sample paired t-test was applied to the known methylation sites to investigate differences between the tumor and normal tissues of the same patient. The resulting *P*-values were corrected for multiple testing to account for the analysis of the 21 present methylation sites. *P*-values annotated as significant passed the threshold for multiple testing at P-value < 0.05. *Dr. Alida Kindt* and *Prof. Zlatko Trajanoski* have performed these two types of analyses.

Overall survival analyses in breast, ovarian and gastric cancer patients were performed as described (32) by *Dr. Martin Pichler*. The online available software tool combines Affymetrix gene expression data from multiple annotated cancer studies into a single database which can be then queried for associations of patient outcome with the expression of individual genes. For these Kaplan-Meier survival analyses an optimal cut-off value was calculated by the software (32) to dichotomize the cohort according to the *ATGL* gene expression values and significant differences with regard to the endpoint overall survival were tested by the log-rank test. Hazard ratio (HR) and 95% confidence interval (CI) were calculated and a P-value of < 0.05 was considered statistically significant.

The author has analyzed gene copy number variation data from TCGA projects. These data were generated at the Broad institute (Cambridge, MA, USA) as described (33). For somatic copy number analysis, q-values are the false discovery (the proportion of false positive tests among all rejected tests). q-value <0.25 is considered to be significant as recommended (33).

6.5 Animal Experiments

We performed three types of experiments involving mice. First, we isolated bone marrow cells from either *Atgl* knockout mice (*Atgl-/-*) or *Hsl* knockout mice (*Hsl-/-*), as well as from the appropriate control mice. In the second type of experiments, we implanted transformed B-cells subcutaneously into wild type animals (control) from *C57BL/6* strain, or into three immune-deficient mouse models that exhibit severe combined immune deficient (SCID) phenotype. *NSG*, NOD scid gamma mice; *RAG2-/-*, Recombinase activating gene-2 knockout mice; and *RAG2-/-/gamma (c)-/-*, RAG2/gammac double-knockout mice. We also injected transformed B-cells and B16f10 mouse melanoma cells intravenously in control *C57BL/6* mice. Third, we examined mice for spontaneous tumor development upon the deletion of *Atgl*. For this purpose it was not possible to use *Atgl-/-* mice because these mice have a short life expectancy due to a congestive heart failure (10). To overcome this phenotype, *Haemmerle* and colleagues expressed the *Atgl* gene only in the myocytes of *Atgl-/-* mice (*Atgl-/-* ctg mice) (34). Therefore, we examined *Atgl+/+* ctg, *Atgl+/-* ctg and *Atgl-/-* ctg mice for the above mentioned purpose. *Silvia Schauer* has provided help during animal handling and samples collection for almost all animal experiments. A number of *Atgl-/-* ctg mice were kindly provided by *Dr. Renate Schreiber* from the Institute of Molecular Biosciences, University of Graz.

6.5.1 Animal Care

All animals were housed in filter-top plastic cages and maintained on a regular light-dark cycle (12 h light, 12 h dark) and kept on a standard laboratory chow diet

(4.5% w/w fat). Mice used for tumor cells inoculation or injection were 8-9 weeks of age. During experiments, food intake as well as body weight was monitored. All animal studies were performed in accordance with the guidelines and provisions of the Commission for Animals Experiments of the Austrian Ministry of Science and recommendations of the local ethics committee (Animal license numbers: BMWF-66.010/0140-II/3b/2012; BMWF-66.010/0025-II/3b/2012; BMWF-66.010/0013-II/3b/2010). The author contributed to writing the approved applications.

6.5.2 Establishment of Transformed B-cells

Experiments to establish transformed B-cells (TPBC) from *Atgl+/+, Atgl-/-* , *Hsl+/+* and *Hsl-/-* mice were performed at the Institute of Pharmacology and Toxicology, University of Veterinary Medicine, Vienna, at the lab of *Prof. Veronika Sexl*. Researchers from the group of *Prof. Sexl* have established the *Atgl+/+* and *Atgl-/-* B cells and the author has established transformed B-cells from *Hsl+/+* and *Hsl-/-* mice with the help of *Mag. Florian Bellutti* and *Dr. Iris Z. Uras*. Bone marrow cells were isolated from fore- and hind legs of mice and transduced by p185bcr-abl viral supernatant from Φ-NX (Phoenix) cells as previously described (35). *GFP* is co-expressed with *p185bcr-abl* as a transduction marker. To assess lineage, transformed precursors B-cells (TPBC) were tested for B-cell precursor's markers B220, CD43 and CD19 at the Institute of Pharmacology and Toxicology. *Atgl+/+* and *Atgl-/-* TPBC were propagated at 37°C; 5% CO2 in RPMI 1640 medium (cat#21875-091, Life Technologies, CA, USA) supplemented with 10% FBS and 50 µM 2-mercaptoethanol (cat#M6250, Sigma-Aldrich, St. Louis, MO, USA).

6.5.3 Tumor Cell Inoculation and Injection

Control *C57BL6*, or immune-deficient mice were anesthetized using isoflurane. *Atgl+/+*, *Atgl-/-* TPBC cells, or B16F10 cells were inoculated subcutaneously or injected intravenously. After a defined time period (6 - 19 days) mice were anaesthetized using isoflurane and blood samples were collected by retro-orbital puncture. Mice were sacrificed by cervical dislocation. Tumors and tissues were

excised, weighed and either frozen in liquid nitrogen or stored in formalin for further analysis.

6.5.4 NNK and Sodium Benzoate Treatment

Atgl+/+ ctg, *Atgl+/-* ctg, and *Atgl-/-* ctg mice were treated with nitrosamine 4-(methyl-nitrosamino)-1-(3-pyridyl)-1-butanone (NNK) (Cat# sc-214216, Santa Cruz Biotechnology) dissolved in water (4 mg/ml) for 10 months as previously descried (36-38). For sodium benzoate treatment, *C57BL6* mice received (500mg/kg/day) of sodium benzoate in drinking water for 14 days (Cat# 109169, Sodium benzoate, ReagentPlus®, 99%, Sigma). Body weight, and food and water intake was monitored during the study.

6.5.5 Blood and Serum Analysis

Blood was collected as mentioned above. White blood cell count was performed using cell blood counter (cell counter Analyzer MS9-5V, Melet Schloesing Lab, France) at the institute for “Biomedizinsche Forschung” with the help of *Mag. Gabriela Horwath*. For serum preparation, blood was collected in 1.5 ml Eppendorf tubes and left on ice for 30 min. Next, tubes were centrifuged at for 30 min. Serum was transferred to 0.5 ml tubes. Serum samples were shipped to the “Universitätsklinik für Kinder- und Jugendheilkunde”, Salzburg for measurements of amino acids concentrations (please see information on amino acids measurements under the section “Amino Acids, Pyruvate and Lactate”)

6.5.6 Gene Microarray Analysis

This experiment was performed by *Dr. Tamilarasan Kuppusamy Palaniappan* with the help of *Karin Wagner* from the core facility molecular biology at the ZMF. The author evaluated and summarized relevant findings from the data that have been already obtained and analyzed: *PhD-Thesis, “Studies on the Role of Lipoprotein*

Lipase Mediated Lipotoxicity of Skeletal Muscle and the Effect of Adipose Triglyceride Lipase in the Tumor Metabolism" by *Dr. Tamilarasan Kuppusamy Palaniappan.* In addition, the author also validated the results for a certain number of genes using the standard quantitative real-time PCR (qPCR) method.

6.5.7 Assessment of Spontaneous Tumor Development

Atgl+/+ ctg, *Atgl+/-* ctg, and *Atgl-/-* ctg mice were housed and maintained as described under animal care. Mice from a defined age group were sacrificed by isoflurane inhalation. These mice were dissected and a number of organs including lungs, liver, spleen and pancreases were isolated. Enlarged lymph nodes were also collected if they had been found. Two-micrometer sections were used for H&E staining using standard techniques by *Silvia Schauer* as described under "Tissue Processing and Staining" section. At least five sections were stained for H&E from each block and evaluated for the presence of neoplastic lesions by the investigator.

6.6 *In Vitro* Experiment

The majority of the *in vitro* experiments were performed at the ZMF laboratories. A number of experiments were performed to characterize and analyze the previously mentioned B-cells tumor model.

6.6.1 Analysis of Proliferation and Apoptosis

Cell number was counted by CASY cell counter (Roche). DNA staining by bromo-deoxyuridine (BrdU) was perfumed using BrdU APC assay kit (BD Bioscience) according to the manufacturer's instructions. Propidium iodide (PI) staining solution was obtained from BD Bioscience and DNA staining by PI was performed according to standard procedures. Cell preparation and labeling were performed by the author and the flow cytometer analyses were performed by *Dr. Beate*

Rinner and *Katharina Meditz* at the ZMF core facility using the FACSCalibur instrument (BD Bioscience). Cell cycle phases were analyzed with the ModFit.LT V3.3.11 software. Caspase 3/7 was measured using an available kit, Caspase-Glo 3/7 Assay (cat# G8090, Promega, Madison, WI, USA). An appropriate number of cells were cultured for 24 hours in RPMI media without serum. The following steps were performed according to the Promega protocol.

6.6.2 Determination of *ATGL* mRNA

Total RNA was isolated from phosphate buffered saline (PBS) washed *Atgl+/+* or *Atgl-/-* TPBC pellets using TRIzol Reagent (cat#15596-018, Life Technologies, CA, USA) following the manufacturer's protocol. Extracted RNA was measured with a Nanodrop 1000 spectrophotometer (Thermo Scientific, DE, USA). 1 µg of the total RNA was used to synthesize cDNA. cDNA synthesis was performed using the High Capacity cDNA Reverse Transcription Kit with RNase Inhibitor (cat#4374966, Life Technologies, CA, USA) according to the manufacturer's protocol. Power SYBR Green PCR Master Mix (cat#4367659, Life Technologies, CA, USA) and the Applied Biosystems 7900HT Fast Real-Time PCR System (Life Technologies, CA, USA) were used for quantitative real-time polymerase chain reaction (qPCR). Beta actin (Actb) was used as an internal control gene. (Oligonucleotide sequences: *Atgl* forward primer (F): *5'-aacgccactcacatctac-3'*; *Atgl* reverse primer (R): *5'-gcctccttggacacctca-3'*; *Actb* F: *5'-acggccaggtcactattg-3'*; *Actb* R: *5'-caagaaggaaggctggaaaag-3'*). Relative quantification of *Atgl* gene expression from the real-time PCR data was calculated using the 2(-Delta Delta C(T)) method.

6.6.3 Measurements of Cellular and Extra Cellular Metabolites

6.6.3.1 Oxygen Consumption Rate

The author has measured oxygen consumption rate (OCR) and acidification rate (ECAR) *in vitro* at the "Institut für Molekularbiologie und Biochemie", MUG at the lab of *Prof. Wolfgang Graier* with the help from *Dr. Roland Malli* and *Dr. Lukas*

Groschner. We used two different methods to measure the OCR of transformed B-cells. First we performed the measurement using the conventional oxygraph chamber (OROBOROS Oxygraph-2k). Next, we measured OCR and ECAR using the Seahorse XFe96 Analyzer according to standard protocol. Because the established tumor B-cells are suspension cells, we used the Cell-Tak reagent (Corning® Cell-Tak™ Cell and Tissue Adhesive) to enable the cell adhere to the 96-wells plate according to recommendations provided from the Seahorse team.

6.6.3.2 Glucose and Fatty Acids Uptake

These experiments were performed at the "Institut für Molekulare Biowissenschaften" Universität Graz, at the laboratory of *Prof. Rudolf Zechner* with the help form *Dr. Martina Schwieger*. Briefly, for glucose or fatty acids uptake and incorporation, cells were incubated with serum free media that contains radioactively labeled glucose or radioactively labeled oleic acid, respectively, at 37 degrees. 15µl of cell lysate were used for radioactive measurements and 20µl for the determination of protein concentration. Oleic acid incorporation into lipid species was determined using the thin-layer chromatography (TLC) method. Cells were incubated with serum free media containing radioactively labeled oleic acid for 5 hours at 37 degrees. Next, lipids were extracted using hexane and isopropanol. The lipid (liquid) phase was transferred into tubes for evaporation whereas the pellet was used for the determination of protein concentration. After reconstitution in chloroform, lipids were spotted in silica plate (TLC Plate- Silica Gel 60- Merck). Standards for TG, DG, MG and for FAs (Sigma, Vienna, Austria) was used for control. Lipid spots were visualized with iodine, cut and immersed in scintillation fluid for measurements.

6.6.3.3 Amino Acids, Pyruvate and Lactate

For determination of cellular and extra cellular concentration of amino acids, pyruvate and lactate, an appropriate number of cells were cultured for 12 hours in media without serum. For amino acids measurements, prepared samples –cells

and their corresponding supernatant– were sent to the “Universitätsklinik für Kinder- und Jugendheilkunde”, Salzburg. The measurement was carried out by *Dr. Johannes Mayr* and *Prof. Barbara Kofler*. The concentration of cellular and secreted pyruvate and lactate were determined using commercially available kits (BioVision, Milpitas, CA, USA): pyruvate, cat# K609-100; Lactate, cat# K627-100. The measurements were performed by the author at the ZMF laboratories according to the manufacturer's recommendations.

6.6.4 *Atgl* Gene Knockdown

This experiment was performed by *Dr. Suman Das* and the author summarized the procedure according to information provided by *Dr. Das*. HEK293T cells were transfected with 5 µl lentiviral packaging mix (SHP001, Sigma- Aldrich, St. Louis, MO, USA) and 1 µg of MISSION® shATGL plasmid DNA (SHCLND-NM_025802, Sigma-Aldrich, St. Louis, MO, USA) (shRNA Atgl) or MISSION® pLKO.1-puro non-mammalian shRNA control plasmid DNA (SHC002, Sigma-Aldrich, St. Louis, MO, USA) (shRNA Ctrl) using lipofectamine 2000 (cat#11668, Life Technologies, CA, USA). The cells were maintained in growth medium for 3 days and lentiviral particles were harvested from supernatant on day 4 and day 5. B16F10 cell line were transduced with lentiviral particles carrying either *shRNA Atgl* or *shRNA Ctrl* and selected in puromycin.

6.7 Images and Image Analysis

All bright-field microscopy images presented in this work were captured using Nikon Eclipse 80i microscope supplied with camera (Nikon's Digital Sight DS-Fi1) and the NIS-Elements D software. Florescent microscopy images were captured using a confocal laser scanning microscope (Inverted Microscope, LSM 510 META Laser Scanning Microscope, Carl Zeiss) supplied with the Zen software. For blood vessels density evaluation, labeled sections with CD31 antibody were scanned using ScanScope ® AT System. In order to establish CD31 IHC quantification method, the author has tried four image analysis software solutions: HistoQuest,

from TissueGnostics; Tissue Studio, from Definiens; ScanScope, from Aperio; IQM, developed by *Prof. Helmut Ahammer*, MUG. Quantification was possible using the four software solutions and resulted in similar results. The data presented in this study are from the ScanScope software. Introductions to the instruments and software were given by *Prof. Helmut Popper*, for Definiens; *Iris Halbwedl*, for Aperio; *Mag. Markus Absenger* (ZMF), for Aperio at the ZMF; *Andrea Lackner*, for NIS-Elements. *Andrea Koschell* helped in capturing the electron microscopic images.

6.8 Statistical analysis

Statistical analyses of experimental data were performed using Graphpad Prism version 5. Data are presented as means and error bars represent standard deviation of the mean (S.D.). *P*-values were obtained using an unpaired t-test, unless otherwise stated. *P*-values < 0.05 were considered statistically significant. For the analysis of categorical data, analysis of lung neoplasia and adenocarcinoma, the investigator used Fisher's exact test. Cancer-specific survival was calculated using Kaplan-Meier method and compared by the log rank test. Statistical analyses were performed using the Statistical Package for Social Sciences version 17.0 (SPSS Inc., Chicago, IL, USA). A two-sided *P* <0.05 was considered statistically significant.

7 Results

Parts of the results in this section are reproduced with modifications from the published article (30) with the permission of the *Oncotarget* journal.

7.1 ATGL Expression in Healthy Tissues

Haemmerle and his colleagues reported that ATGL depletion in a mouse model (*Atgl-/-* mice) resulted in lipid accumulation in almost all tissues and not only in adipose tissue (10). Tissue distribution of this lipase in humans is expected to be similar to that in mouse. It was reported that ATGL is specifically expressed in the oxidative muscle fibers (type I muscle fibers) in humans and that mutations in the human *ATGL* gene (*PNPLA2*) lead to muscle dystrophy and cardiomyopathy (34, 39-41). To study ATGL protein expression pattern in human tissues, we analyzed proteomics data accessible to the public and performed ATGL immunohistochemistry (IHC) on several different types of normal human tissue.

Results from the human protein map show that ATGL is expressed only in differentiated tissues; none of the studied fetal organs has detectable ATGL expression (**Figure. 2**) (42). This suggests that lipid metabolism might differ according to cell differentiation status. Indeed, expression levels of other key enzymes involved in the lipogenic pathway, such as ACLY, ACACA, and FASN, were more abundant in fetal organs than in differentiated tissues and the opposite was observed for the main three lipolytic key enzymes (**Figure. 2**). These data suggest that proliferating cells in fetal organs use *de novo* synthesized fatty acids to build up organelles required for cellular division, whereas specialized cells can utilize stored lipids via lipolysis to produce energy required to perform cellular functions.

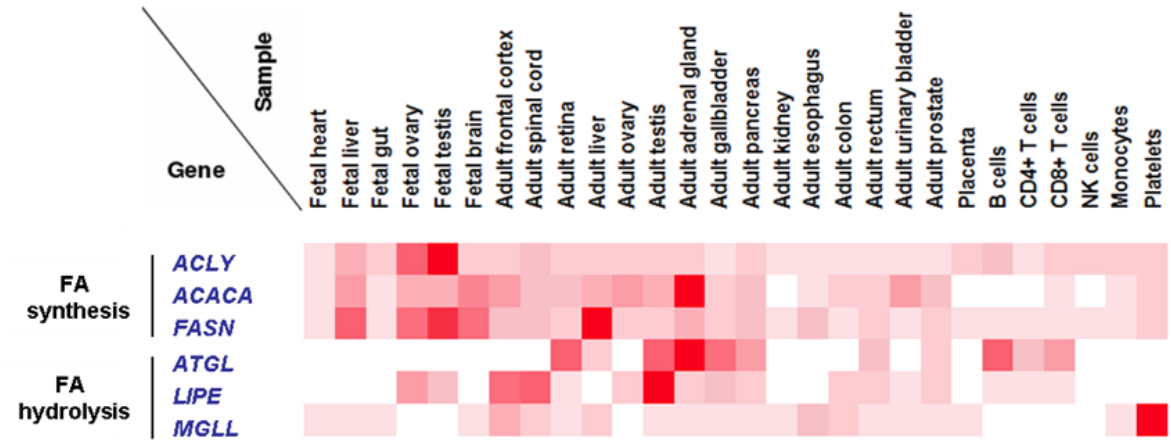

Figure .2 ATGL protein levels in fetal and adult tissues*. Heat map shows protein levels of important enzymes that regulate lipid storage and mobilization. In fetal organs, enzymes that play role in FAs synthesis have higher levels than those that mediate FAs hydrolysis. ATGL levels in fetal organs are undetectable. FAs, fatty acids; ACLY, ATP citrate lyase; ACACA, acetyl-CoA carboxylase alpha; FASN, fatty acid synthase; ATGL, adipose triglyceride lipase (); LIPE, lipase hormone-sensitive (also known as HSL); MGLL, monoglyceride lipase (also known as MGL).*

Our results which we obtained by applying ATGL IHC methods on several tissue types showed a similar tissue distribution pattern. We have evaluated protein levels of ATGL by applying an antibody which can detect this enzyme on formalin-fixed, paraffin-embedded (FFPE) samples. We stained several tissue microarrays contain samples from human mesenchymal and epithelial healthy tissues (**Figure. 3**). Expression pattern of ATGL protein detected using this method was in line with the previously mentioned human proteome map as well as with our current knowledge about this lipase from both human and animal studies. For example, *Atgl-/-* mice suffer from an increased accumulation of neutral lipids in the heart indicating that ATGL is required for efficient hemostasis in mouse cardiac muscle; it lacks an alternate pathway. In our analysis, human cardiomyocytes showed the

highest signal intensity (**Figure. 3**). This is also in agreement with the reports on the *ATGL* gene (*PNPLA2*) mutations and cardiomyopathy (40, 41). In addition, our IHC results on skeletal muscles show that it is highly expressed in skeletal muscles and importantly, only one type of muscle fibers express detectable levels of ATGL. This is consistent with published studies showed that ATGL is exclusively expressed in type I (oxidative) muscle fibers (43, 44) and also consistent with what we know on the association between *ATGL* gene mutations and myopathy (39, 45-47). Most interestingly for us was that the tissue distribution pattern of ATGL protein detected by IHC is similar to the above-mentioned human proteomic data with regard to the differentiation status; ATGL levels in differentiated and terminally differentiated cells were generally higher than the levels in proliferating cells (**Figure. 3**). Taken together, these data verify the specificity of the ATGL anti-body we used and support the idea that there is an inverse relationship between ATGL expression and the ability of cells to enter the cell cycle and divide (**Figure. 3**).

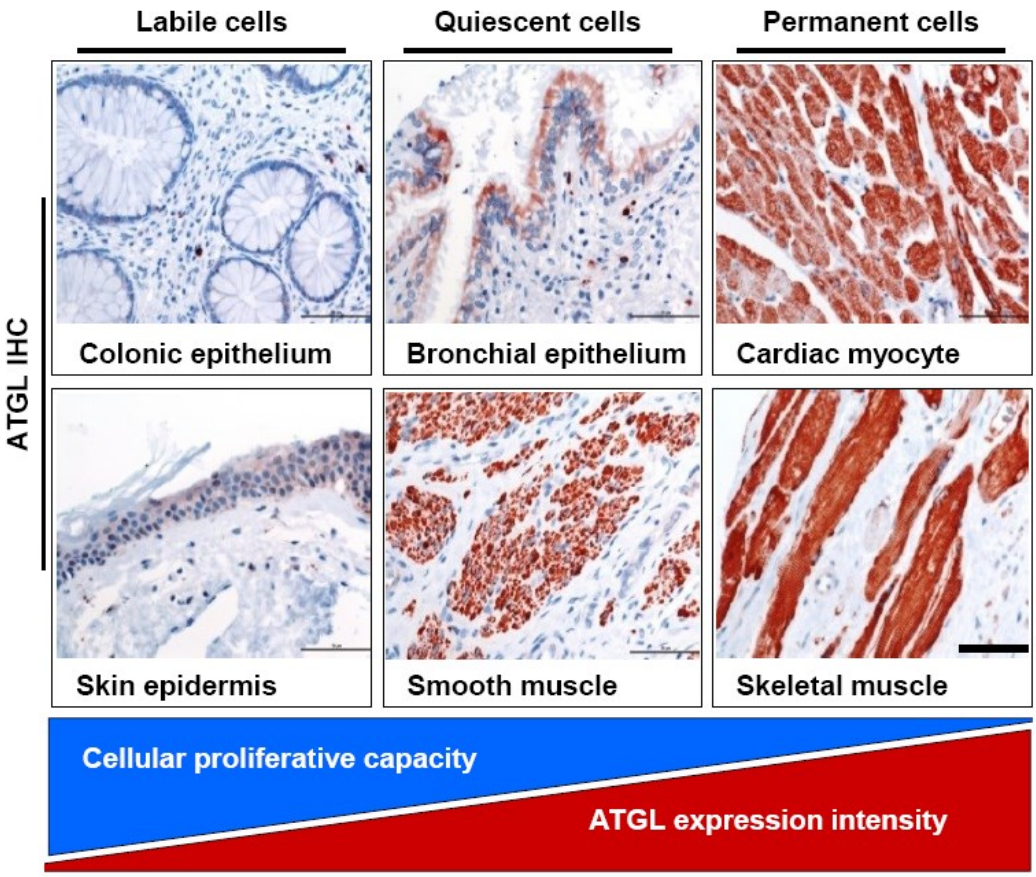

Figure .3 ATGL protein levels across normal cells. *Representative microscopic images for six different types of tissues stained with ATGL antibody. The cells are grouped according to their ability for proliferation and to their differentiation status. Left panels show cells known to have a high rate of proliferation; colonic epithelium and skin epidermis. ATGL signal is either weak, as seen in the skin epidermis, or even undetectable as in the colonic epithelium. Right panels show strong signal for ATGL IHC in two types of cells known to be terminally differentiated; Cardiac and skeletal muscles. Quiescent cells from bronchial epithelium and smooth muscles, in the middle panels, show strong to moderate ATGL expression. Scale bar, 50μm.*

7.2 ATGL Expression Levels in Tumors

Several metabolic pathways that operate in fast proliferating –but normal (non-transformed)—cells are similar to those essential pathways needed in cancer cells (12, 13). Because ATGL levels were low in normal proliferating cells in comparison to specialized cells, we investigated whether ATGL expression is differentially regulated during tumorigenesis. We mainly focused our analyses on tumors which develop in tissues that have high ATGL levels.

We retrospectively analyzed ATGL expression in epithelial and mesenchymal normal and cancer samples including, smooth muscle tumors, pancreatic carcinomas and pancreatic pre-cancerous lesions, and non-small cell lung cancers. All the cases studied had been diagnosed by expert pathologists. We are aware that adjacent morphologically normal tissues might nevertheless harbor pathological changes, yet histo-morphologically, they resemble normal healthy tissues. For reasons of readability, we refer to all adjacent morphologically normal looking tissues in this thesis as “normal tissues”.

7.2.1 Smooth Muscle Tumors

We analyzed benign and malignant tumors that arise from smooth muscles of the uterus and compared distribution and intensity of ATGL IHC signal between tumor and adjacent normal smooth muscle. Levels of ATGL in normal tissues were high and evenly distributed. For this pattern of staining intensity we assigned a numerical value (score) equal to three (= 3), and estimated the percentage of stained cells as (equal to 100%) (**Figure. 4A**) and (**Figure. 5**). Next, we evaluated ATGL IHC in malignant smooth muscle tumors (leiomyosarcoma). Remarkably, we observed that ATGL expression in this type of cancer was low to undetectable in the majority of cancer cells. We assigned score (= 0) for cells that do not show detectable staining using 200X magnification. Score (=1) and score (=2) were assigned to cells express low and moderate IHC intensity respectively, at 200X magnification (**Figure. 4A**) and (**Figure. 5**). Based on the values of ATGL staining

intensity and the percentage of stained cells, we calculated the H-Score as described in the Methods section (**Figure. 4B)** (right panel) (31). We also performed immunofluorescent staining on vascular smooth muscle cell line (VSMC) cells and confirmed that smooth muscles cells have high levels of ATGL expression (**Figure. 4C**)

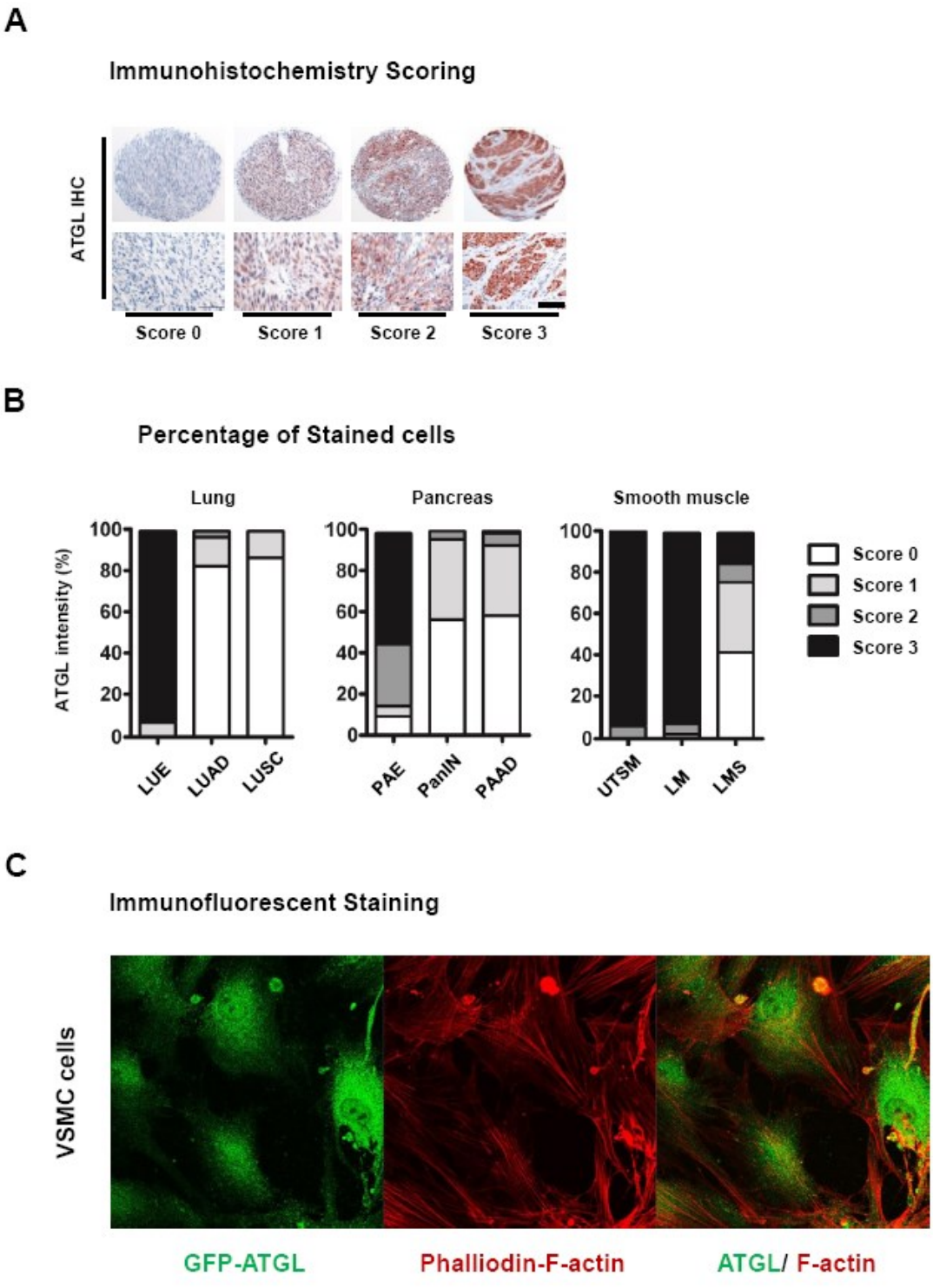

Figure .4 Evaluation of ATGL protein levels. A. *Microscopic images illustrating ATGL IHC staining intensity score. Regions from the upper panels are shown in higher magnification in the lower panels. Scale bar, 50μm.* ***B.*** *Bar graphs show percentages of ATGL IHC staining intensity in neoplasia of lung epithelium, pancreatic epithelium or smooth muscle. LUE, normal lung epithelium; LUAD, lung adenocarcinoma; LUSC, lung squamous cell carcinoma; PAE, normal pancreatic epithelium; PanIN, pancreatic intraepithelial neoplasia; PAAD, pancreatic adenocarcinoma; UTSM, normal uterus smooth muscle; LM, benign smooth muscle tumor (leiomyoma); LMS, malignant smooth muscle tumor (leiomyosarcoma).* ***C.*** *Immunofluorescent staining for ATGL on healthy vascular smooth muscle cell line (VSMC). GFP, green fluorescent protein; Phalliodin, a high-affinity F-actin probe conjugated to the red-orange fluorescent dye that can label cellular filaments and is used in this experiment for counter staining. It was not possible to use the standard counter staining –DAPI; (4',6-diamidino-2-phenylindole)—for nuclear staining due to a technical limitation with laser confocal microscope. This explains why a detectable ATGL signal is seen localized to cell nuclei.*

ATGL IHC H-Score results show that leimyosarcoma cells exhibit significantly lower ATGL protein levels when compared to normal smooth muscle cells (**Figure. 5**). These data clearly indicates that ATGL levels are reduced in this malignant tumor. In fact, this observation raised the question whether ATGL levels are also reduced during the development of common benign tumors that arise from the same tissue type i.e. leiomyoma. It is reported that 70-80% of women by age 50 have developed leiomyoma of the uterus and, importantly, this benign tumor is characterized by a slow growth rate and low rate of mitosis (48-50). We found that ATGL levels in leiomyoma were similar to that in normal uterine smooth muscle (**Figure. 5**) (left panel; LM vs. UTSM), suggesting that the reduced protein levels of this enzyme observed in leimyosacomas (**Figure. 5**) (LMS vs. UTSM) is linked to biological and/or genetic events that are prominent specifically in malignant tumors. This might be important for a better understanding how leiomyosarcoma develop.

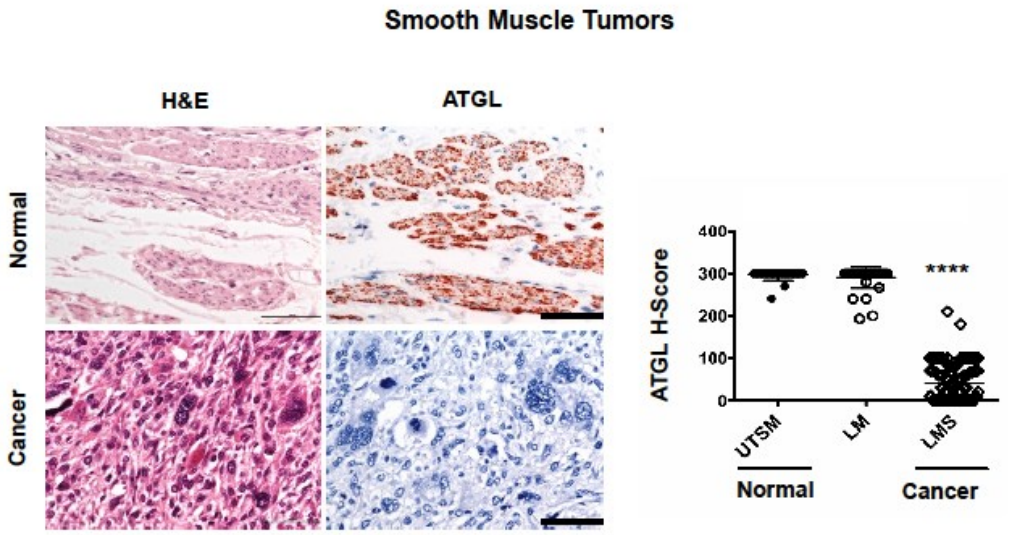

Figure .5 ATGL protein levels are reduced in leiomyosarcoma compared to leiomyoma and normal smooth muscle. *Left, representative microscopic images from haematoxylin and eosine (H&E) stained sections and from immunohistochemical analysis (IHC) using antibodies against ATGL. Normal tissues (upper panels) are compared to cancers (lower panels). Right, dot plot show the results of ATGL IHC semi quantification; H-Score of ATGL protein levels determined by IHC takes into account the proportion (P, 0-100) of positive cells and the respective intensity score (I, 0-3) according to the formula [(I(0)xP(0))+(I(1)xP(1))+(I(2)xP(2))+(I(3)xP(3))]. UTSM, normal uterus smooth muscle; LM, benign tumor of smooth muscle (leiomyoma); LMS, malignant tumor of smooth muscle (leiomyosarcoma). ****P < .0001. Error bars represent SD. (UTSM: mean = 296.5; n =26. LMS: mean = 42.53; n = 83. LM: mean = 291.0; n = 42). Scale bar, 50μm.*

7.2.2 Pancreatic Ductal Carcinomas and Pancreatic Pre-cancerous Lesions

We also studied whether ATGL protein levels are changed during transformation of normal epithelial cells of pancreatic ducts to invasive adenocarcinoma. We observed that normal epithelial cells have high levels of this enzyme. In agreement with other studies reporting that ATGL is expressed in Beta cells (51) from the neuroendocrine part of the pancreas, our IHC shows that cells in the islets of Langerhans express moderate levels of ATGL protein. Percentage of the positive cells suggest that these are Beta cells, however, it was not possible for us to clearly document whether or not Alpha and Delta cells in the Langerhans islets express ATGL.

Unlike the normal ductal epithelium, invasive cells from ductal adenocarcinomas showed low to undetectable IHC signals (**Figure. 6A**). Using the previously mentioned H-Score scoring system we found that the difference in ATGL IHC signal between normal epithelium and pancreatic cancer cells is statistically highly significant. In addition, we observed that the intensity of the staining was low or even lost in pre-cancerous lesions of the pancreas known as pancreatic intraepithelial neoplasia (PanIN). ATGL levels in PanIN lesions were similar to those in invasive cancer cells and significantly lower than those in normal (non-transformed) epithelial cells (**Figure. 6A** and **B**). This indicates that a reduction of cellular ATGL protein concentrations occurs at early stage of the transformation from pancreatic epithelial cells to pancreatic carcinoma cells.

The author also observed that neuroendocrine tumors of the pancreas have an obvious decrease of ATGL protein signal (data not shown). I did not study a sufficient number of cases, but think that this would be an important tumor entity to be evaluated in future studies.

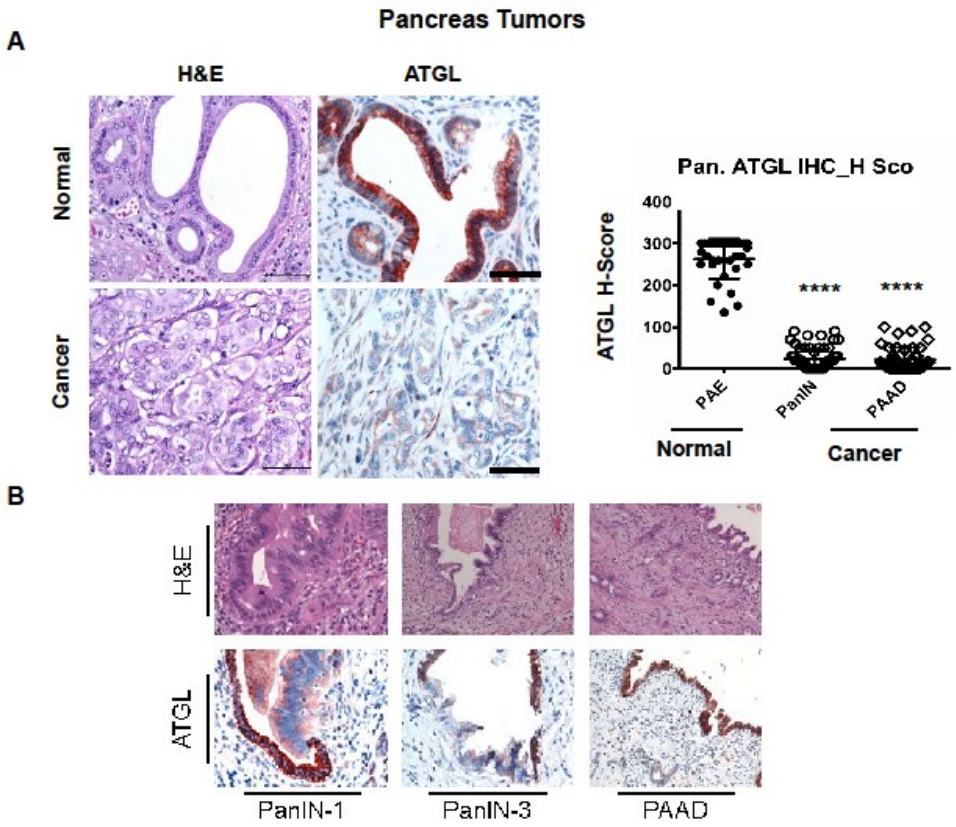

Figure .6 ATGL expression in pancreatic adenocarcinoma and in pre-invasive neoplastic lesions. A. *microscopic* images from pancreas tissue sections stained with *H&E or with ATGL IHC. Normal tissues (upper panels) are compared to cancers (lower panels). Dot plot shows data obtained by evaluating ATGL IHC according to the previously described H-Score system. PAE, normal pancreatic epithelium; PanIN, pancreatic intraepithelial neoplasia; PAAD, pancreatic adenocarcinoma. ****P < .0001. Error bars represent SD. (PAAD: mean = 22.02; n = 47. PanIN: mean = 23.48; n = 66). Scale bar, 50μm.* ***B.*** *Representative microscopic images show H&E staining and IHC using antibodies against ATGL of pre-invasive neoplastic lesions and invasive adenocarcinoma of the pancreas. PanIN-1, pancreatic intraepithelial neoplasia (low grade); PanIN-3, pancreatic intraepithelial neoplasia (high grade); PAAD, pancreatic adenocarcinoma.*

7.2.3 Non-small cell lung cancers

Our results obtained by studying ATGL expression in non-small cell lung cancers provided additional evidence that the levels of this enzyme are reduced during cancer cell development. We evaluated ATGL IHC signals in tissue microarrays (TMA) that contain samples from two common types of cancer that arise from lung epithelia cells: squamous cell carcinomas and adenocarcinomas of the lung. Normal lung epithelium showed specific and strong signal for ATGL IHC whereas cells from the two cancer types studied showed low or no positive staining for ATGL. Statistically, ATGL levels are significantly reduced in non-small cell lung cancers when compared to the signal in normal lung epithelial tissues (**Figure. 7**).

We also evaluated ATGL protein expression in a number of tumor types that develop in tissues that have low ATGL expression, including colon and prostatic epithelium. I did not detect a prominent difference between normal and tumor tissues. However, it was clear that there was no increase in ATGL protein levels in these two types of tumors.

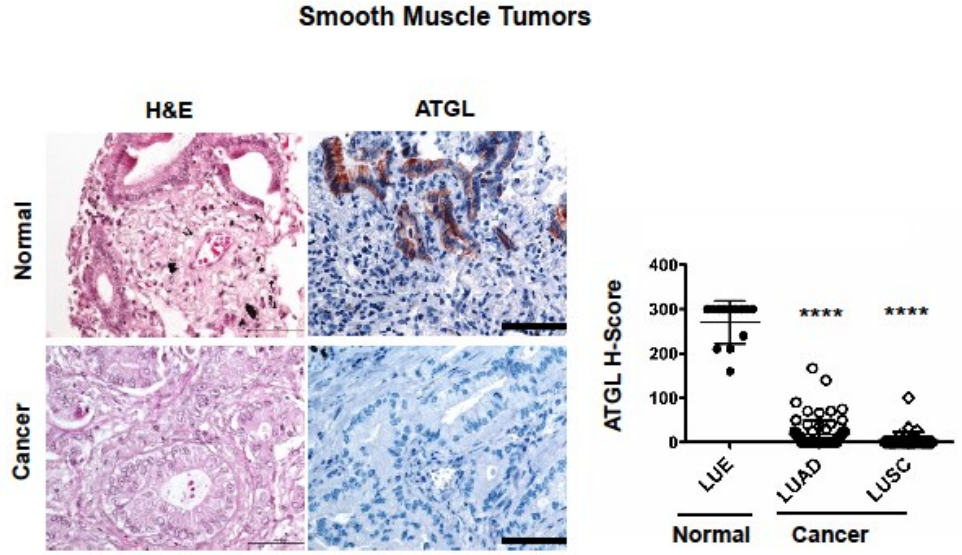

Figure .7 ATGL protein levels are reduced in lung cancer. *Representative microscopic images from lung sections stained with H&E stained or labeled with ATGL Anti-body. Normal epithelial cells (upper panels) are compared to adeno carcinoma cells c (lower panels). Data from ATGL IHC semi quantification (H-Score) are presented in the dot plot to the right. LUE, normal lung epithelium; LUAD, lung adenocarcinoma; LUSC, lung squamous cell carcinoma. ****P < .0001. Error bars represent SD. (LUE: mean = 13.47; n =13. LUAD: mean = 17.31; n = 70. LUSC: mean = 5.623; n = 34.) Scale bar, 50μm.*

7.3 *ATGL* mRNA Levels in Tumors

IHC data show that ATGL protein levels are reduced in several types of human epithelial and mesenchymal cancers. To gain an insight on how mRNA levels of this enzyme might be altered in cancers, we analyzed data available to the public and performed our analysis on samples obtained from the archives of the Biobank, MUG.

We extracted data for *ATGL* mRNA expression levels from four datasets of The Cancer Genome Atlas (TCGA) database. In accordance with our results on the protein levels, we found a highly significant decrease in *ATGL* mRNA levels in several cancer tissues compared to their matched normal tissue. We observed a pronounced reduction in breast carcinoma, lung adenocarcinoma and squamous cell carcinoma, as well as head and neck squamous cell carcinoma (**Figure. 8**) and (**Table. 1**)

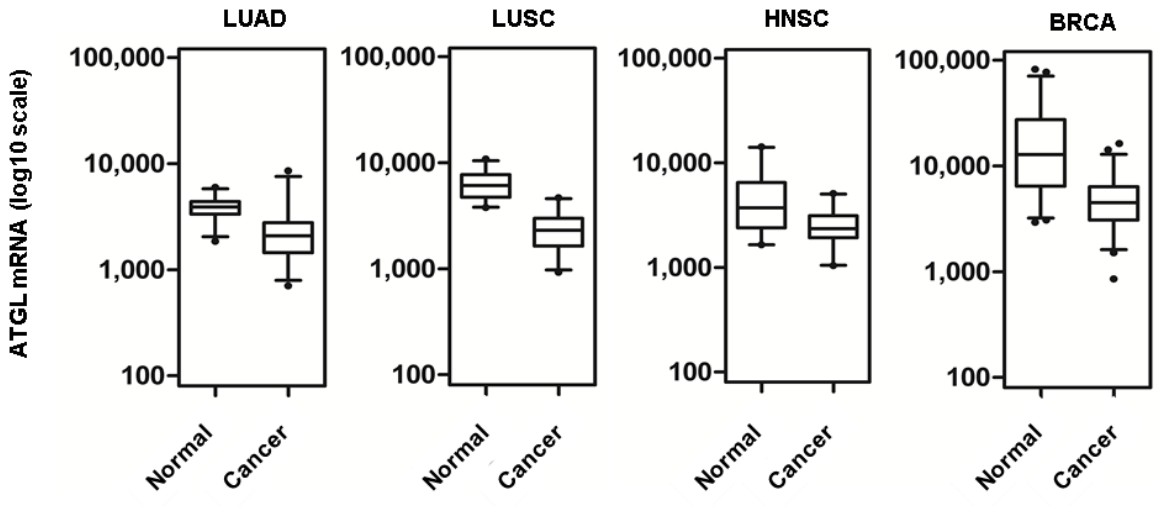

Figure .8 ATGL mRNA expression levels in tissue samples of four types of cancer*. LUAD, lung adenocarcinoma; LUSC, lung squamous cell carcinoma; HNSC, head and neck squamous cell carcinoma; BRCA, breast ductal carcinoma. (See also* ***Table. 1****). The data were obtained from The Cancer Genome Atlas*

(TCGA) database and were provided by Dr. Alida Kindt and Prof. Zlatko Trajanoski at the Division of Bioinformatics, Medical University of Innsbruck.

Table .1 Analysis of ATGL mRNA levels

Dataset	Number of Patients	Log2 fold Change	Adjusted P value
LUAD	57	- 0,87	$1.47X10^{-17}$
LUSC	50	- 1,42	$6.23x10^{-50}$
HNSC	40	- 0,71	$1.57X10^{-7}$
BRCA	108	- 1,52	$6.17x10^{-33}$

[a] *Tumors are compared to matched normal tissues*

In addition, we also evaluated *ATGL* mRNA levels using reverse transcriptase quantitative polymerase chain reaction (RT-qPCR) method in tumor and control samples from patients diagnosed with lymphomas, liver carcinomas or leukemia. In these tumor types we were not able to detect a significant difference in *ATGL* mRNA expression between tumor and non-tumor samples (**Figure. 9**).

Because epigenetic events, including DNA methylation, are able to regulate gene expression, we studied whether DNA methylation might play a role in down regulating *ATGL* gene expression in cancer tissues. We analyzed data on *ATGL* gene methylation statues using the same four datasets from TCGA that showed reduced *ATGL* mRNA levels (**Figure. 8**). The Infinium HumanMethylation450 BeadChip Kit contains 21 methylation sites before and within the ATGL gene. These sites were analyzed in patients for which matched tumor and normal tissue samples exist. Our analyses show that the lung adenocarcinoma dataset contained no significantly different methylated sites in and around the *ATGL* gene after multiple testing was taken into account. In the other three datasets, the mean differences between tumor and normal tissues were small –ranging between -0.20 and 0.20 (**Figure. 10**). Based on these results a relation between the observed

downregulation of *ATGL* mRNA expression and the methylation statues of the *ATGL* gene is unlikely.

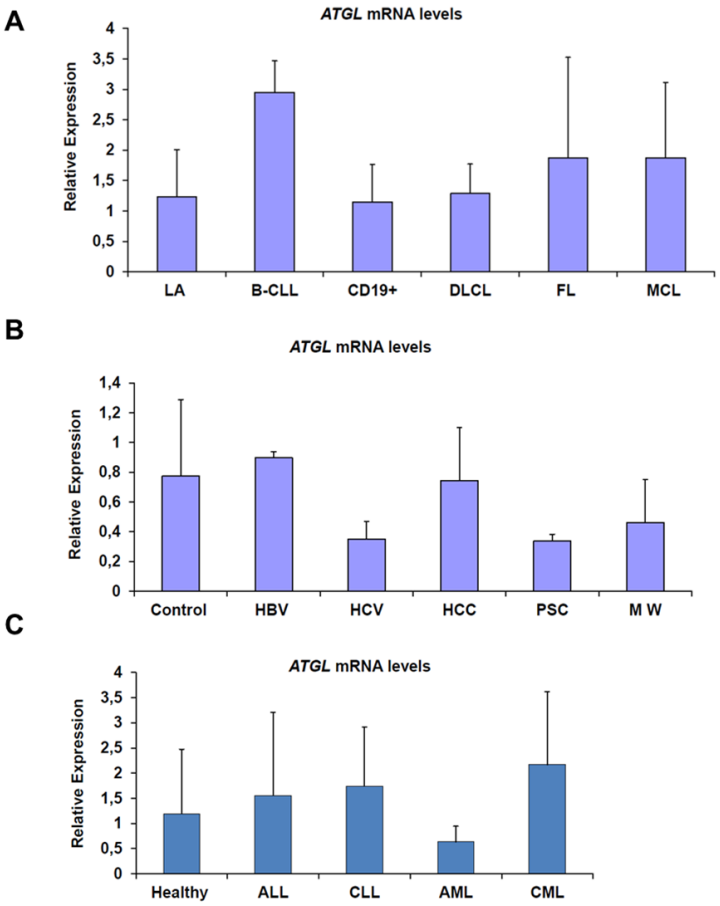

Figure .9 ATGL mRNA levels. *The data presented in this figure were obtained by analyzing control and tumor samples using the quantitative reverse transcriptase quantitative PCR (RT-qPCR) method.* ***A.*** *ATGL mRNA levels in lymphoma and control samples: LA, lymphadenitis (n = 9); B-CLL; B-cell chronic lymphocytic leukemia/small lymphocytic lymphoma (B-CLL/SLL) (n = 6); CD19+, B-cell lymphoma express the surface marker CD19 (cluster of differentiation 19) (n = 4); DLBCL, diffuse large B-cell lymphoma (n = 20); FL, follicular lymphoma (n = 22); MCL, mantle cell lymphoma (n = 9).* ***B.*** *ATGL mRNA levels in samples from liver disease caused by hepatitis B or C viruses, by an autoimmune disorder and one type of liver carcinoma (hepatocellular carcinoma). Control, healthy liver (n = 4); HBV, hepatitis B virus (n = 5); HCV, hepatitis C virus (n = 6); HCC, hepatocellular carcinoma (n = 6); Primary sclerosing cholangitis (n = 2); MW, Mowat-Wilson syndrome (n = 2). The samples were kindly provided by Dr. Johannes Haybaeck's research group.* ***C.*** *ATGL mRNA levels in samples from leukemia patients. Healthy, blood from healthy donors (n = 5), ALL, acute lymphocytic leukemia (n = 10); CLL, chronic lymphocytic leukemia (n = 10); AML, acute myeloid leukemia (n = 10),*

CML, chronic myeloid leukemia (n = 10). The samples were kindly provided by Prof. Heinz Sill's research group with the help of Ms. Karin Lind.

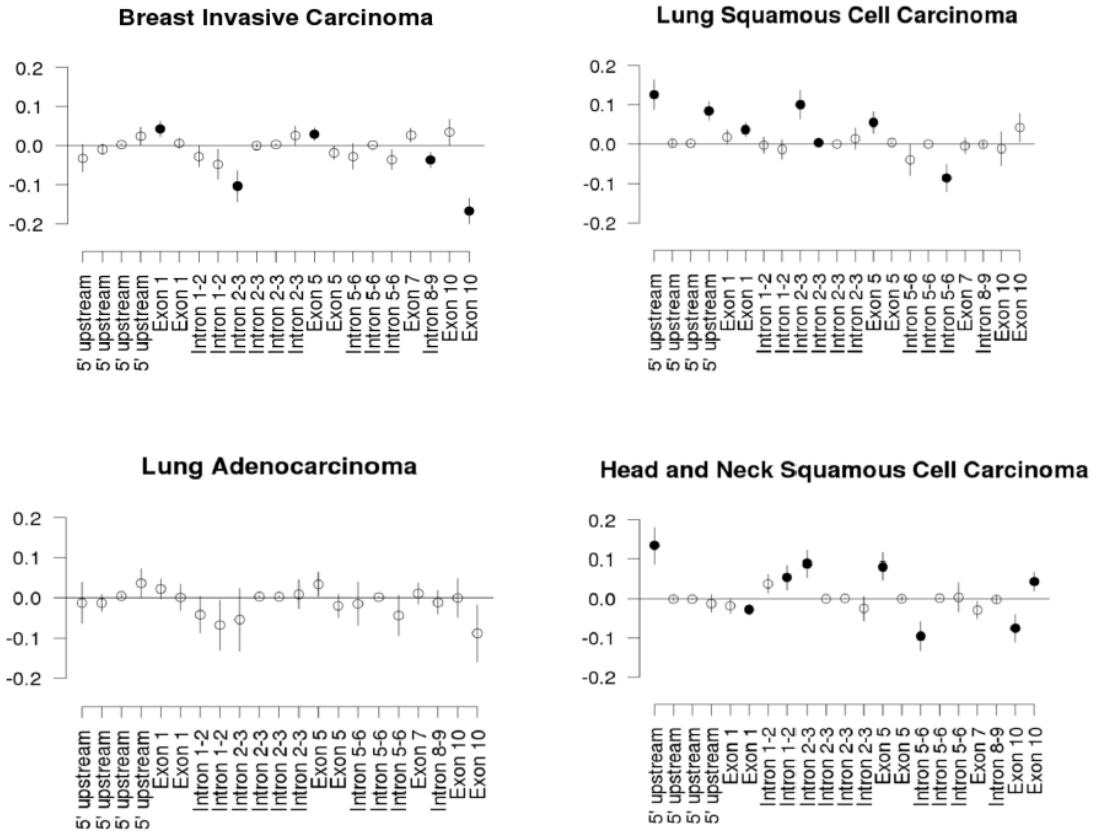

***Figure .10 the ATGL gene methylation status**. Mean differences and 95% confidence intervals of methylation in four cancer datasets. X-axis shows position of methylation sites relative to the ATGL gene. Values on the Y-axis indicate percentages of methylation at the sites; the differences range between -20 and 20 %. Solid symbols (●) show significant mean differences. Empty symbols (○) are not significant after correcting for multiple testing. Values above zero indicate that tumors are more methylated than normal tissue, while values below show the opposite. The data were kindly provided by Dr. Alida Kindt and Prof. Zlatko Trajanoski at the Division of Bioinformatics, Medical University of Innsbruck.*

Next, we analyzed genetic alterations of the *ATGL* gene, including DNA mutations and copy number alterations. We found that the *ATGL* gene has a very low rate of mutations in all type of cancers (**Figure. 11**) indicating that other genetic events might be responsible for the observed reduced levels of this enzyme. Notably, analysis of copy number alteration from the TCGA data indicated a deletion of the *ATGL* gene in 24.7 % of all cancers analyzed (q-value = 5.64x10-72). We found that the *ATGL* gene is deleted in about 38% of lung cancer (n = 1016, q-value = 1.74x10-13). Moreover, it is significantly (q-value <0.25) deleted in tumors from 14 cancer types (**Table. 2**). It is worth noting that the *ATGL* gene was not significantly amplified in any tumor type (**Table. 2**). The later observation supports our IHC data because we did not detect any tumor type with an increased ATGL IHC signal. Taken together, these results suggest that deletion of the *ATGL* gene might account –at least in a number of tumor samples— for the low levels of this enzyme in tumors compared to normal tissues. These data provide further support for the importance of the observed loss of ATGL during malignant transformation of several tissue types.

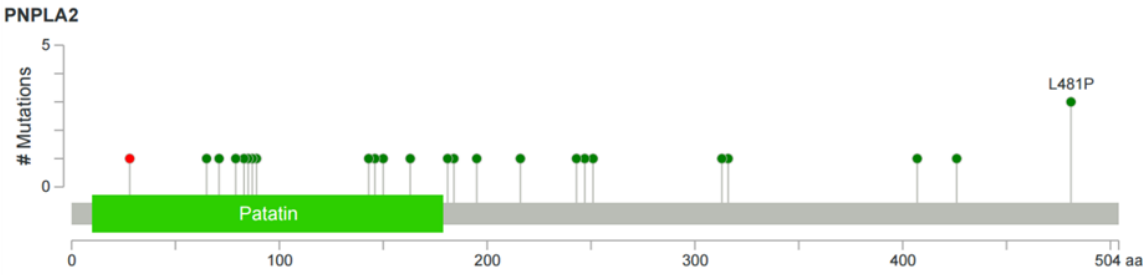

Figure .11 Frequency of the ATGL gene mutations in human cancer. *Mutation diagram shows reported mutations for the human ATGL gene (PNPLA2) in TCGA. Green circles correspond to missense mutations. Red circle corresponds to a truncating mutation; a frameshift insertion was reported in renal cell carcinoma.*

Table .2 Analysis of the ATGL gene copy number alteration across multiple cancer types collected in The Genome Cancer Atlas (TGCA)

[a] *Analysis version: 2014-11-03 stddata__2014_10_17; dataset of 10570 tumors*

Cancer subset	Amplifications		Deletions	
	Frequency	q-value	Frequency	q-value
All cancers	0.09	1.0	0.25	**5.64E-72**
Epithelial cancers	0.10	1.0	0.25	**3.18E-53**
Ovarian serous cystadenocarcinoma	0.10	1.0	0.59	**6.39E-31**
Lung cancers	0.12	1.0	0.38	**1.74E-13**
Brain lower grade glioma	0.06	1.0	0.21	**5.94E-13**
Breast invasive adenocarcinoma	0.13	1.0	0.28	**6.35E-12**
Glial cancers	0.04	1.0	0.22	**7.6E-12**
Lung squamous cell carcinoma	0.09	1.0	0.49	**5.32E-11**
Uterine corpus endometrioid carcinoma	0.07	1.0	0.19	**9.54E-8**
Sarcoma	0.09	1.0	0.42	**2.98E-6**
Lung adenocarcinoma	0.16	1.0	0.27	**0.00281**
Glioblastoma multiforme	0.04	1.0	0.23	**0.00765**
Bladder urothelial carcinoma	0.06	1.0	0.52	**0.0213**
Esophageal carcinoma	0.16	1.0	0.40	**0.0219**
Stomach adenocarcinoma	0.13	1.0	0.20	**0.0296**
Pancreatic adenocarcinoma	0.05	1.0	0.156	**0.103**
Pheochromocytoma and Paraganglioma	0.04	1.0	0.35	**0.126**
Head and neck squamous cell carcinoma	0.13	1.0	0.31	**0.244**
Uterine carcinosarcoma	0.11	1.0	0.46	0.412
Adrenocortical carcinoma	0.09	1.0	0.3	0.596
Acute myeloid leukemia	0.02	1.0	0.01	0.635
Blood cancers	0.06	1.0	0.01	0.884
Cervical squamous cell carcinoma	0.05	1.0	0.36	1.0
Cutaneous melanoma	0.12	1.0	0.31	1.0
Melanomas	0.12	1.0	0.26	1.0
Liver hepatocellular carcinoma	0.10	1.0	0.17	1.0
Rectum adenocarcinoma	0.2	1.0	0.15	1.0
Kidney chromophobe	0.23	1.0	0.14	1.0
Colorectal cancers	0.15	1.0	0.13	1.0
Colon adenocarcinoma	0.13	1.0	0.12	1.0
Mesothelioma	0.15	1.0	0.06	1.0
Kidney renal papillary cell carcinoma	0.04	1.0	0.06	1.0
Kidney cancers	0.07	1.0	0.05	1.0
Prostate adenocarcinoma	0.05	1.0	0.04	1.0
Kidney renal clear cell carcinoma	0.06	1.0	0.04	1.0
Uveal melanoma	0.13	1.0	0.03	1.0
Diffuse large B-cell lymphoma	0.21	1.0	0.02	1.0
Thyroid carcinoma	0.01	1.0	0.02	1.0

7.4 ATGL Expression Levels and Clinical Out-comes

To test a possible impact of *ATGL* gene expression on clinical outcome in different types of cancer, we analyzed overall survival in breast, ovarian, gastric and non-small cell lung cancer patients using Kaplan-Meier Plotter (*www.kmplot.com*). This online available software tool combines Affymetrix gene expression data from multiple annotated cancer studies into a single database which can be then queried for associations of patient outcome with the expression of individual genes (32). Our analyses show that high levels of *ATGL* mRNA in tumor samples correlate with better prognosis of the disease in patients (**Figure 12**).

To test whether the ATGL protein levels in pancreatic cancer is associated with clinic-pathological parameters or with clinical outcomes, we dichotomized 51 patients according to their ATGL protein levels determined by the IHC method. There was no association with age, gender, tumor grade or stage (*P* Values > 0.05). No survival differences between the groups of ATGL negative and ATGL positive pancreatic cancer patients could be observed (*P* = 0.612) (**Figure. 13**). It is important to consider that ATGL protein levels in pancreatic cancer cells were low and this might influence the outcomes of the analysis. Based on this result, we think that classifying the groups of patients based on mRNA levels might provide a better insight on the relation between ATGL expression and patient outcome. This might be also the case for other types of cancer.

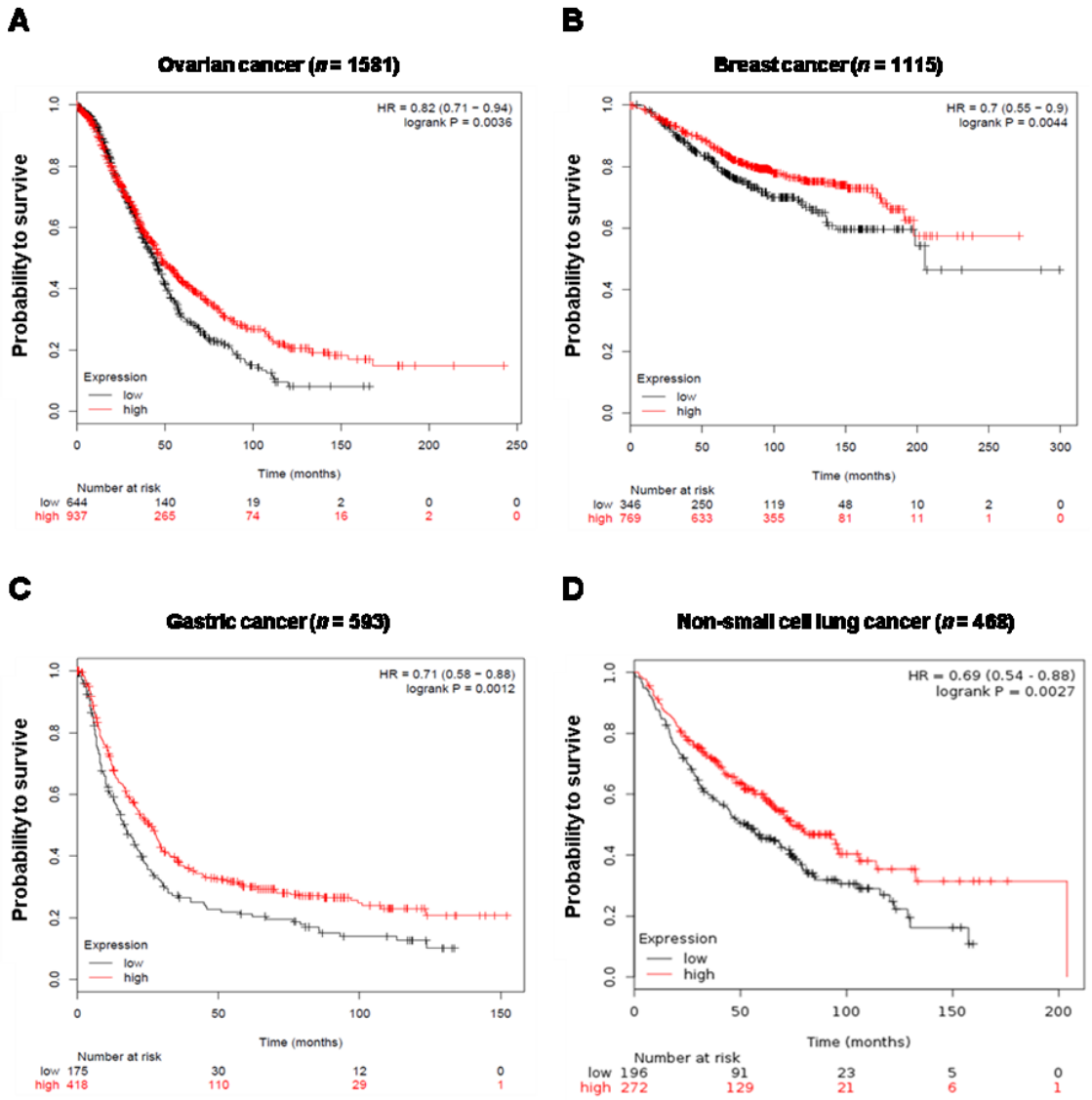

Figure .12 ATGL gene expression level is a prognostic factor in multiple cohorts of different types of cancer. *Overall survival of 1581 ovarian cancer patients (**A**), 1115 breast cancer patients (**B**), 593 gastric cancer patients (**C**), 486 non-small cell lung cancer patients (CAARRAY cohort) (**D**) after dichotomization according to the ATGL expression levels. HR: hazard ratio.*

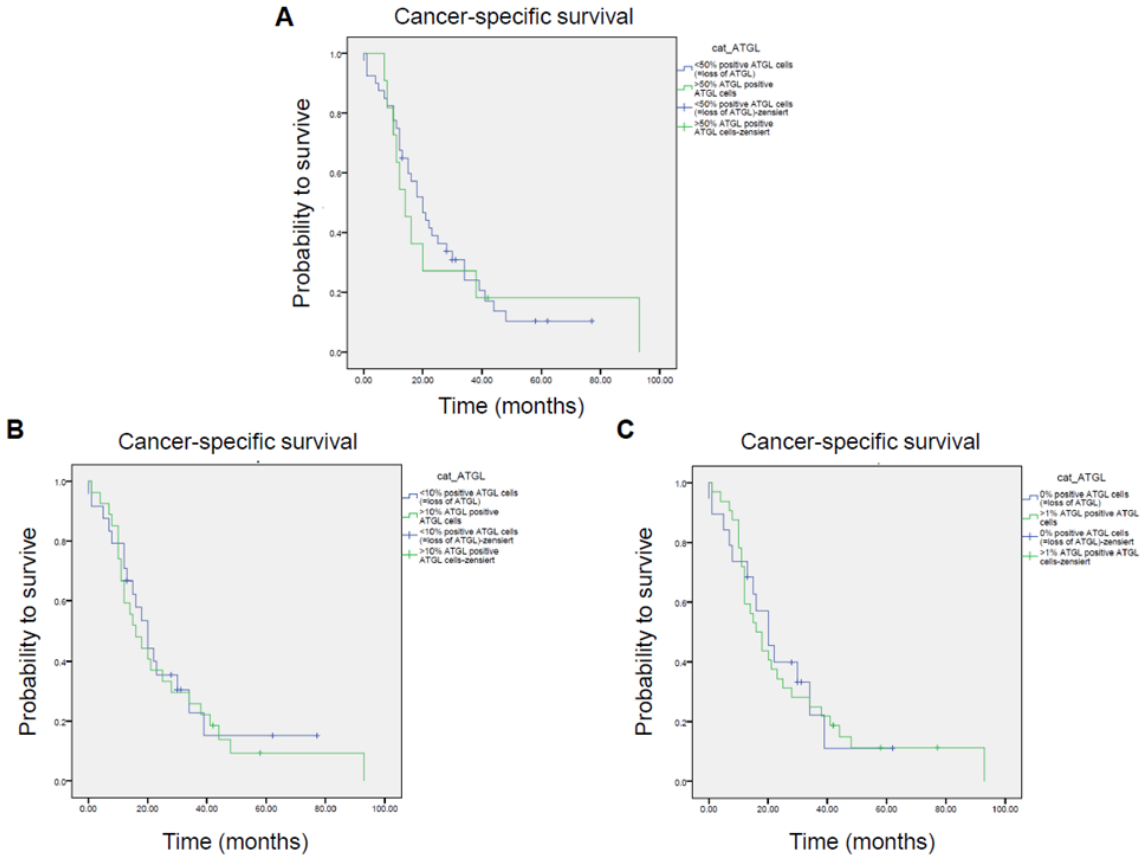

Figure .13 ATGL protein levels and survival of pancreatic cancer patients. *Survival curves show Kaplan-Meier analyses of the prognostic relevance of ATGL protein expression in pancreatic cancer tissues. Percentage of cancer cells is considered for cut off; (**A**) 50 % of cancer cells show detectable ATGL expression, (**B**) 10 % of cancer cells show detectable ATGL expression, (**C**) 1% of cancer cells show detectable ATGL expression.*

7.5 Loss of ATGL in Experimental Mouse Tumor Models

Data obtained from analyzing ATGL protein and *ATGL* mRNA levels, as well as *ATGL* gene copy number variations reveal that the levels of this lipase are reduced or even lost during carcinogenesis. This suggests that the loss of ATGL is beneficial for cancer cells. To test this hypothesis we performed several *in vitro* and *in vivo* experiments on tumor and animal models that lack ATGL.

7.5.1 Establishment of an Experimental B-Cell Tumor Model

To study the consequences of ATGL loss on tumor cell properties and biology, an experimental B-cell tumor model was created using Bcr-Abl transformed B-cell precursors from wild type (*Atgl+/+*) and *Atgl-/-* mice bone marrow (35) (**Figure. 14A-C**). The establishment of this model was performed with the help of *Prof. Veronika Sexl* and members of her research group at the "Institut für Pharmakologie und Toxikologie", Veterinärmedizinische Universität, Vienna. *Bcr-Abl* is a fusion gene formed by a (9;22)(q34;q11) translocation; Abl1 (Abelson murine leukemia viral oncogene homolog 1) gene on chromosome 9 (region q34) translocated within the part of the BCR (breakpoint cluster region) gene on chromosome 22 (region q11). The resulting fusion gene encodes a fusion protein that varies in size, depending on the breakpoint in the BCR gene: fusion protein of 230kD molecular mass (P230); or of 210kD molecular mass (P210); or of 185kD molecular mass (P185) (35, 52-55). Because the short form (P185) is associated with acute lymphocytic leukemia (ALL) ─a hematological malignancy defined by clonal proliferation of lymphoid precursors in human─ this form was used to transform mouse B-cell precursors.

In this work we refer to transformed B-cells precursors derived from *Atgl+/+* mice as *Atgl+/+* TPBC, and to transformed B-cells precursors derived from *Atgl-/-* mice as *Atgl-/-* TPBC. *Atgl+/+* TPBC cells have a considerable *Atgl* mRNA levels and, as expected, *Atgl* mRNA levels were undetectable in *Atgl-/-* TPBC providing an appropriate model to carry out our investigation (**Figure .14D**).

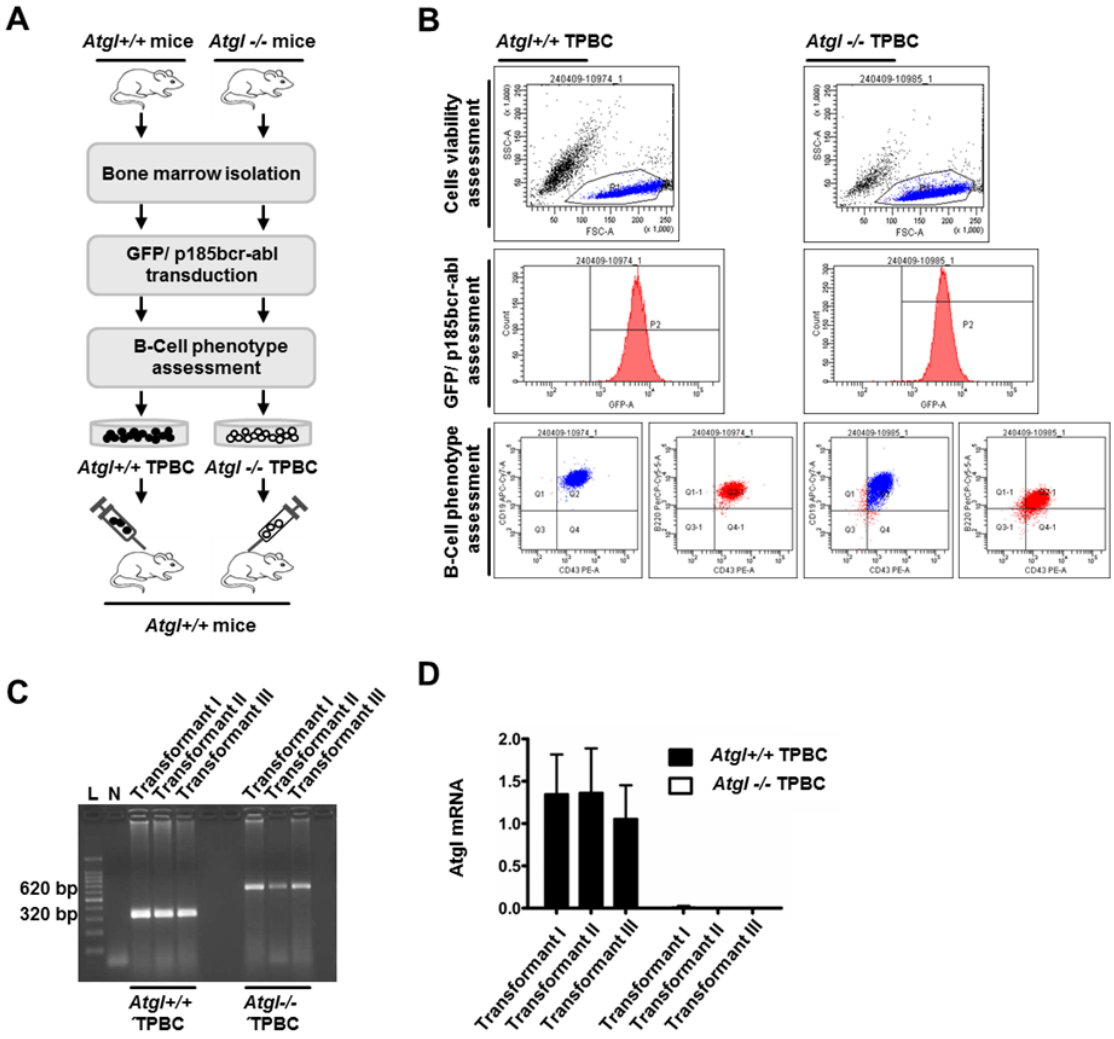

Figure .14 Outline of Atgl+/+ or Atgl-/- experimental transformed precursor B-cell lymphoma/ leukemia model establishment and assessment. (***A***) *Diagram outlining Atgl+/+ or Atgl-/- experimental TPBC development and investigating strategy.* (***B***) *Selection of bcr-abl transformed B-cells using fluorescence activated cell sorting (FACS). Cells were isolated from bone marrow of Atgl+/+ or Atgl-/- mice (n= 3). Viable cells (upper panels) were transduced with p185bcr-abl viral supernatant in which GFP is co-expressed. GFP positive cells were isolated by FACS (middle panels) and assessed for expression of B-cell phenotype markers B220, CD43 and CD19 (lower panels). This procedure yielded 3 independent cell lines of each genotype, Atgl+/+ or Atgl -/-. Dot plots and histograms were provided by the group of Prof. Veronika Sexl.* (***C***) *Confirmation of*

*Atgl+/+ or Atgl -/- TPBC genotype. The gel images were provided by Dr. T. K. Palaniappan. (**D**) Relative Atgl mRNA levels in Atgl+/+ or Atgl-/- TPBC cells (n= 5). Error bars represent SD.*

7.5.2 Measurements of Proliferation Rate *in Vitro*

Several cell count measurements performed at the Institut für Pharmakologie und Toxikologie, Vienna, as well as at the ZMF Graz showed that there was no difference in the *in vitro* proliferation rate between *Atgl+/+* TPBC and *Atgl-/-* TPBC cells. However, *Atgl-/-* TPBC cells developed significantly larger tumors compared to *Atgl+/+* TPBC cells when injected into mice. This important finding was reported by *Dr. T. K. Palaniappan*. Because of these two findings, it was concluded that the loss of ATGL increased proliferation rate of TPBC cells *in vivo* only and not *in vitro*. Further experiments were later performed by *Dr. T. K. Palaniappan* and by the author to explore the observed phenotype *in vivo*.

For each *in vivo* experiment, frozen TPBC cells were recovered and cultured until the viability of the cells reach a high percentage (> 95%) and until enough cells needed for injection were obtained. Interestingly, we observed that *Atgl-/-* TPBC cells recover faster than *Atgl+/+* TPBC cells *in vitro*. The observed difference in the recovery rate can be due to several reasons, including freezing conditions. Therefore, the author performed several experiments to optimize all steps required for maintaining and propagating the cells, including the freezing process. We repeated the recovery procedure under the new conditions.

We observed again that *Atgl-/-* TPBC cells recover faster than *Atgl+/+* TPBC cells, suggesting that this difference is indeed a cells-specific feature rather than an artificial effect (**Figure .15A**). This observation prompted us to further characterize the TPBC cells proprieties *in vitro*. In fact, the author found that *Atgl-/-* TPBC cells proliferate 1.5-2-fold faster than faster *Atgl+/+* TPBC cells under various cell culture conditions (**Figure. 15B**). This observation was confirmed by several researchers, who worked with these particular TPBC cells under appropriate cell culture conditions – data are not shown.

A

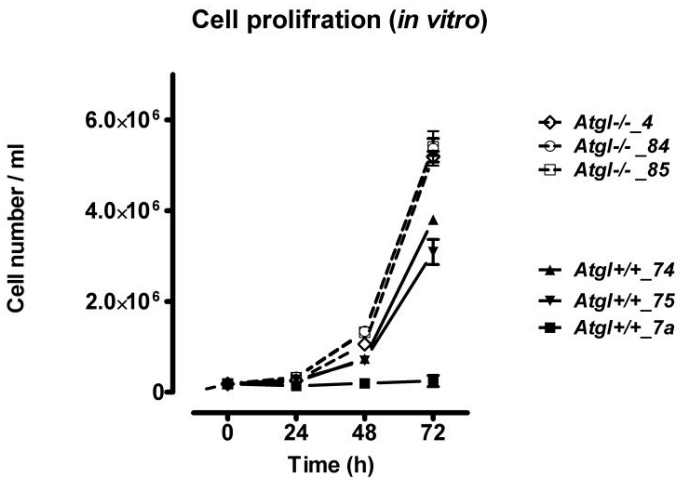

B

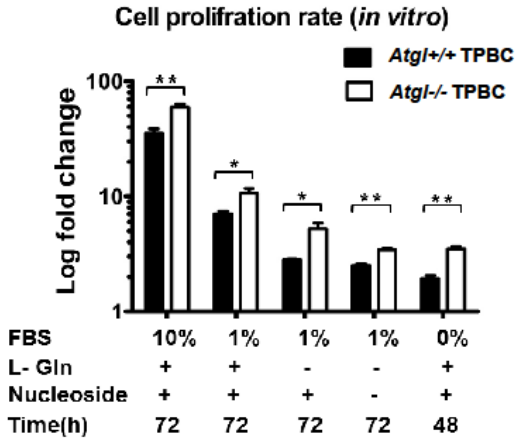

Figure .15 Ablation of ATGL enhances the in vitro tumor cell proliferation capacity. ***A.*** *Proliferation curve of Atgl+/+ TPBC or Atgl-/- TPBC cells in vitro (n = 4). Cell count was performed by Dr. Spela Klemen under the guidance of the author* ***B****. Fold changes of Atgl+/+ TPBC or Atgl-/- TPBC cell numbers upon culturing under the indicated media conditions; (FBS) Fetal bovine serum, (L-Gln) L-glutamine (n=3). ** P < 0.05, ** P < 0.01. Error bars represent SD.*

These results were also supported by additional two independent experiments using flow cytometry. First, we performed cell cycle analysis after DNA labeling with propidium iodide (PI) (**Figure. 16A**). Our results show that the largest portion of *Atgl-/-* TPBC and *Atgl+/+* TPBC cells were in the synthesis phase (S-phase). This indicates that both genotypes have high rate of DNA synthesis and have the ability for rapid proliferation. However, *Atgl-/-* TPBC cells have a significantly higher number of cells in S-phase and significantly lower number in gap 1 (G1) phase when compared to *Atgl+/+* TPBC. In the second experiment, we incubated cells with Bromo-deoxyuridine (BrdU) which incorporates with the newly synthesized DNA (**Figure. 16B**). Here we also found similar results regarding the S-phase and G1 phase, revealing a significant difference in the cell cycle phases between the two genotypes. Because the cell number can be influenced also by apoptosis, we measured 3/7 caspase activity in these cells. Importantly, the rate of apoptosis *in vitro* was similar between *Atgl-/-* TPBC and *Atgl+/+* TPBC cells (**Figure. 16C**). All these results indicate that the increased cell number of *Atgl-/-* TPBC cells is due to a higher proliferation rate suggesting that the loss of ATGL resulted in a faster proliferating tumor cells.

Next, we asked whether the loss of this metabolic enzyme altered the metabolic status of the cells, which in turn might enable the cells to proliferate faster. To address this question we performed several experiments.

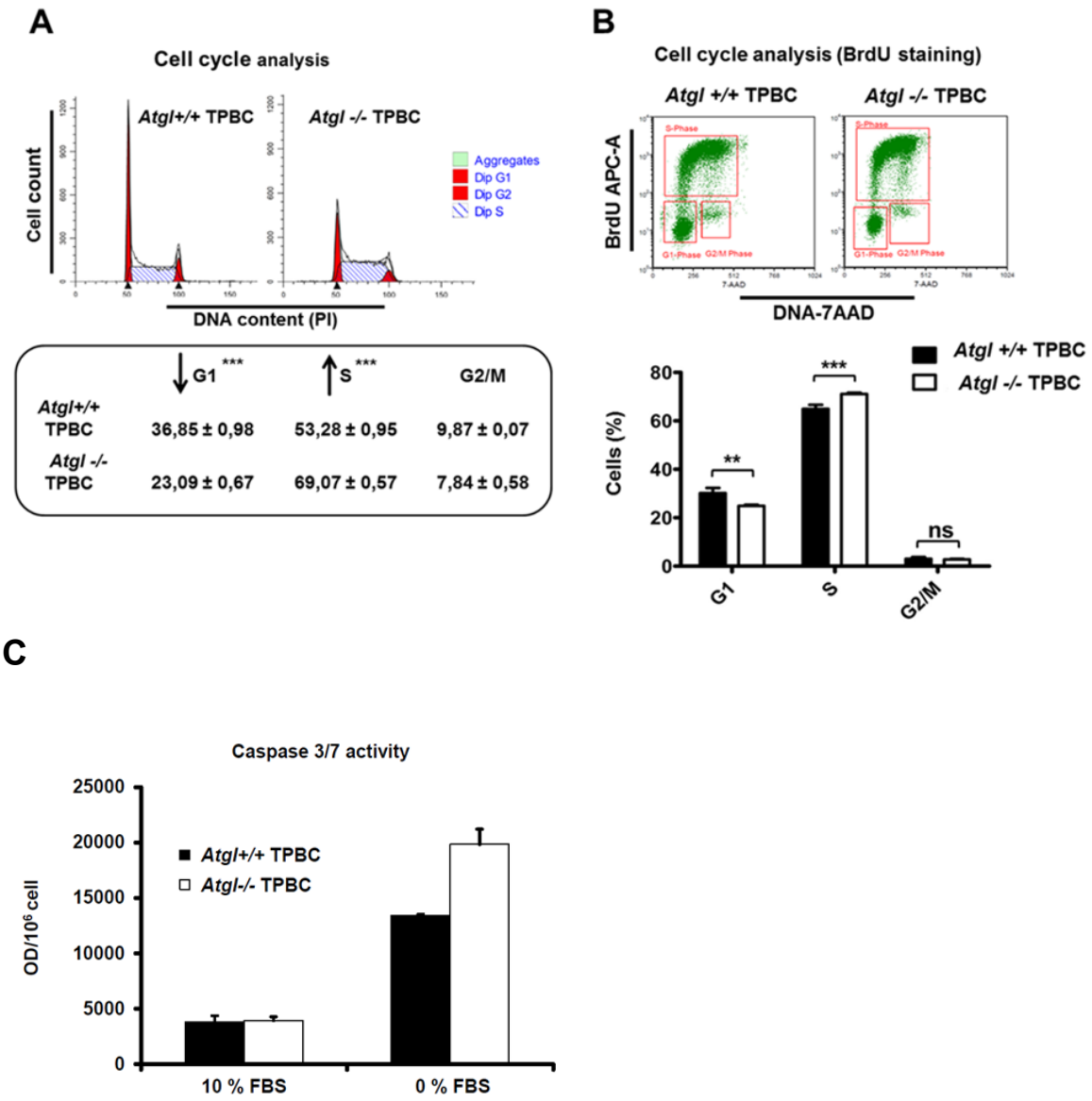

Figure .16 Proliferation and apoptosis rate of TPBC cells. ***A***. *Histograms (upper panels) show the percentage of TPBC cells in three stages of the cell cycle: G1, .the gap 1 phase; S, the synthesis phase; G2/M, the gap2 phase and the mitotic phase. Averages and standard deviations are listed in the lower panel.* ***B***. *Plots show BrdU labeled DNA content in TPBC cells (upper panels). Bar graphs show the percentage of TPBC cells in cell cycle phases (lower panel).* ***C.*** *Bar graphs show caspase 3/7 activity in TPBC cells determined by standard colorimetric assay under two growth conditions; RPMI medium supplemented by 10 % fetal bovion serum (FBS) or RPMI medium without FBS supplementation. ** P < 0.01, *** P < 0.001. Error bars represent SD.*

7.5.3 Levels of Cellular and Extracellular Metabolites

A large body of evidence emphasizes the importance of the utilization of metabolites for proliferation of tumor cells and for tumor growth (56, 57). Therefore, we investigated how ATGL loss might change cellular metabolism in our B-cell tumor model. We studied a number of metabolites using standard assays. In parallel to our work, Prof. Birner-Gruenberger's group from the MUG performed similar investigations on this tumor model using a more systemic approach: metabolic profiling.

Our IHC data on the PanIN lesions suggest that the reduction in ATGL levels in transformed epithelial cells occurs before the upregulation of GLUT1 expression (30). This might suggest that these cells increase the uptake of glucose to compensate the loss of ATGL. To test this hypothesis in our TPBC model, we compared the glucose uptake rate between *Atgl+/+* and *Atgl-/-* TPBC cells. Using a radioactive assay, we found that cells from the two genotypes uptake similar amounts of glucose (**Figure. 17A**). *Atgl+/+* TPBC cells took up more glucose than *Atgl-/-*TPBC, the difference was, however, not significant. We also measured glucose uptake after insulin stimulation. Glucose uptake in the cells of both genotypes remained unchanged with or without insulin stimulation (we expected an increase in glucose uptake rate after 10min of insulin stimulation). The results also show that *Atgl+/+* TPBC cells took up more glucose than *Atgl-/-*TPBC cells (**Figure. 17B**). However, we concluded from both experiments that the loss of ATGL in these cells does not affect glucose uptake rate significantly. Next, we decided to investigate whether FA uptake and incorporation differ between the two genotypes. For this experiment we incubated the cells with radioactive oleic acid and measured FA incorporation into lipid species using a standard thin-layer chromatography (TLC) method. No difference in oleic acid uptake rate was found and the concentrations of lipid species measured were similar in the two groups (**Figure. 17C, D**).

To investigate glucose utilization, we measured extracellular lactate and pyruvate concentration in cell culture. *Atgl-/-* TPBC cells secreted significantly less lactate and pyruvate than *Atgl+/+* TPBC cells (**Figure 18**).

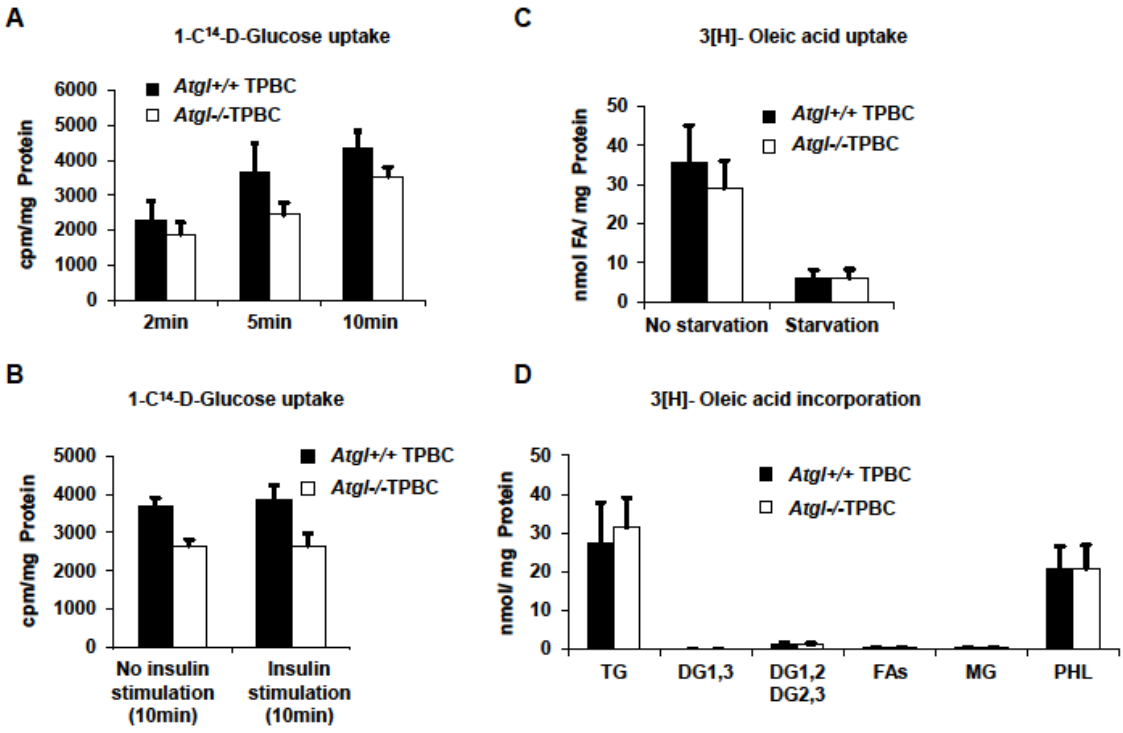

Figure .17 Radioactive measurement of 1- C14-D- Glucose uptake 3[H]-Oleic acid uptake and incorporation*. Bar graphs in (**A**) and (**B**) show that there is no significant difference in1- C14-D- Glucose uptake under normal culture conditions (**A**) and also after insulin stimulation (**B**). Surprisingly, there was only minimal increase in the rate of 1- C14-D- Glucose uptake after 10 minutes of insulin stimulation. **C**. Bar graphs show that cells from both genotypes of TPBC cells have a similar 3[H]-Oleic acid uptake rate. **D.** Bar graphs show that there was no difference in 3[H]-Oleic acid uptake incorporation into several lipid species. TG, triacylglycerol; DG, diacylglycerol; FAs, free fatty acids; MG, monoacylglycerol; PHL, phospholipids. Error bars represent SD.*

We measured also the oxygen consumption rate (OCR) and the extracellular acidification rate (ECAR). Results from two different platforms for OCR showed that *Atgl-/-* TPBC cells consume significantly higher amount of oxygen; OROBOROS Oxygraph-2k (**Figure. 19A**) and seahorse FX analyzer (**Figure. 19B**) were used. In addition, the ECAR rate was higher in *Atgl+/+* TPBC cell medium. Interestingly, the ECAR results are consistent with the OCR results and also with our extra cellular lactate measurements results. Collectively, these data suggest that *Atgl-/-* TPBC cells have the capacity to oxidize glucose better than *Atgl+/+* TPBC cells.

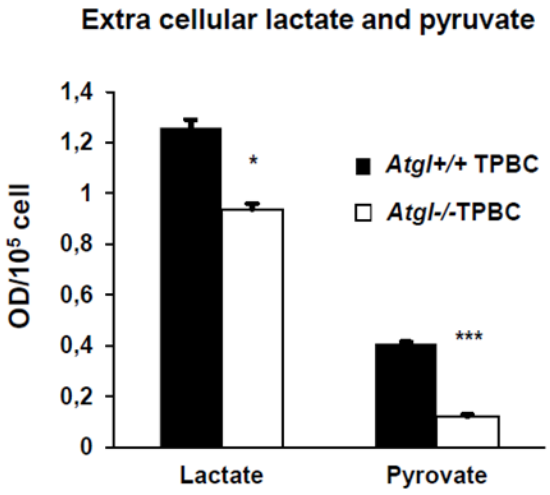

Figure .18 Measurements of extracellular lactate and pyruvate. *Bar graphs show levels of lactate and pyruvate secreted into medium by TPBC cells determined by standard colorimetric assays. Optical density (OD) values were normalized to OD values of the same type of medium kept under the same culture condition without cells. * P < 0.05, *** P < 0.001. Error bars represent SD.*

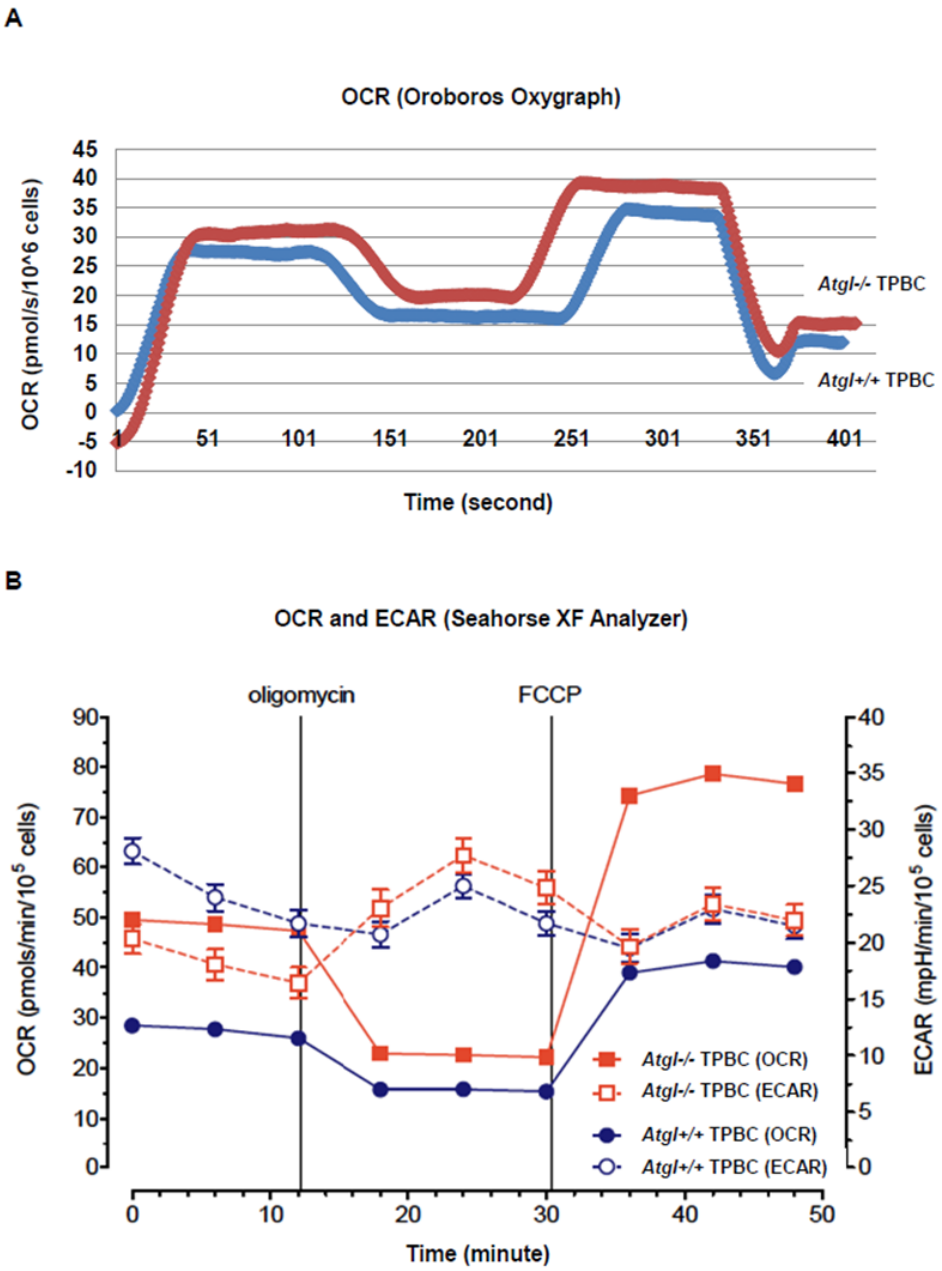

Figure .19 Extracellular oxygen and hydrogen concentration. A. *Oxygen consumption rate (OCR) measurements for one sample per group using the OROBOROS Oxygraph-2k instrument (this instrument has two chambers and therefore allows to compare (measure) the OCR for two samples simultaneously). We performed this experiment three times and all measurements showed similar pattern; OCR of Atgl-/- TPBC was higher than the OCR of Atgl+/+ TPBC.* ***B.*** *OCR*

and extracellular acidification rate (ECAR) measurements using the Seahorse XF-Analyzer. Atgl-/- TPBC have higher OCR and lower ECAR comparing to Atgl+/+ TPBC. Measurements during the first 12 minutes document the basal cell respiration. Measurements after oligomycin injection until 30 minutes document minimal cell respiration. After injecting carbonilcyanide p-triflouromethoxyphenylhydrazone (FCCP) –which uncouples the mitochondrial oxidative phosphorylation—measurements document the maximal respiration. We measured six samples per each group and repeated the experiment three times using the same cell line linages. These two experiments were performed with support from Prof. Wolfgang Graier at his lab and with the help from Dr. Lukas Groschner.

7.5.4 *In Vivo* Proliferation of TPBC Tumors

As previously mentioned, *Dr. T. K. Palaniappan* found that *Atgl-/-* TPBC cells forms larger tumors when injected subcutaneously into mice. These results were confirmed by several researchers, including the author. The work described here was performed mainly by the author in order confirm this result and to investigate possible mechanisms that led to this phonotype.

We injected subcutaneously a low number of TPBC cells (50.000) of the two genotypes into the same mouse at two different locations. Theoretically, these cells were growing under same macro-environment conditions from the host. As expected, we found that *Atgl-/-* TPBC cells develop larger tumor (**Figure. 20A**). In another experiment, we wanted to monitor the development of the injected cells into tumors. First, an ultrasound imaging devices was used at the “Institut für Biomedizinische Forschung” with the help of *Mag. Alexander Hofmeister* to measure tumor volumes. The device could not detect small tumors that formed 5-6 days after TPBC cell inoculation. In the second experiment we injected the TPBC cells into several mice which were later scarified at different time points. We evaluated tumor formation macroscopically and measured tumor volume after sacrificing the mice either microscopically for small tumors or by using a ruler for tumors that can be measured macroscopically. The results show that ATGL loss

enhances tumor growth as early as 6 days after tumor cell inoculation (**Figure. 20B**).

To extend these *in vivo* results, the TPBC cells were injected intravenously. This might better mimic the clinical behavior of ALL cells in patients. When injected intravenously, *Atgl-/-* TPBC cells caused severe lymphocytosis (**Figure. 20C**). All injected mice had high number of white blood cells (>16500/µ) while white blood cells counts in healthy mice vary between 2000 -10000/µl. Because the transformed B-cells (TPBC cells) are derived from precursors B-cells and represent small blast cells, it was expected that the cell counter identifies these cells as lymphocytes. Therefore, the increased numbers of lymphocytes determined by the blood cell counter indicates a higher number of *Atg-/-* TPBC cells in blood. Moreover, *Atg-/-* TPBC cells invaded the soft tissues adjacent to the bone marrow and infiltrated the liver after 12 days while *Atgl+/+* TPBC infiltration was restricted to bone marrow (**Figure. 20D**). Importantly, mice injected with *Atgl+/+* TPBC cells lived significantly longer than mice injected with the corresponding *Atg-/-* TPBC cells (**Figure. 20E**).

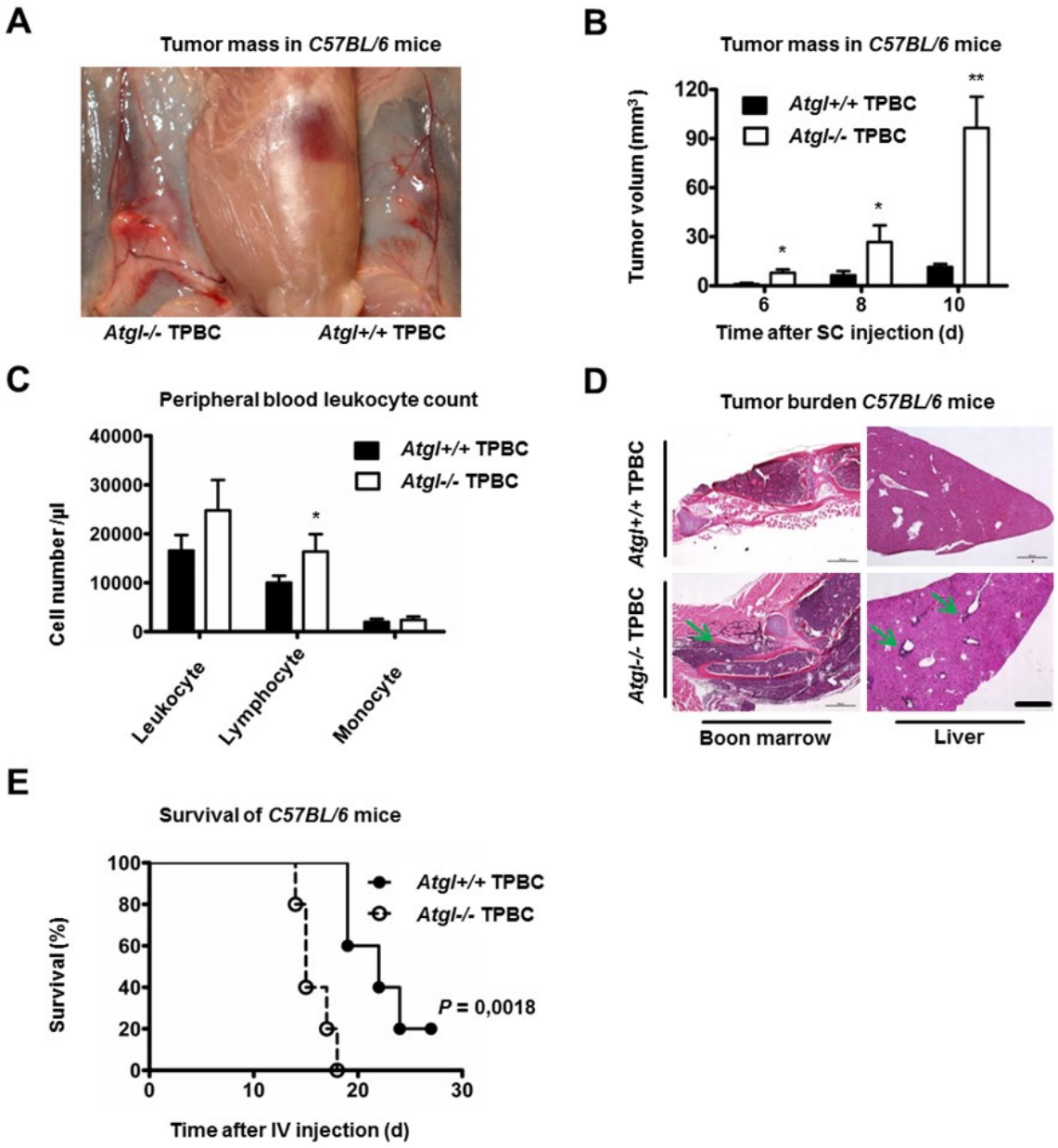

Figure .20 Ablation of ATGL enhances tumor growth and spread. A. *Macroscopic image shows tumor formation in C57BL/6 mouse injected with 50,000 Atgl+/+ TPBC cells on the left flank and 50,000 Atgl-/- cells on the right flank. Compared to the ATGL+/+ (wild type) tumor, the Atgl-/- TPBC tumor had a larger tumor mass and showed increased vascularization.* ***B.*** *Tumor volume after subcutaneous injection of 150,000 Atgl+/+ TPBC or Atgl-/- TPBC cells each in C57BL/6 mice. Mice were scarified at the time points indicated. Areas of injection were dissected and microscopically assessed for tumor formation and tumor*

*volume was calculated (n = 3-4). * P < 0.05, ** P < 0.01.* ***C.*** *Peripheral blood leukocyte count 12 days after intravenous injection of 50.000 Atgl+/+ TPBC or Atgl-/- TPBC cells each in C57BL/6 mice. (n = 5) * P < 0.05.* ***D.*** *Histological analysis of tumor cell infiltration in bone marrow and liver 12 days after intravenous injection of 50.000 Atgl+/+ TPBC or Atgl-/- TPBC each in C57BL/6 mice (n = 5). Green arrows highlight tumor cell infiltration. Scale bar, 50 µm.* ***E.*** *Kaplan–Meier survival analysis of C57BL/6 mice injected intravenously with 50.000 Atgl+/+ TPBC or Atgl-/- TPBC cells each and monitored for 28 days (n = 5). Median survival: Atgl+/+ TPBC = 22, Atgl-/- TPBC = 15. P value = 0.0018.*

7.5.5 Loss of ATGL Altered the Immune Response

Our data from the *in vitro* and the *in vivo* experiments indicate that ATGL is critical for controlling tumor cell proliferation and tumor burden in the TPBC tumor model. The influence of ATGL loss was more profound *in vivo* than *in vitro*, which suggests that ATGL might interact, directly or indirectly, with the tumor microenvironment.

To study the effect of ATGL loss on tumor microenvironment in the TPBC model, we evaluate histologically TPBC tumors for potential differences between *Atgl+/+* TPBC and *Atgl-/-* TPBC tumors using samples from the time course experiment described above. Inspection of critical components of the tumor microenvironment revealed that ATGL loss led to a significant increase in blood vessel formation and a decrease in T-cell infiltration compared to *Atgl+/+* tumors (**Figure. 21A, B**). These changes were independent of tumor size or time after tumor cell inoculation. We did not observe a significant difference in macrophage infiltration between *Atgl-/-* and *Atgl+/+* tumors. Knowing that T-cells play a critical role in the induction of antitumor immunity, one might expect that the antitumor immune response is not efficiently stimulated in *Atgl-/-* TPBC tumor bearing mice.

In agreement, levels of multiple mRNAs specifying proteins known to modulate immune response were decreased in *Atgl-/-* TPBC tumors. Expression profiling and subsequent functional analysis revealed that a significant number of genes

that encode proteins functionally related to innate and adaptive immune pathways were downregulated in *Atgl-/-* TPBC tumors (**Table. 3**). The numbers of genes which were upregulated in *Atgl-/-* TPBC tumors in those eight pathways were not significant (**Table. 3**). Because *Atgl-/-* TPBC tumors show only few infiltrating T-cells, it was not surprising that the T-cell activation pathway is among the deregulated pathways. Of note, the fact that the antigen processing and presentation pathway is deactivated in *Atgl-/-* TPBC tumors may indicate that *Atgl* ablation impaired, at least partially, the ability of *Atgl-/-* TPBC cells or infiltrating macrophages to processes and present antigens.

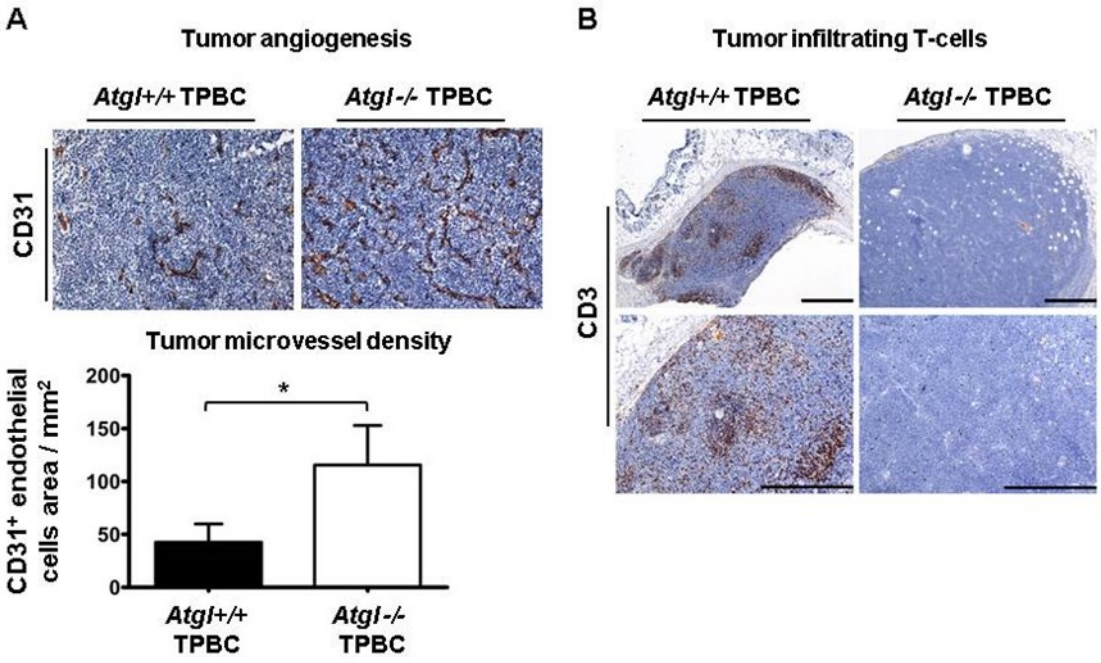

***Figure .21 Atgl-/- TPBC tumors elicit only a reduced tumor-induced immune reaction**. **A.** Immunohistochemical analysis of Atgl+/+ or Atgl-/- tumors using antibodies against CD31 highlighting endothelial cells. Representative microscopic images (upper panel) and quantification of the positive endothelial cells area at day 8 after subcutaneous inoculation of 150.000 Atgl+/+ or Atgl-/- TPBC each in C57BL/6 mice (n= 4). *P < 0.05. **B**. Immunohistochemical analysis of Atgl+/+ or*

Atgl-/- tumors with antibodies against CD3 highlighting T-cells. Representative microscopic images show infiltration of CD3 positive T-cells into tumors at day 8 after subcutaneous inoculation of 150.000 Atgl+/+ or Atgl-/- TPBC each in C57BL/6 mice (n= 4). Regions from upper panels are shown in higher magnification in lower panels. Scale bar, 50 µm.

Table 3: Functional analysis of affymetrix gene list

Pathway	# genes up in *Atgl-/-* tumors	p-value	# genes down in *Atgl-/-* tumors	p-value
Immune system process	18	1,00E+00	116	5,26E-28
Immune response	6	1,00E+00	69	1,42E-26
Antigen processing and presentation	0	1,00E+00	28	2,06E-12
Response to interferon-gamma	1	1,00E+00	18	5,99E-11
T-cell activation	0	1,00E+00	13	2,05E-06
Inflammation mediated by chemokine	2	1,00E+00	20	1,04E-05
Macrophage activation	3	1,00E+00	24	1,76E-06
Natural killer cell activation	2	1,00E+00	12	3,68E-04

[a] *Analysis of affymetrix gene expression profiles using the PANTHER (Protein ANalysis THrough Evolutionary Relationships) site. This analysis was performed by Karin Wagner from the molecular biology facility at the ZMF.*

[b] *The table lists number of genes which altered (≥ 1.5 fold or ≤ 1.5 fold) in the pathways indicated upon Atgl ablation.*

In accordance with this finding, we observed a loss of cells surface microvilli in *Atgl-/-* TPBC cells compared to *Atgl+/+* TPBC cells by transmission electron microscope analysis (**Figure. 22**). These microvilli structures exhibit high density of antigen presenting molecules and have been shown to play a role in presenting antigens (58). Quantitative polymerase chain reaction (qPCR) assays were performed on tumors to measure the levels of mRNAs of chemokines, chemokine (C-X-C motif) ligand 9 (CXCL9) and chemokine (C-X-C motif) ligand 10 (CXCL10), interferon gamma (IFNγ) cytokine, and protein kinase C theta (PKC theta)

because they are known to play central role in chemo-attraction and activation of T-cells, as well as in inhibition of tumor growth and angiogenesis (59-61). As expected, their mRNAs levels were significantly reduced (2-5-fold) in *Atgl-/-* TPBC tumors compared to control tumors (**Figure. 23**). Collectively, these data are consistent with the interpretation that *Atgl-/- TPBC* tumors do not stimulate strong antitumor immune response in *C57BL6* mice as compared to *Atgl+/+* TPBC tumors. This finding suggests that ATGL in the B-cell tumor model is important to stimulate the host immune defense against tumor cells.

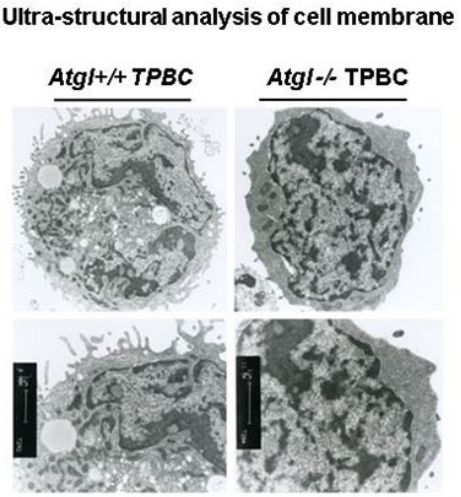

Figure .22 Ultrastructural analysis of the TPBC cells*. Transmission electron microscope images of Atgl+/+ TPBC or Atgl-/- TPBC cultured in vitro, showing the ultrastructure of cell membrane. Compared to Atgl+/+ TPBC shown here, Atgl-/- TPBC shows a decrease of the microvilli structures. Regions from the upper panels are shown in higher magnification in the lower panels.*

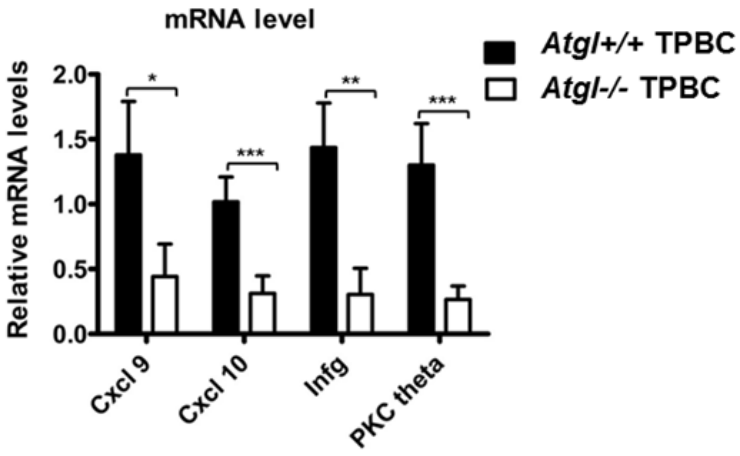

Figure .23 mRNA analysis in TPBC tumors. *Relative expression of the indicated genes, as determined by RT-PCR, in Atgl+/+ TPBC or Atgl-/- B-cell tumors at day 14 after subcutaneous inoculation of 150.000 Atgl+/+ TPBC or Atgl-/- bcr-abl transformed cells each in C57BL/6 mice (n= 4). * P < 0.05, ** P < 0.01, *** P < 0.001.*

Because the immune system is capable of suppressing tumor growth, we hypothesized that the impaired immune response observed against *Atgl-/-* TPBC tumors may contribute to the enhanced *Atgl-/-* TPBC tumors growth as compared with *Atgl+/+* TPBC tumors. To test this hypothesis, we pursued two strategies: First, we compared *Atgl+/+* TPBC and *Atgl-/-* TPBC tumor growth in control *C57BL6* mice (immuno-competent mice) and in three immune-deficient mice models that exhibit a severe combined immune deficient (SCID) phenotype. *NSG*, NOD scid gamma mice; *RAG2-/-*, Recombinase activating gene-2 knockout mice; *RAG2-/-/gamma (c)-/-*, RAG2/gammac double-knockout mice. *Atgl+/+* TPBC tumors grew to a significantly larger (5-10-fold) size in the three different immune-deficient mice strains compared to the one in immune-competent mice. In contrast, *Atgl-/-* TPBC tumor growth was similar (0.8-1.3-fold) in immune-deficient and immune-competent *C57BL6* mice (**Figure. 24A, B**). Second, we tested the antitumor effect of the immune response in *C57BL6* mice following the inoculation of a low number of transformed B-cells precursors. After 16 days, 3 out of 10 mice inoculated with *Atgl+/+* TPBC cells developed tumors whereas all mice, 5 out of 5, inoculated with *Atgl-/-* TPBC cells developed tumors already after 12 days post

inoculation (**Figure. 24C**). Additionally, *Atgl-/-* TPBC tumor size was again consistently up to 20-fold larger than *Atgl+/+* TPBC tumor size (**Figure. 24D**). Together, these results suggest that the enhanced *Atgl-/-* TPBC tumors growth seen in *C57BL6* mice, is at least in part due to the ineffective antitumor immune response. Thus, it could be concluded that *Atgl+/+* TPBC tumors elicit a more robust immune response in immune-competent mice than *Atgl-/-* TPBC tumors resulting in decreased tumor formation and growth. This difference is not seen in immune-deficient mice supporting the assumption that ATGL in B-cell tumor model is critically required to stimulate an effective antitumor immune response.

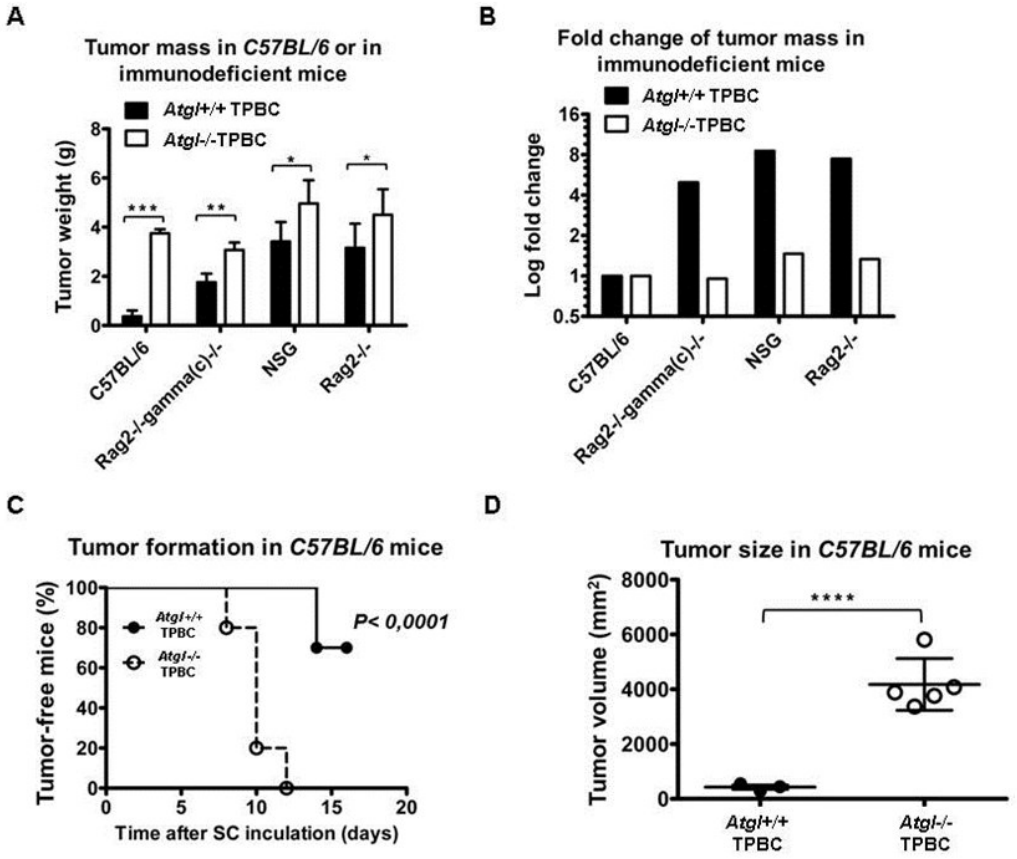

Figure .24 TPBC tumor growth in immunocompetent and immunodeficient mice. A. *Weight of tumors 14 days after subcutaneous inoculation of 150,000 cells of Atgl+/+ or Atgl-/- TPBC each in C57BL/6 mice (immunocompetent mice) or in immunodeficient mice of the genotype indicated (n= 4-5). *P < 0.05, **P < 0.01, ***P < 0.001. Results are combined from three different experiments.* ***B.*** *Bar graph shows log fold change in tumor mass of the tumors in (**A**); tumor mass of tumors that developed in immunodeficient mice is compared (normalized) to the mean of tumor mass of tumors —of the same genotype (Atgl+/+ or Atgl-/-) that developed in C57BL/6 mice.* ***C.*** *Tumor formation in C57BL/6 mice inoculated subcutaneously with 50,000 cells of Atgl+/+ or Atgl-/- TPBC each. All mice inoculated with Atgl-/- TPBC developed tumors (n= 5) whereas 30% of mice inoculated with Atgl+/+ TPBC developed tumors (n= 10).* ***D.*** *Tumor mass of the tumors in (**C**) at day 16 after inoculation. ****P < 0.0001. All error bars represent SD.*

7.5.6 Amino Acid Metabolism in TPBC Cells and Tumors

The previously described results from the immune-deficient mice show that *Atgl-/-* tumors were larger than *Atgl+/+* tumors. In addition, the difference in proliferation rate of the TPBC cells observed *in vitro* is independent from the anti-tumor immune response. These two facts point to another mechanism, or several mechanisms, that need to be understood to explain why *Atgl-/-* TPBC cells and tumors proliferate faster than the *Atgl+/+* controls *in vitro* as well *in vivo*.

In an attempt to find what factors are involved, we utilized the previously mentioned data from the gene expression array experiment. We found that mRNA levels of one gene that regulates glycine metabolism, glycine dehydrogenase (decarboxylating) (*Gldc*), is remarkably low in *Atgl-/-* TPBC tumors compared to *Atgl+/+* TPBC tumors. Because the RNA samples which were analyzed for this experiment have been extracted from implanted tumors in *C57BL6* mice, we validated the results by using the standard qPCR method on another set of samples from tumors which were implanted and prepared by the author. In addition, we compared the mRNA levels of *Gldc* between *Atgl+/+* and *Atgl-/-* TPBC cells *in vitro* by qPCR. Our results confirmed that *Gldc* mRNA levels are lower in *Atgl-/-* tumors *in vivo* and showed that *Atgl-/-* TPBC have lower levels than *Atgl+/+* TPBC *in vitro* as well (**Figure. 25A**). These data suggested that *Gldc* gene might be an interesting candidate for further investigations.

GLDC is a mitochondrial enzyme that is essential for glycine degradation. Patients with germline *GLDC* gene mutation have high glycine levels in the blood and suffer from nonketotic hyperglycinemia (62). It is reported that glycine and serine, the precursor of glycine, support purines biosynthesis in fast proliferation cells (57, 63). Because *Atgl-/-* TPBC cells have lower levels of *Gldc* mRNA, we hypothesized that these cells can better convert glycine and serine to generate purine nucleotides, providing a growth advantage to *Atgl-/-* TPBC cells and tumors. To test this hypothesis, we cultured the cells in media depleted from all non-essential amino acids, including glycine and serine. Interestingly, cells from the two genotypes proliferated at similar rate under this condition (**Figure. 25B**). Although in this experiment the cells were deprived from several non-amino acids and not only from glycine and serine, this preliminary result prompted us to study

the effects of lowering glycine levels on the *in vivo* tumor growth. Therefore, we treated mice bearing tumors of *Atgl+/+* TPBC or *Atgl-/-* TPBC with a chemical compound known to reduce serum glycine levels, sodium benzoate. The growth advantage of *Atgl-/-* TPBC tumors was abolished; *Atgl+/+* and *Atgl-/-* tumors were in the same weight range (**Figure. 25C**).

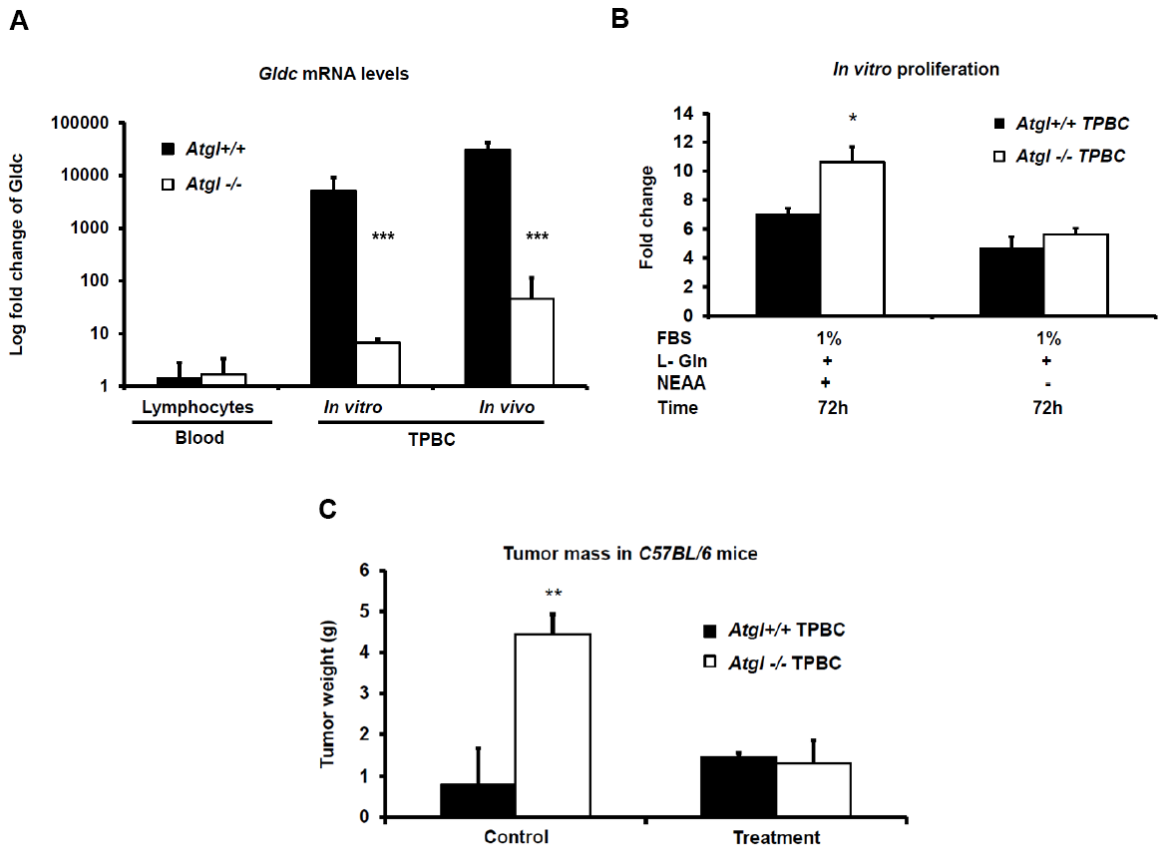

Figure .25 Potential role for GLDC in TPBC proliferation*. **A.** Gldc mRNA levels in peripheral blood lymphocytes isolated from Atgl+/+ and Atgl-/- mice, as well as in Atgl+/+ and Atgl-/- TPBC and tumors. **B.** Bar graphs show fold change in proliferation rate for TPBC when cultured under two different conditions. FBS, Fetal bovine serum; L-Gln, L-glutamine; NEAA, non-essential amino acids **C.** Tumor weight in mice treated with sodium benzoate, 0.5 mg/kg of body weight per day dissolved in drinking water, compared to control mice. Tumors were assessed*

*14 days after subcutaneous inoculation of Atgl+/+ or Atgl-/- TPBC. Sodium benzoate treatment started 2 days before the inoculation (n = 4). * P < 0.05, ** P < 0.01, *** P < 0.001. Error bars represent SD.*

7.5.7 Silencing of ATGL in Mouse Cell Lines

To study the effect of ATGL on tumor cell growth in an additional model system, we used B16-F10 melanoma (B16-F10) cell line –a tumor model for studying lung metastasis (64, 65) –and compared the *in vivo* systemic spread potential to the lungs. Partial *Atgl* downregulation by RNA interference (shRNA *Atgl*) resulted in enhanced spread potential of B16-F10 cells when compared to control cells (shRNA Ctrl) (**Figure. 26A, B**). This difference was observed when this experiment was repeated several times by other colleagues from our lab. Importantly, there was no difference in *in vitro* or *in vivo* proliferation rate between shRNA *Atgl* and shRNA Ctrl cells.

In another set of experiments, researchers from our lab used the same RNA interference technology to establish additional ATGL knock-down cells from the B16-F10 melanoma cell line. Studying these newly established cells showed no difference in the spread of the B16-F10 cells to the lung. Therefore it was not possible to conclude whether or not the reduction of ATGL levels in the B16-F10 cells has an effect on lung metastasis.

Colleagues from our lab and other labs silenced this enzyme also in different mouse cell lines such as Lewis lung carcinoma cell line and colon carcinoma cell line (CT26). The results were conflicting; in early experiments, it was observed that the loss of ATGL enhanced proliferation rate in culture and in mice. These results were not reproducible in later experiments. This can be due to several reasons mainly related to the cell culture conditions. However, it is possible that the loss of ATGL in immortalized tumor cell lines provides no growth advantage.

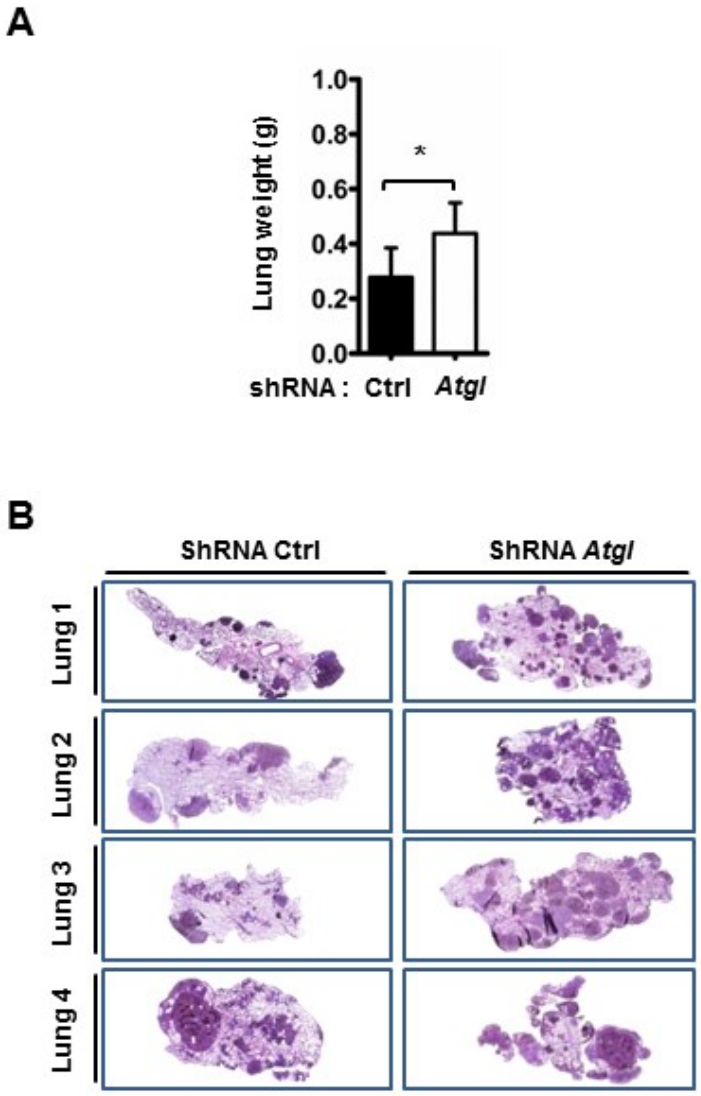

Figure .26 Downregulation of ATGL enhances B16-f10 cells spread. A. *Lung weight of C57BL/6 mice 16 days after intra venous injection with 1.5 x10^5 B16-F10 cells transduced either with shRNA Atgl (shRNA Atgl) or shRNA Ctrl. (n = 4). (shRNA Ctrl: Mean = 0.2775; shRNA Atgl: Mean = 0.4375; P = 0.0427). Error bars represent SD.* ***B.*** *Representative microscopic images of H&E stained sections show tumor nodules in lungs of C57BL/6 mice from (**A**).*

7.6 Spontaneous Tumor Development in *Atgl-/- ctg* Mice

Because ATGL levels in several human malignancies are reduced, and because loss of ATGL in a B-cell tumor model resulted in enhanced tumor progression and reduced immune recognition, we investigated whether ATGL loss is also associated with a higher risk of *de novo* tumor development in aged mice using a mouse model.

Atgl-/- mice die early in life due to cardiac failure (10, 34). Therefore, we investigated *Atgl+/+, Atgl+/-* and *Atgl-/-* mice, from *C57BL6* background, which expresses *Atgl* in cardiac muscles and have longer life expectancy (34). Hereafter, we refer to these mice as *Atgl+/+* ctg*, Atgl+/-* ctg and *Atgl-/-* ctg. We examined tumor development in several organs. We found an increased occurrence of lung tumors in *Atgl-/-* ctg mice at high frequency. The loss of both *Atgl* alleles in lung epithelium of *Atgl-/- ctg* mice resulted in the development of multifocal lung epithelial neoplastic lesions in mice within the first three months. Comparing with control mice the difference was, however, not significant (**Figure. 27A, B** and **table. 4**). Of note, however, none of the *Atgl+/+ ctg* or *Atgl+/- ctg* mice developed neoplastic lesion in the lungs. It is important to consider that age is a critical factor in neoplastic transformation and tumor development processes, especially in epithelial tumors (66).

Indeed, after three months of age, the difference in formation of neoplastic foci was highly significant. All *Atgl-/- ctg* mice older than six months (7-30 months) developed extensive neoplastic lesions, and importantly, these neoplastic lesion further developed into invasive adenocarcinomas (**Figure. 27B, C** and **Table 4**). We found invasive tumors in lung samples from 5 out of 20 *Atgl -/- ctg* mice that were older than 10 months. We did not detect any distant metastases and none of the invasive tumors has become lethal.

We also observed a number of neoplastic lesions and invasive tumors in *Atgl+/- ctg* mice. The frequency was lower than the frequency in *Atgl-/- ctg* mice and the neoplastic lesions formed later in life (**Figure. 26B**). We detected adenocarcinoma in 4 out of 21 *Atgl+/- ctg* mice that were older than 10 months.

Only two neoplastic lesion were found in *Atgl+/+ ctg* mice (22 mice) older than 10 months (**Figure. 27B** and **table. 4**). and no lung adenocarcinoma were detected at any age–which is consistent with the reported fact that the *C57BL6* mice strain is resistant to spontaneous lung tumor development (37, 67).

We also examined lung tumor development in *C57BL6* mice treated with nitrosamine 4-(methyl-nitrosamino)-1-(3-pyridyl)-1-butanone (NNK). NNK is a compound found in tobacco leaves and known to induce high rate of lung tumorigenesis in *A/J* mice (38). In our experiment, we did not observe a significant increase in lung tumors in *C57BL6* mice and therefore our data suggest that NNK has no histo-morphologically detectable effect that is associated with lung tumor development in this mice strain (*C57BL6)* in contrast to *A/J* mice.

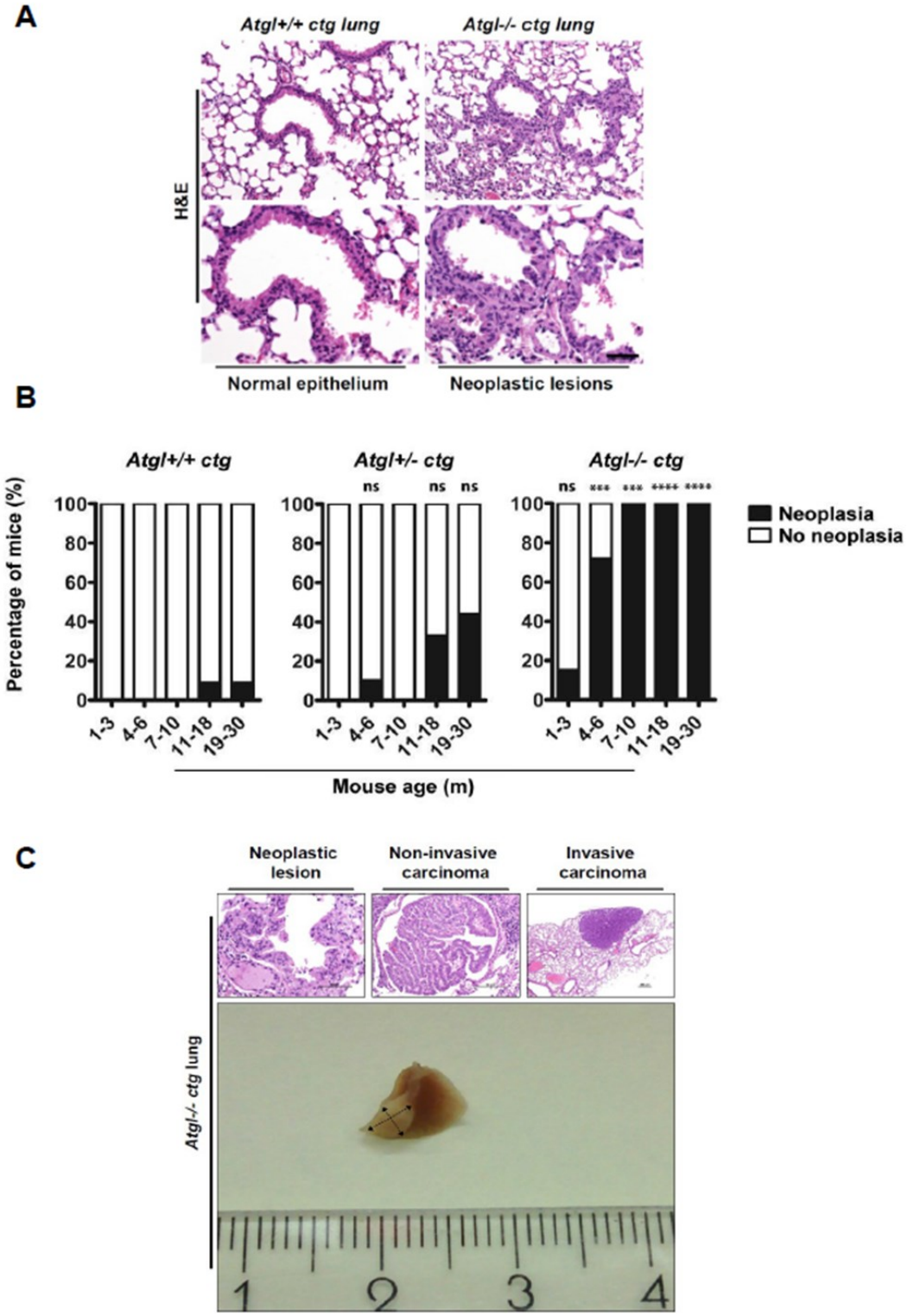
A
Atgl+/+ ctg lung
Atgl-/- ctg lung
H&E
Normal epithelium
Neoplastic lesions
B
Atgl+/+ ctg
Atgl+/- ctg
Atgl-/- ctg
Percentage of mice (%)
ns
***
****
Neoplasia
No neoplasia
1-3
4-6
7-10
11-18
19-30
Mouse age (m)
C
Neoplastic lesion
Non-invasive carcinoma
Invasive carcinoma
Atgl-/- ctg lung

Figure .27 Loss of ATGL results in spontaneous lung tumors. A. *Histopathological analysis of intraepithelial neoplastic lesions in lungs of Atgl+/+ ctg and Atgl-/- ctg mice. Representative microscopic images show early neoplastic lesions in Atgl-/- ctg mice compared to morphologically normal lung epithelium in Atgl+/+ ctg mice. Representative regions are shown at higher magnification in the lower panels.* ***B.*** *Bar graphs show the percentage of mice in which one or more pulmonary neoplastic lesions were detected. Atgl+/+ ctg mice, (n = 50); Atgl+/- ctg mice (n = 49); Atgl-/- ctg mice (n = 49).* ***C.*** *Representative microscopic images (upper panels) display three consecutive stages (from left to the right) of lung tumor development in Atgl-/- ctg mice. In old mice lung tumors can be even detected by macroscopic examination (lower panel). We did not detect lung adenocarcinoma in any of the mice from the three genotypes that were younger than 10 months. In mice older than 10 month, no lung adenocarcinoma were detected in Atgl+/+ ctg mice (n = 22). Out of 20 Atgl-/- ctg mice, we detected adenocarcinoma in 5 mice (P value = 0.0182). We also detected adenocarcinoma in 4 out of 21 Atgl+/- ctg mice (P value = 0.0485). ***P ≤ 0.001; ****P ≤ 0.0001*

Table 4: Number of animals with neoplastic lesions detected in lungs of *Atgl+/+ ctg*, *Atgl +/- ctg* and *Atgl -/- ctg* mice

Age group (months)	Number of animals with pulmonary neoplasia Neoplasia/Total[(Statistical significance)]		
	Atgl +/+ ctg	***Atgl +/- ctg***	***Atgl -/- ctg***
1-3	0/8	0/13 [(ns)]	2/13 [(ns)]
4-6	0/10	1/10 [(ns)]	8/11[(***)]
7-10	0/10	0/5 [(ns)]	5/5 [(***)]
11-18	1/11	4/12 [(ns)]	12/12 [(****)]
19-30	1/11	4/9 [(ns)]	8/8 [(****)]

[a] ***ns*** *P > 0.05; ***P ≤ 0.001; ****P ≤ 0.0001.*

[b] *Frequency of neoplasia in Atgl+/- ctg or Atgl-/- ctg mice is compared to frequency of neoplasia in Atgl+/+ ctg mice.*

ATGL IHC showed that ATGL is expressed in human bronchial lung epithelium and, therefore, we expected that ATGL is also expressed in bronchial epithelium of mouse lungs. For technical reasons, we were not able to establish ATGL IHC detection in mouse tissues. Therefore we tested whether ATGL plays a role in lipid homeostasis in these particular epithelia cells. We stained lung frozen section with Oil Red O stain, a lipid soluble dye that is widely used to stain neutral lipids. Our results indicate that bronchial epithelial cells from *Atgl-/- ctg* mice have profound lipid accumulation as visualized with Oil Red O staining compared to control cells in *Atgl+/+ ctg* mice which show no microscopically detectable Oil Red O staining (**Figure. 28A**). To gain better insight into what type of lung bronchial epithelial cells exhibit lipid accumulation, we examined lung sections by using a transmission electron microscopy. First, we observed that lipid droplets are only found in epithelial cells from *Atgl-/- ctg* mice — which confirms the results from the Oil Red O experiment—and secondly, we found that only non-ciliated cells show lipid droplets (**Figure. 28B**). This strongly suggest that lipid homeostasis in these cells is disrupted upon the loss of ATGL providing an indirect evidence that indeed ATGL is an essential metabolic enzyme for regulating homeostasis in non-ciliated bronchial epithelial cells.

A

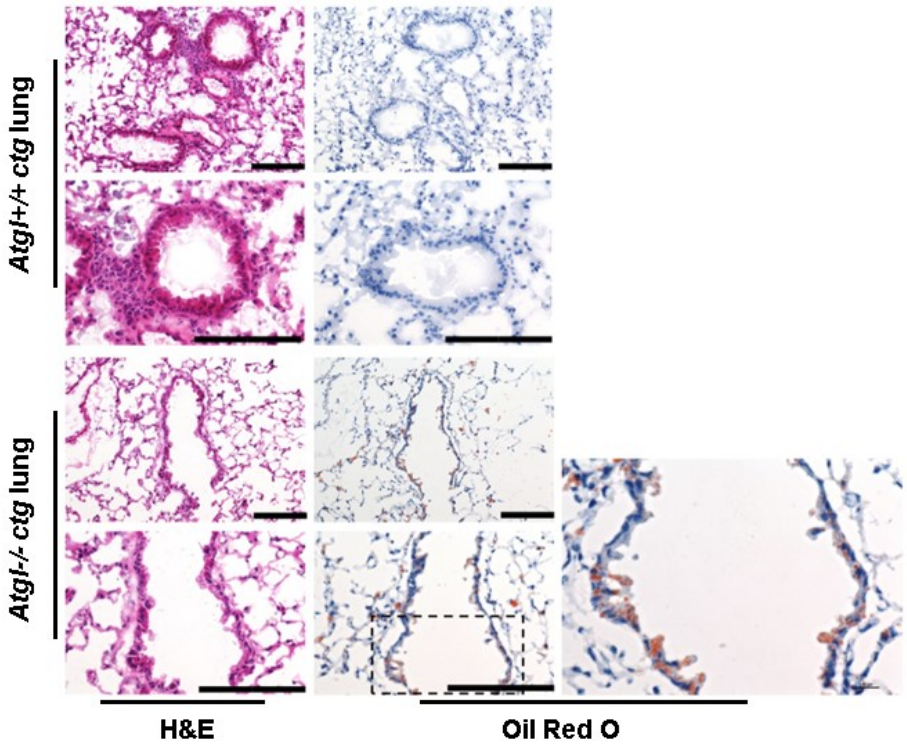

B

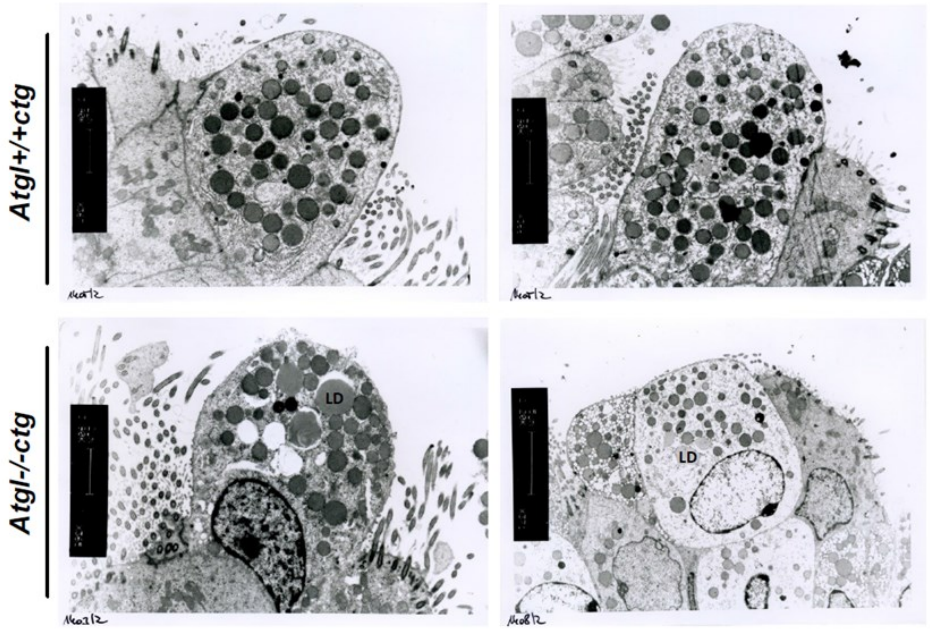

***Figure .28 Accumulation of neutral lipids in ATGL deficient bronchial epithelial cells**. **A.** Representative microscopic images show H&E and Oil Red O staining of lung sections. Bronchial epithelium of Atgl-/- ctg mice stains positive for Oil Red O whereas bronchial epithelium of Atgl+/+ ctg mice is negative. Regions from the upper panels are shown in higher magnification in the lower panels. Scale bar, 100µm. **B.** Representative electron-microscopic images of lung epithelium. Lipid droplets (LD) are only seen in non-ciliated cells from Atgl-/- mice. Images were captured at 365X magnification.*

Almost all neoplastic lesions detected at early stages in *Atgl-/- ctg* mice were formed at the terminal bronchioles. This suggests that epithelial cells at this anatomical location of the bronchial tree are the origin of the neoplastic lesions. Because we observed lipid accumulation in the non-ciliated cells at the same location, it is possible that ATGL has a crucial role for cellular homeostasis regulation in these cells which give rise to the observed neoplastic lesion and, subsequently, invasive tumors. Therefore, the disruption of the cellular hemostasis shown in *Atgl-/- ctg* could thus be a key event in promoting multifocal expansion of the bronchial epithelial cells as indicated by the observed neoplastic lesions. Subsequently, accumulations of additional genetic and metabolic alterations might occur in a number of cells that result in invasive lung tumors in these mice. Several additional studies are necessary to confirm our hypothesis, in particular to investigate in detail the molecular changes involved. However, our results clearly show that loss of ATGL increased the risk of lung tumor development in a time- and gene-dose dependent manner.

8 Discussion

Altered cellular metabolism has been recognized as one of the hallmarks of tumor cells and is emerging as a therapeutic target, yet further understanding of the metabolic differences between normal and cancer cells is the key for success in developing novel therapeutic approaches. In this work, we first identify a previously undescribed difference in the lipolytic pathway in cancer cells, and second we provide evidence for a novel function of ATGL, the principal enzyme in TG lipolysis, as metabolic tumor suppressor. Although the detailed mechanisms are still unclear, our work will have broad implications for the field of cancer metabolism.

The observation that cancer cells exhibit a high rate of glycolysis under normal concertation of oxygen has led to decades of research that resulted in the current knowledge about cancer metabolism (11). Several studies showed that cancer linked proteins involved in tumor development and progression are indeed dysregulated metabolic enzymes (12, 13). Recent work revealed that mutant forms of metabolic enzymes play a role in tumor formation and growth. Moreover, other investigations suggested that cancer cells switch on a number of catalytic enzymes in glycolysis cascade to promote rapid tumor growth (18, 19). Interestingly, tumor specific metabolic changes have become a target in cancer therapy. Studies on this flied not only helped for better understanding of tumor metabolism, but also rose up the fact that altered metabolism in tumor cells is crucial for cancers progression; altered metabolism is currently considered one of the hallmarks in cancer (14).

Unlike glucose metabolism, lipid metabolism has only recently been established as a research focus in tumor metabolism (3). Cancer cells use *de novo* synthesis of fatty acids to fulfill their requirement of lipids for biosynthesis of macromolecules (22). This induction of lipogenesis is mainly regulated by the PI3K/Akt/ mTORC1 pathway (24, 68). Yet, little is known about how lipolytic pathway is altered in proliferating tumor cells (4). Few studies showed that MGL plays a role in tumor growth (69-71). Whether MGL promotes tumor development (69, 71, 72), or has a tumor suppressive function is still not clear (70). Because cancer cells mostly rely

on *de novo* FAs synthesis rather than on hydrolyzed FAs, it is unlikely that the role of MGL in cancer growth is directly linked to the availability of intra cellular FAs. It is possible that the loss of MGL mostly has an effect on intracellular lipid signaling and signal transduction. Therefore, it is most important to study the intracellular lipolytic pathway by investigating the role of other lipases in cancer development.

ATGL is the rate limiting enzyme in the intracellular lipolysis. Consequently, the loss of ATGL function has various pathological consequences in several organs and tissues. *Atgl-/-* mice die at age of 14-18 weeks due to impaired FAs beta-oxidation in cardiac muscle (10, 34). In humans, the discovery that mutation in *PNPLA2* gene (the gene encoding human ATGL) causes neutral lipid storage disease with myopathy (NLSDM) and cardiomyopathy, helps to better understand the etiology and pathogenesis of these diseases (34, 39-41, 45-47, 73). Together, these reports confirm the importance of ATGL in cellular homeostasis of normal tissue. To our knowledge, this is the first study showing that ATGL expression is differentially regulated in human cancer and investigates a potential role for this enzyme *in vitro* and *in vivo* tumor models, as well in animal models.

Our results revealed a relationship between ATGL expression and cellular proliferation and differentiation. In healthy tissues, ATGL is more abundant in differentiated cells than in proliferating ones. Because ATGL is essential for providing FAs for ß-oxidation, and thereby providing energy for serval cellular function, it was not surprising that this enzyme is expressed in several types of tissues with active lipid metabolism and not only in adipocytes. It was also not surprising that highly differentiated cells like cardiomyocytes and muscles have high ATGL concentration since these cells require permanent mobilization of FAs to perform the desired function. Interestingly, cardiomyocytes and skeletal muscle are tissues that lack self-renewal capability and are terminally differentiated. These cells are in G0 phase and are not able to divide or enter the G1 phase (74). In contrast, cells with a short lifespan (days) that have the ability for rapid self-renewal, show low levels of this enzyme. In fact, these levels were so low that we were not able to document a specific IHC signal when the tissues were labeled by ATGL antibodies. The data we obtained from the human map indicate that fetal organs have undetectable ATGL expression. It is known that cells in fetal organs

exhibit a high rate of cell cycle activity which in turn is reduced during the development (75).

Recently, a number of studies demonstrated a relation between cell cycle regulation and the requirement for precise control of lipolysis. In two studies it was shown that ATGL activity is reduced by the G0/G1 switch gene 2 (G0S2) during the transition of cells between G0 and G1 phase of the cell cycle (76, 77). But on the other hand, triacylglycerol lipase (Tgl4), the functional ortholog of ATGL in yeast, is shown to be required for cell cycle progression in another study (78). Our data are indeed in line with the first two studies and I think that cell cycle regulation in mammalian cells is more complex than in yeasts. The *in vitro* studies on ATGL expression during 3T3-L1 cells differentiation into fully differentiated adipocytes are consistent with our observation in human tissues. ATGL protein is not detectable in proliferating 3T3-L1 cells and it is induced only on day three of differentiation; the cells at this time point are not proliferating (79). Based on our results and these studies, it is possible to establish a relationship between ATGL levels and the cell differentiation statutes.

We documented also multiple lines of evidence that ATGL loss is associated with the development of human cancers. The importance of this finding is highlighted by the broad range of human malignant tumors that show loss of ATGL. Our immunohistochemical analysis shows that AGTL protein is severely reduced or absent in non-small cell lung cancer and adenocarcinoma of the pancreas, as well as in malignant smooth muscle tumors. Expression data from the TCGA indicate that *ATGL* mRNA reduction is highly significant in invasive carcinoma of the breast, lung as well as of the head and neck compared to respective normal tissues. Low levels of *ATGL* mRNA correlate with significantly reduced survival in patients with ovarian, breast and gastric cancers. And, moreover, copy number variation data indicates frequent deletions of the *ATGL* gene in various forms of human cancers.

The loss of ATGL in human cancer may have a diagnostic application. Our data show that ATGL protein expression levels are low to undetectable in three tumor entities compared to normal tissues and that this is highly significant. Therefore, ATGL IHC can be considered as a potential histological tool that can complement

other morphological criteria and immunohistchemical markers to discriminate between normal tissues that express ATGL and cancers arising from these tissues. For example cancer cells originating from smooth muscle cells have no ATGL expression whereas normal cells and cells from benign smooth muscle tumors express high levels of ATGL. This remarkable difference in ATGL protein expression between benign and malignant can be ideal application for ATGL IHC, especially when dealing with small fragmented biopsies, where the standard criteria for distinguishing benign from malignant smooth muscle tumor cannot be applied. To establish ATGL IHC as a routine diagnostic marker, confirmatory data from several other labs are needed to validate the methods.

We do not provide data regarding the mechanism(s) by which the levels of this enzyme are reduced in cancer tissues. However, the finding that cancer cells have low ATGL levels may be deduced based on our current knowledge about the regulation of ATGL in normal tissues. The master catabolic enzyme AMP-activated protein kinase (AMPK) enhances ATGL hydrolase activity (80) and the transcription factor forkhead box O1 (Foxo1) directly stimulates ATGL expression (79, 81). In contrast, the phosphoinositide 3-kinase (PI3K/Akt/ mTORC1) pathway not only induces lipogenesis but inhibits the main two TG lipases: ATGL and HSL (82).

AMPK functions as a sensor for energy and regulates cytosolic ATP levels and thereby this kinase is involved in several metabolic pathways. Recent work from several research groups linked AMPK to cancer suggesting that it functions as a metabolic tumor suppressor protein (83). Because AMPK is dysregulated in many cancer types, including lung cancer, it is possible that ATGL activity in cancer cells is also reduced as a consequence. It will be interesting to investigate a potential relation between ATGL regulation and AMPK activity in cancer tissues and cells. The second important regulator for ATGL is FOXO1 which is also considered as a tumor suppressor protein (84). FOXO1 belongs to forkhead transcription factors and regulates transcription of many genes that controls cell proliferation and cellular metabolism, including the *ATGL* gene. Because FOXO1 levels are reduced in many tumor tissues, it is not surprising that the levels of downstream target genes are also downregulated. We think that the loss of FOXO1 in pancreatic epithelium (data are not shown) might contribute to the observed low

levels of ATGL in this particular cancer type. Further work is still needed to study how FOXO1 is altered in non-small lung cancers and smooth muscles tumors to extend this observation.

While proteins with “anti-tumor” effects, such as AMPK and FOXO1, can positively regulate ATGL levels and activity, pathways known to be activated during tumorigenesis and support tumor growth are able to negatively regulate lipases. Large number of experimental studies support the notion that PI3K/Akt/ mTORC1 is an essential metabolic pathway for regulating cellular metabolism to support uncontrolled tumor cell proliferation. In addition to activating the lipogenic pathway, the PI3K/Akt/ mTORC1 signaling pathway has been recently implicated in the negative regulation of lipolysis; ATGL and HSL levels were inhibited by mTORC activation in 3T3-L1 adipocytes (82). The author performed preliminary experiments to validate these results in our lab by over expressing the Ras homolog enriched in brain (RHEB). Our preliminary results (data not shown) were in line with the reported data. However, these data need to be confirmed. Nevertheless, all the later reports suggest that ATGL is not required for cancer cells to proliferate and survive and that several players are involved in the regulation of ATGL levels.

In agreement with this hypothesis, we found that ablation of ATGL increased the tumor cell proliferation rate *in vitro* and tumor growth rate *in vivo*. In an experimental B-cell lymphoma mouse model, *Atgl-/-* TPBC cell number was higher than control cells under standard cell culture conditions. The higher number of cells can theoretically be due to several factors include a) an increased proliferation rate; and b) a decrease in the rate of apoptosis in *Atgl-/-* TPBC cells. We did not detect a significant difference in the rate of apoptosis between the both genotypes, rather we noticed that *Atgl-/-* TPBC cells have slightly higher apoptotic rate than *Atgl+/+* TPBC cells arguing against the second possibility. To determine whether or not *Atgl-/-* TPBC cells exhibit a higher proliferation rate *in vitro* we performed two cell cycle analysis experiments. Our data indicate that loss of ATGL in TPBC cells facilitated the S phase entry enabling *Atgl-/-* TPBC cells to proliferate faster. We expected that the increased rate of S phase entry is due to, or at least is associated with, an increase in glucose or FAs uptake. However, our results show that there was no increase in the uptake rate of these two energy

sources by *Atgl-/-* TPBC cells. Further analysis of other metabolites showed that OCR is higher in *Atgl-/-* TPBC cells and that these cells secret less lactate and pyruvate. Nevertheless, these data indicate that the loss of ATGL promotes cell cycle progression in this mouse model.

In vivo, the difference in tumor weight between *Atgl-/-* TPBC and *Atgl+/+* TPBC tumors was high –up to 10 fold. Unlike in the *in vitro* systems, *in vivo* tumor growth is a complicated process because of the interaction between tumor cells in one side and many factors related to both, tumor microenvironment and tumor macro-environment from the host side. In addition, tumors are composed of tumor cells and other cells, such as stromal and endothelial cells, as well as inflammatory cells. To estimate proliferation and apoptosis rate in these tumors we performed IHC for Ki67 and Caspase3. We did not detect a significant difference. To extend our analysis on these tumors beyond tumor cells, we analyzed components from the tumor microenvironment. Here we could see an interesting phenotype; *Atgl-/-* TPBC tumors show an increased blood vessel formation and a profound decrease in infiltrating T-cells compared to *Atgl+/+* TPBC tumors. This phenotype suggests that the microenvironment plays a role in the observed growth difference, in that, *Atgl-/-* TPBC cells were able to escape the tumor immune surveillance. Data from a gene expression array performed at our lab further supported this hypothesis.

To confirm the role of the immune system in the observed tumor growth difference, we implanted TPBC cells in three different immune deficient mice strains. Although *Atgl-/-* TPBC tumors have higher tumor weight –the difference in tumor weight is significantly reduced in immune deficient mice. This result provides evidence that indeed the loss of ATGL in the TPBC tumor model impaired, at least to a degree, the ability of the host immune system to reduce tumor growth rate. Until now, it is not clear how the loss of ATGL might affect the immune recognition. Our preliminary data points to a structural defect in *Atgl-/-* TPBC cells. This observation still needs to be confirmed and further studied. Nevertheless, we can conclude from our *in vivo* and *in vitro* results that the loss of ATGL in this tumor model enhances tumor proliferation and growth.

The results obtained from studying changes on TPBC cell and tumors proliferation upon manipulating the metabolism of the non-essential amino acids, glycine and

serine, *in vitro* and *in vivo* might open interesting questions regarding the interaction between cellular lipid and protein metabolism pathways. The result that sodium benzoate (SB) reduced only *Atgl-/-* TPBC tumor growth needs to be confirmed by other researchers using several cell linages of TPBC cells. In addition, it would be very interesting to study how amino acids metabolism is changed in the media of TPBC cells as well as in the serum of TPBC tumor bearing mice, upon several conditions including sodium benzoate treatment. Our preliminary data show that SB altered the concentration of several non-essential amino acids in the serum of TPBC tumor bearing mice. An important note here is finding the optimal method to normalize serum values since the mice have different tumor volumes and body weights. The second limitation is that the measurement was performed once from samples obtained at the end of the experiment. Monitoring how serum values for the non-essential amino acids change during the course of the experiment will provide more accurate results. I think it is also important to study how SB treatment might affect anti-tumor immune response against TPBC tumors. This can help to clarify whether or not the effect of SB is independent of the suppression effect of the anti-tumor immune response.

To independently verify the role of ATGL in tumor development and mainly in tumor initiation, we assessed the risk of spontaneous tumor development in a mouse mode that lack ATGL in all tissues except the heart. Our results show a significant increase in lung tumor development upon the genetic ablation of *Atgl*. It is worth mentioning that I do not have an explanation why the deference in tumor development is only seen for lung tumors. We did not find a significant increase in the development of other tumor types in these mice. In a small number of *Atgl-/- ctg* mice we were able to identify tumors in the liver as well as lymphoid tumors. Because the incidence of these tumors were low, it was not possible to extract a conclusion. Future work to investigating a larger number of mice might be important to address this point. Since the immune system is an important player in lung tumor development and progression (85), and because we have an evidence that *Atgl-/-* loss impaired the anti-tumor immune response in the TPBC cells, it is conceivable that the increased lung tumor occurrence detected in *Atgl-/-* ctg mice is a consequence of both increased proliferation and defective anti-tumor immune response. However, at present no data exists that tumor immune surveillance

plays a role in the development of the documented lung tumors in *Atgl-/- ctg mice*. This hypothesis and other possible underlying mechanisms are being investigated by researchers in our group.

To further investigate the role of ATGL in lung tumor development in mice, it might be essential to design a set of experiments to answer the following two questions: I) is the increased occurrence of neoplastic lesions linked to the well-known function for ATGL as lipase?; II) is it possible that this enzyme may have another— yet unidentified—function in regulating cell cycle?

We clearly show that broncho-epithelial cells have a disrupted lipid metabolism as evidenced by the accumulation of lipid droplet in these cells which do not store lipids under physiological conditions. This raise two possibilities: a) first, it is possible that the accumulated intracellular lipids in lung epithelium is the driving metabolic event that initiate or provoke transformation of broncho-epithelial cells to neoplastic cells; b) second, the disrupted lipid metabolism is associated with the loss of ATGL but has no essential role in transforming the cells, rather it is another molecular event linked to ATGL reprograms these cells and is waiting to be discovered.

Whether it is one of the two events initiates the development of the lung neoplastic lesions or a combination of both, it is clear that our data from the *Atgl-/- ctg+* mice and their littermates provide proof that ATGL contributes to the suppression of lung tumor formation in mice suggesting that ATGL may also contribute to suppress human tumors. Indeed, the human *ATGL* gene is located in the gene region 11p15.5. Alterations in this region have been implicated in a broad variety of childhood and adult malignancies including non-small cell lung cancer and, therefore, it is considered to be an important tumor-suppressor gene region (86-92). Consequently, loss of *ATGL* located in the tumor suppressor region, may therefore represent a critical event during tumor formation (**Figure. 29**).

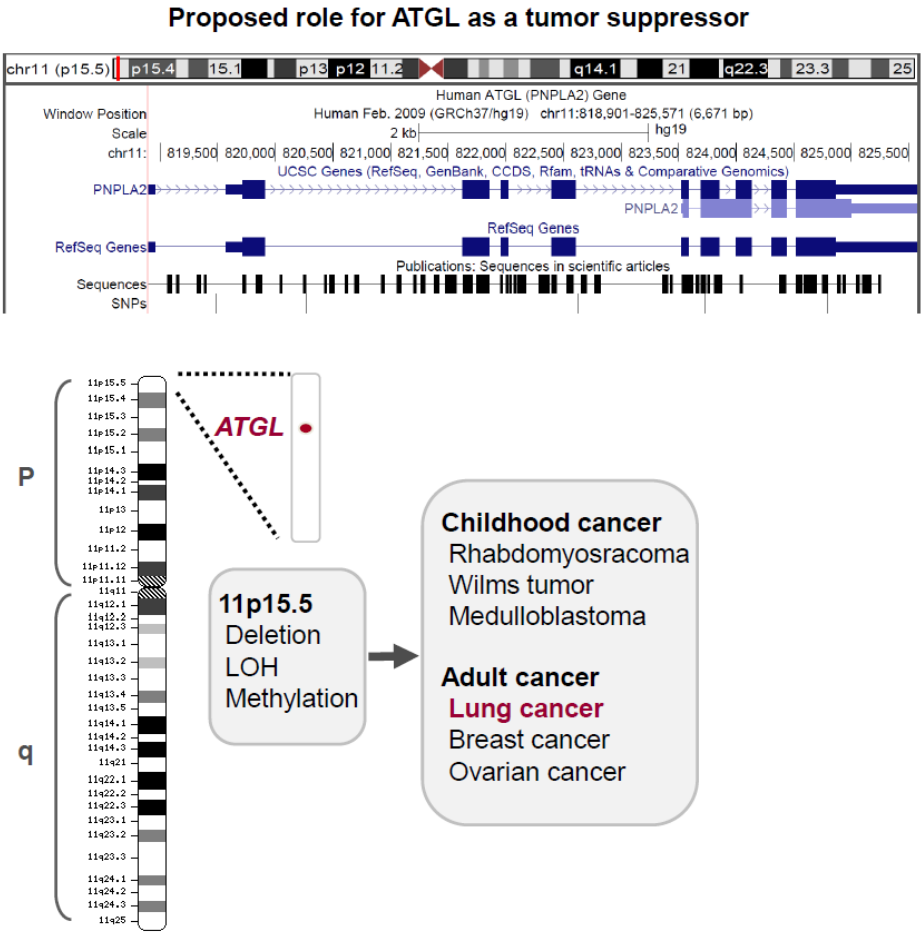

Figure .29 Proposed tumor suppressive function of ATGL*. Schematic representation of chromosome 11 illustrates the location of the human ATGL gene in the tumor suppressor region, 11p15.5, and human cancers associated with somatic alterations in this region. The figure was generated based on data from the UCSC Genome Browser.*

We conclude that the essential lipolytic enzyme in TG hydrolysis, ATGL, carries out a tumor suppressive function. Tumor suppressor proteins control cellular growth and proliferation, and –as the name indicates— suppress tumor formation and development. Inactivation of these proteins leads to uncontrolled cell division. Several lines of evidence support our conclusion. First, ATGL expression is positively correlated with cell differentiation status and inversely correlated with proliferation potential of the cells. Second, various types of human epithelial and mesenchymal tumors display undetectable ATGL protein levels, low *ATGL* mRNA levels, and deletion of the *ATGL* gene. Third, the loss of this lipolytic enzyme in tumor model leads to an increased proliferation rate *in vitro* and tumor growth rate *in vivo*. Fourth, genetic ablation of *Atgl* in mice leads to spontaneous formation of lung adenocarcinomas. Finally, the human *ATGL* gene lies within an important tumor suppressor region of chromosome 11. Thus, this work identifies a novel function for ATGL as a metabolic tumor suppressor protein.

9 References

1. Al-Zoughbi W, Huang J, Paramasivan GS, Till H, Pichler M, Guertl-Lackner B, et al. Tumor macroenvironment and metabolism. Seminars in oncology. 2014;41(2):281-95.
2. Zimmermann R, Strauss JG, Haemmerle G, Schoiswohl G, Birner-Gruenberger R, Riederer M, et al. Fat mobilization in adipose tissue is promoted by adipose triglyceride lipase. Science (New York, NY). 2004;306(5700):1383-6.
3. Prentki M, Madiraju SR. Glycerolipid metabolism and signaling in health and disease. Endocrine reviews. 2008;29(6):647-76.
4. Zechner R, Zimmermann R, Eichmann TO, Kohlwein SD, Haemmerle G, Lass A, et al. FAT SIGNALS--lipases and lipolysis in lipid metabolism and signaling. Cell metabolism. 2012;15(3):279-91.
5. Haemmerle G, Zimmermann R, Strauss JG, Kratky D, Riederer M, Knipping G, et al. Hormone-sensitive lipase deficiency in mice changes the plasma lipid profile by affecting the tissue-specific expression pattern of lipoprotein lipase in adipose tissue and muscle. The Journal of biological chemistry. 2002;277(15):12946-52.
6. Haemmerle G, Zimmermann R, Hayn M, Theussl C, Waeg G, Wagner E, et al. Hormone-sensitive lipase deficiency in mice causes diglyceride accumulation in adipose tissue, muscle, and testis. The Journal of biological chemistry. 2002;277(7):4806-15.
7. Zimmermann R, Haemmerle G, Wagner EM, Strauss JG, Kratky D, Zechner R. Decreased fatty acid esterification compensates for the reduced lipolytic activity in hormone-sensitive lipase-deficient white adipose tissue. Journal of lipid research. 2003;44(11):2089-99.
8. Villena JA, Roy S, Sarkadi-Nagy E, Kim KH, Sul HS. Desnutrin, an adipocyte gene encoding a novel patatin domain-containing protein, is induced by fasting and glucocorticoids: ectopic expression of desnutrin increases triglyceride hydrolysis. The Journal of biological chemistry. 2004;279(45):47066-75.
9. Jenkins CM, Mancuso DJ, Yan W, Sims HF, Gibson B, Gross RW. Identification, cloning, expression, and purification of three novel human calcium-independent phospholipase A2 family members possessing triacylglycerol lipase and acylglycerol transacylase activities. The Journal of biological chemistry. 2004;279(47):48968-75.
10. Haemmerle G, Lass A, Zimmermann R, Gorkiewicz G, Meyer C, Rozman J, et al. Defective lipolysis and altered energy metabolism in mice lacking adipose triglyceride lipase. Science (New York, NY). 2006;312(5774):734-7.
11. Ward PS, Thompson CB. Metabolic reprogramming: a cancer hallmark even warburg did not anticipate. Cancer cell. 2012;21(3):297-308.
12. Vander Heiden MG, Cantley LC, Thompson CB. Understanding the Warburg effect: the metabolic requirements of cell proliferation. Science (New York, NY). 2009;324(5930):1029-33.

13. Vander Heiden MG. Targeting cancer metabolism: a therapeutic window opens. Nature reviews Drug discovery. 2011;10(9):671-84.
14. Hanahan D, Weinberg RA. Hallmarks of cancer: the next generation. Cell. 2011;144(5):646-74.
15. Lyssiotis CA, Cantley LC. SIRT6 puts cancer metabolism in the driver's seat. Cell. 2012;151(6):1155-6.
16. Warburg O. On the origin of cancer cells. Science (New York, NY). 1956;123(3191):309-14.
17. Cairns RA, Harris IS, Mak TW. Regulation of cancer cell metabolism. Nature reviews Cancer. 2011;11(2):85-95.
18. Cantor JR, Sabatini DM. Cancer cell metabolism: one hallmark, many faces. Cancer discovery. 2012;2(10):881-98.
19. DeBerardinis RJ, Lum JJ, Hatzivassiliou G, Thompson CB. The biology of cancer: metabolic reprogramming fuels cell growth and proliferation. Cell metabolism. 2008;7(1):11-20.
20. Kelloff GJ, Hoffman JM, Johnson B, Scher HI, Siegel BA, Cheng EY, et al. Progress and promise of FDG-PET imaging for cancer patient management and oncologic drug development. Clinical cancer research : an official journal of the American Association for Cancer Research. 2005;11(8):2785-808.
21. Simpson K. Cancer metabolism: Lipid addiction. Nature medicine. 2014;20(8):813-.
22. Currie E, Schulze A, Zechner R, Walther TC, Farese RV, Jr. Cellular fatty acid metabolism and cancer. Cell metabolism. 2013;18(2):153-61.
23. Anastasiou D, Cantley LC. Breathless cancer cells get fat on glutamine. Cell research. 2012;22(3):443-6.
24. Menendez JA, Lupu R. Fatty acid synthase and the lipogenic phenotype in cancer pathogenesis. Nature reviews Cancer. 2007;7(10):763-77.
25. Mashima T, Seimiya H, Tsuruo T. De novo fatty-acid synthesis and related pathways as molecular targets for cancer therapy. British journal of cancer. 2009;100(9):1369-72.
26. Selak MA, Armour SM, MacKenzie ED, Boulahbel H, Watson DG, Mansfield KD, et al. Succinate links TCA cycle dysfunction to oncogenesis by inhibiting HIF-alpha prolyl hydroxylase. Cancer cell. 2005;7(1):77-85.
27. Yan H, Parsons DW, Jin G, McLendon R, Rasheed BA, Yuan W, et al. IDH1 and IDH2 mutations in gliomas. The New England journal of medicine. 2009;360(8):765-73.
28. Figueroa ME, Abdel-Wahab O, Lu C, Ward PS, Patel J, Shih A, et al. Leukemic IDH1 and IDH2 mutations result in a hypermethylation phenotype, disrupt TET2 function, and impair hematopoietic differentiation. Cancer cell. 2010;18(6):553-67.
29. Sebastian C, Zwaans BM, Silberman DM, Gymrek M, Goren A, Zhong L, et al. The histone deacetylase SIRT6 is a tumor suppressor that controls cancer metabolism. Cell. 2012;151(6):1185-99.

30. Al-Zoughbi W, Pichler M, Gorkiewicz G, Guertl-Lackner B, Haybaeck J, Jahn SW, et al. Loss of adipose triglyceride lipase is associated with human cancer and induces mouse pulmonary neoplasia. Oncotarget. 2016.
31. Cohen DA, Dabbs DJ, Cooper KL, Amin M, Jones TE, Jones MW, et al. Interobserver agreement among pathologists for semiquantitative hormone receptor scoring in breast carcinoma. American journal of clinical pathology. 2012;138(6):796-802.
32. Miller TW, Balko JM, Ghazoui Z, Dunbier A, Anderson H, Dowsett M, et al. A gene expression signature from human breast cancer cells with acquired hormone independence identifies MYC as a mediator of antiestrogen resistance. Clinical cancer research : an official journal of the American Association for Cancer Research. 2011;17(7):2024-34.
33. Mermel CH, Schumacher SE, Hill B, Meyerson ML, Beroukhim R, Getz G. GISTIC2.0 facilitates sensitive and confident localization of the targets of focal somatic copy-number alteration in human cancers. Genome biology. 2011;12(4):R41.
34. Haemmerle G, Moustafa T, Woelkart G, Buttner S, Schmidt A, van de Weijer T, et al. ATGL-mediated fat catabolism regulates cardiac mitochondrial function via PPAR-alpha and PGC-1. Nature medicine. 2011;17(9):1076-85.
35. Sexl V, Piekorz R, Moriggl R, Rohrer J, Brown MP, Bunting KD, et al. Stat5a/b contribute to interleukin 7-induced B-cell precursor expansion, but abl- and bcr/abl-induced transformation are independent of stat5. Blood. 2000;96(6):2277-83.
36. Hecht SS. Tobacco smoke carcinogens and lung cancer. Journal of the National Cancer Institute. 1999;91(14):1194-210.
37. Meuwissen R, Berns A. Mouse models for human lung cancer. Genes & development. 2005;19(6):643-64.
38. Castonguay A, Rioux N. Inhibition of lung tumourigenesis by sulindac: comparison of two experimental protocols. Carcinogenesis. 1997;18(3):491-6.
39. Fischer J, Lefevre C, Morava E, Mussini JM, Laforet P, Negre-Salvayre A, et al. The gene encoding adipose triglyceride lipase (PNPLA2) is mutated in neutral lipid storage disease with myopathy. Nature genetics. 2007;39(1):28-30.
40. Pasanisi MB, Missaglia S, Cassandrini D, Salerno F, Farina S, Andreini D, et al. Severe cardiomyopathy in a young patient with complete deficiency of adipose triglyceride lipase due to a novel mutation in PNPLA2 gene. International journal of cardiology. 2016;207:165-7.
41. Muggenthaler M, Petropoulou E, Omer S, Simpson MA, Sahak H, Rice A, et al. Whole exome sequence analysis reveals a homozygous mutation in PNPLA2 as the cause of severe dilated cardiomyopathy secondary to neutral lipid storage disease. International journal of cardiology. 2016;210:41-4.
42. Kim MS, Pinto SM, Getnet D, Nirujogi RS, Manda SS, Chaerkady R, et al. A draft map of the human proteome. Nature. 2014;509(7502):575-81.

43. Jocken JW, Smit E, Goossens GH, Essers YP, van Baak MA, Mensink M, et al. Adipose triglyceride lipase (ATGL) expression in human skeletal muscle is type I (oxidative) fiber specific. Histochemistry and cell biology. 2008;129(4):535-8.
44. Meex RC, Hoy AJ, Mason RM, Martin SD, McGee SL, Bruce CR, et al. ATGL-mediated triglyceride turnover and the regulation of mitochondrial capacity in skeletal muscle. American journal of physiology Endocrinology and metabolism. 2015;308(11):E960-70.
45. Schweiger M, Lass A, Zimmermann R, Eichmann TO, Zechner R. Neutral lipid storage disease: genetic disorders caused by mutations in adipose triglyceride lipase/PNPLA2 or CGI-58/ABHD5. American journal of physiology Endocrinology and metabolism. 2009;297(2):E289-96.
46. Pennisi EM, Missaglia S, Dimauro S, Bernardi C, Akman HO, Tavian D. A myopathy with unusual features caused by PNPLA2 gene mutations. Muscle & nerve. 2015;51(4):609-13.
47. Ash DB, Papadimitriou D, Hays AP, Dimauro S, Hirano M. A novel mutation in PNPLA2 leading to neutral lipid storage disease with myopathy. Archives of neurology. 2012;69(9):1190-2.
48. Yamazaki K, Yakumaru K, Eyden BP. Lipid-rich residual bodies and cathepsin D in the human uterus: ultrastructural and quantitative comparison between normal myometrium and leiomyoma. Journal of submicroscopic cytology and pathology. 1993;25(3):437-47.
49. Styer AK, Rueda BR. The Epidemiology and Genetics of Uterine Leiomyoma. Best practice & research Clinical obstetrics & gynaecology. 2015.
50. Sparic R, Mirkovic L, Malvasi A, Tinelli A. Epidemiology of Uterine Myomas: A Review. International journal of fertility & sterility. 2016;9(4):424-35.
51. Peyot ML, Guay C, Latour MG, Lamontagne J, Lussier R, Pineda M, et al. Adipose triglyceride lipase is implicated in fuel- and non-fuel-stimulated insulin secretion. The Journal of biological chemistry. 2009;284(25):16848-59.
52. Melo JV. BCR-ABL gene variants. Bailliere's clinical haematology. 1997;10(2):203-22.
53. Tan Y, Chen X, Qi X, Li G, Wang J, Bian S, et al. Acute lymphoblastic leukemia expressing b3a2 (p210), e1a2 (p190), and variant e1a2 BCR-ABL transcripts: a case report and review of the literature. Acta haematologica. 2012;128(2):119-23.
54. Pane F, Intrieri M, Quintarelli C, Izzo B, Muccioli GC, Salvatore F. BCR/ABL genes and leukemic phenotype: from molecular mechanisms to clinical correlations. Oncogene. 2002;21(56):8652-67.
55. Chiarella P, Summa V, De Santis S, Signori E, Picardi E, Pesole G, et al. BCR/ABL1 fusion transcripts generated from alternative splicing: implications for future targeted therapies in Ph+ leukaemias. Current molecular medicine. 2012;12(5):547-65.
56. Zhang WC, Shyh-Chang N, Yang H, Rai A, Umashankar S, Ma S, et al. Glycine decarboxylase activity drives non-small cell lung cancer tumor-initiating cells and tumorigenesis. Cell. 2012;148(1-2):259-72.

57. Jain M, Nilsson R, Sharma S, Madhusudhan N, Kitami T, Souza AL, et al. Metabolite profiling identifies a key role for glycine in rapid cancer cell proliferation. Science (New York, NY). 2012;336(6084):1040-4.
58. Abitorabi MA, Pachynski RK, Ferrando RE, Tidswell M, Erle DJ. Presentation of integrins on leukocyte microvilli: a role for the extracellular domain in determining membrane localization. The Journal of cell biology. 1997;139(2):563-71.
59. Gajewski TF, Schreiber H, Fu Y-X. Innate and adaptive immune cells in the tumor microenvironment. Nat Immunol. 2013;14(10):1014-22.
60. Zaidi MR, Merlino G. The two faces of interferon-gamma in cancer. Clinical cancer research : an official journal of the American Association for Cancer Research. 2011;17(19):6118-24.
61. Brezar V, Tu WJ, Seddiki N. PKC-Theta in Regulatory and Effector T-cell Functions. Frontiers in immunology. 2015;6:530.
62. Takayanagi M, Kure S, Sakata Y, Kurihara Y, Ohya Y, Kajita M, et al. Human glycine decarboxylase gene (GLDC) and its highly conserved processed pseudogene (psiGLDC): their structure and expression, and the identification of a large deletion in a family with nonketotic hyperglycinemia. Human genetics. 2000;106(3):298-305.
63. Maddocks OD, Labuschagne CF, Adams PD, Vousden KH. Serine Metabolism Supports the Methionine Cycle and DNA/RNA Methylation through De Novo ATP Synthesis in Cancer Cells. Molecular cell. 2016;61(2):210-21.
64. Fidler IJ. Biological behavior of malignant melanoma cells correlated to their survival in vivo. Cancer research. 1975;35(1):218-24.
65. Elvin P, Evans CW. Cell adhesion and experimental metastasis: a study using the B16 malignant melanoma model system. European journal of cancer & clinical oncology. 1984;20(1):107-14.
66. DePinho RA. The age of cancer. Nature. 2000;408(6809):248-54.
67. Lemon WJ, Bernert H, Sun H, Wang Y, You M. Identification of candidate lung cancer susceptibility genes in mouse using oligonucleotide arrays. Journal of medical genetics. 2002;39(9):644-55.
68. Birsoy K, Sabatini DM, Possemato R. Untuning the tumor metabolic machine: Targeting cancer metabolism: a bedside lesson. Nature medicine. 2012;18(7):1022-3.
69. Nomura DK, Long JZ, Niessen S, Hoover HS, Ng SW, Cravatt BF. Monoacylglycerol lipase regulates a fatty acid network that promotes cancer pathogenesis. Cell. 2010;140(1):49-61.
70. Sun H, Jiang L, Luo X, Jin W, He Q, An J, et al. Potential tumor-suppressive role of monoglyceride lipase in human colorectal cancer. Oncogene. 2013;32(2):234-41.
71. Hu WR, Lian YF, Peng LX, Lei JJ, Deng CC, Xu M, et al. Monoacylglycerol lipase promotes metastases in nasopharyngeal carcinoma. International journal of clinical and experimental pathology. 2014;7(7):3704-13.

72. Nomura DK, Lombardi DP, Chang JW, Niessen S, Ward AM, Long JZ, et al. Monoacylglycerol lipase exerts dual control over endocannabinoid and fatty acid pathways to support prostate cancer. Chemistry & biology. 2011;18(7):846-56.
73. Kaneko K, Kuroda H, Izumi R, Tateyama M, Kato M, Sugimura K, et al. A novel mutation in PNPLA2 causes neutral lipid storage disease with myopathy and triglyceride deposit cardiomyovasculopathy: a case report and literature review. Neuromuscular disorders : NMD. 2014;24(7):634-41.
74. Baserga R. The Cell Cycle. New England Journal of Medicine. 1981;304(8):453-9.
75. Ahuja P, Sdek P, MacLellan WR. Cardiac myocyte cell cycle control in development, disease, and regeneration. Physiological reviews. 2007;87(2):521-44.
76. Yang X, Lu X, Lombes M, Rha GB, Chi YI, Guerin TM, et al. The G(0)/G(1) switch gene 2 regulates adipose lipolysis through association with adipose triglyceride lipase. Cell metabolism. 2010;11(3):194-205.
77. Lu X, Yang X, Liu J. Differential control of ATGL-mediated lipid droplet degradation by CGI-58 and G0S2. Cell cycle (Georgetown, Tex). 2010;9(14):2719-25.
78. Kurat CF, Wolinski H, Petschnigg J, Kaluarachchi S, Andrews B, Natter K, et al. Cdk1/Cdc28-dependent activation of the major triacylglycerol lipase Tgl4 in yeast links lipolysis to cell-cycle progression. Molecular cell. 2009;33(1):53-63.
79. Chakrabarti P, Kandror KV. FoxO1 controls insulin-dependent adipose triglyceride lipase (ATGL) expression and lipolysis in adipocytes. The Journal of biological chemistry. 2009;284(20):13296-300.
80. Ahmadian M, Abbott MJ, Tang T, Hudak CS, Kim Y, Bruss M, et al. Desnutrin/ATGL is regulated by AMPK and is required for a brown adipose phenotype. Cell metabolism. 2011;13(6):739-48.
81. Chakrabarti P, English T, Karki S, Qiang L, Tao R, Kim J, et al. SIRT1 controls lipolysis in adipocytes via FOXO1-mediated expression of ATGL. Journal of lipid research. 2011;52(9):1693-701.
82. Chakrabarti P, English T, Shi J, Smas CM, Kandror KV. Mammalian target of rapamycin complex 1 suppresses lipolysis, stimulates lipogenesis, and promotes fat storage. Diabetes. 2010;59(4):775-81.
83. Luo Z, Zang M, Guo W. AMPK as a metabolic tumor suppressor: control of metabolism and cell growth. Future oncology (London, England). 2010;6(3):457-70.
84. Greer EL, Brunet A. FOXO transcription factors at the interface between longevity and tumor suppression. Oncogene. 2005;24(50):7410-25.
85. Wrangle J, Wang W, Koch A, Easwaran H, Mohammad HP, Vendetti F, et al. Alterations of immune response of Non-Small Cell Lung Cancer with Azacytidine. Oncotarget. 2013;4(11):2067-79.
86. Koufos A, Hansen MF, Copeland NG, Jenkins NA, Lampkin BC, Cavenee WK. Loss of heterozygosity in three embryonal tumours suggests a common pathogenetic mechanism. Nature. 1985;316(6026):330-4.

87. Karnik P, Paris M, Williams BR, Casey G, Crowe J, Chen P. Two distinct tumor suppressor loci within chromosome 11p15 implicated in breast cancer progression and metastasis. Human molecular genetics. 1998;7(5):895-903.
88. Fearon ER, Feinberg AP, Hamilton SH, Vogelstein B. Loss of genes on the short arm of chromosome 11 in bladder cancer. Nature. 1985;318(6044):377-80.
89. Coppes MJ, Bonetta L, Huang A, Hoban P, Chilton-MacNeill S, Campbell CE, et al. Loss of heterozygosity mapping in Wilms tumor indicates the involvement of three distinct regions and a limited role for nondisjunction or mitotic recombination. Genes, chromosomes & cancer. 1992;5(4):326-34.
90. Besnard-Guerin C, Newsham I, Winqvist R, Cavenee WK. A common region of loss of heterozygosity in Wilms' tumor and embryonal rhabdomyosarcoma distal to the D11S988 locus on chromosome 11p15.5. Human genetics. 1996;97(2):163-70.
91. Bepler G, Garcia-Blanco MA. Three tumor-suppressor regions on chromosome 11p identified by high-resolution deletion mapping in human non-small-cell lung cancer. Proceedings of the National Academy of Sciences of the United States of America. 1994;91(12):5513-7.
92. Andersen TI, Gaustad A, Ottestad L, Farrants GW, Nesland JM, Tveit KM, et al. Genetic alterations of the tumour suppressor gene regions 3p, 11p, 13q, 17p, and 17q in human breast carcinomas. Genes, chromosomes & cancer. 1992;4(2):113-21.

10 Bibliography

Wael Al-Zoughbi, M.D., Pathologist

Ph.D. Candidate, Medical University of Graz

Address

Institute of Pathology
Medical University of Graz
Auenbruggerplatz 25
8036 Graz, Austria
Email: Wael.Alzoughbi@stud.medunigraz.at
Tel: +43 650 9503209

Licenses, Certification

2002	**Medical Doctor, Syrian Ministry of Health**
2008	**Specialist Recognition in Pathology, Syrian Ministry of Health**

Professional registration

2002	**Syrian Medical Association**
2009	**European Society for Medical Oncology**
2010	**European Society of Pathology**
2014	**American Association for Clinical Chemistry**
2016	**Österreichische Gesellschaft für Pathologie**
2016	**Österreichische Gesellschaft für Molekulare Biowissenschaften und Biotechnologie**

Education and Training

2002	**Bachelor of Medicine,** Faculty of Medicine, Damascus University
2007	**Anatomic Pathology,** Faculty of Medicine-affiliated hospitals, Damascus University
2010-	**Ph.D.-Doctoral Program,** Medical University of Graz

Professional Experience

2010-	**Ph.D. Candidate, Ph.D.-Doctoral Programme**	Institute of Pathology, Medical University of Graz
2009-	**Research student, Doctoral Program in Medical Sciences**	Institute of Pathology, Medical University of Graz
2009- 2009	**Visiting Scientist**	Institute of Pathology, Medical University of Graz
2008- 2009	**Lecturer**	Faculty of Medicine, Pathology Department, Damascus University

2007- 2008	**Advanced Trainee in Tumour Pathology**	Al-Baironi University Hospital, Damascus University
2002- 2007	**Pathology Resident**	Faculty of Medicine-affiliated hospitals, Damascus University
1994- 2002	**Medical Student**	Faculty of Medicine, Damascus University

Selected Presentations

2010	**94th Annual Meeting of the German Association of Pathology, Berlin**
2011	**Keystone Symposia, Cancer Control by Tumor Suppressers and Immune Effectors, Santa Fe**
2013	**Tumor Metabolism meets Immunology Symposium, Regensburg**

Awards

2011	**Keystone Symposia Future of Science Fund Scholarship**
	Cancer Control by Tumor Suppressors and Immune Effectors / Santa Fe, USA
2013	**Tumor Metabolism meets Immunology Symposium Scholarship**
	Tumor Metabolism meets Immunology Symposium / Regensburg, Germany
2013	**ESMO Travel Grant**
	ESMO Symposium on Immuno-Oncology / Geneva, Switzerland

11 Appendix

11.1 Publications

1. **Al-Zoughbi W**, Pichler M, Gorkiewicz G, Guertl-Lackner B, Haybaeck J, Jahn SW, Lackner C, Liegl-Atzwanger B, Popper H, Schauer S, Nusshold E, Kindt AS, Trajanoski Z, et al. Loss of adipose triglyceride lipase is associated with human cancer and induces mouse pulmonary neoplasia. Oncotarget. 2016.

2. **Al-Zoughbi W**, Huang J, Paramasivan GS, Till H, Pichler M, Guertl-Lackner B and Hoefler G. Tumor macroenvironment and metabolism. Seminars in oncology. 2014; 41:281-295.

3. Schrammel A, Mussbacher M, Wolkart G, Stessel H, Pail K, Winkler S, Schweiger M, Haemmerle G, **Al Zoughbi W**, Hofler G, Lametschwandtner A, Zechner R and Mayer B. Endothelial dysfunction in adipose triglyceride lipase deficiency. Biochimica et biophysica acta. 2014; 1841:906-917.

4. Szkandera J, Stotz M, Absenger G, Stojakovic T, Samonigg H, Kornprat P, Schaberl-Moser R, **Alzoughbi W**, Lackner C, Ress AL, Seggewies FS, Gerger A, Hoefler G, et al. Validation of C-reactive protein levels as a prognostic indicator for survival in a large cohort of pancreatic cancer patients. British journal of cancer. 2014; 110:183-188.

5. Huang J, Das SK, Jha P, **Al Zoughbi W**, Schauer S, Claudel T, Sexl V, Vesely P, Birner-Gruenberger R, Kratky D, Trauner M and Hoefler G. The PPARalpha agonist fenofibrate suppresses B-cell lymphoma in mice by modulating lipid metabolism. Biochimica et biophysica acta. 2013; 1831:1555-1565.

6. Szkandera J, Stotz M, Eisner F, Absenger G, Stojakovic T, Samonigg H, Kornprat P, Schaberl-Moser R, **Alzoughbi W**, Ress AL, Seggewies FS, Gerger A, Hoefler G, et al. External validation of the derived neutrophil to lymphocyte ratio as a prognostic marker on a large cohort of pancreatic cancer patients. PloS one. 2013; 8:e78225.

7. Stotz M, Gerger A, Eisner F, Szkandera J, Loibner H, Ress AL, Kornprat P, **AlZoughbi W**, Seggewies FS, Lackner C, Stojakovic T, Samonigg H, Hoefler G, et al. Increased neutrophil-lymphocyte ratio is a poor prognostic factor in patients with primary operable and inoperable pancreatic cancer. British journal of cancer. 2013; 109:416-421.

8. Tamilarasan KP, Temmel H, Das SK, **Al Zoughbi W**, Schauer S, Vesely PW and Hoefler G. Skeletal muscle damage and impaired regeneration due to LPL-mediated lipotoxicity. Cell death & disease. 2012; 3:e354.

9. Senanayake U, Das S, Vesely P, **Alzoughbi W**, Frohlich LF, Chowdhury P, Leuschner I, Hoefler G and Guertl B. miR-192, miR-194, miR-215, miR-200c and miR-141 are downregulated and their common target ACVR2B is strongly expressed in renal childhood neoplasms. Carcinogenesis. 2012; 33:1014-1021.

11.2 Permission to Reuse

11.2.1 Oncotarget Journal

Oncotarget applies the Creative Commons Attribution License (CCAL) to all works we publish (read the human-readable summary or the full license legal code). Under the CCAL, authors retain ownership of the copyright for their article, but authors allow anyone to download, reuse, reprint, modify, distribute, and/or copy articles in *Oncotarget* journal, so long as the original authors and source are cited.

11.2.2 Elsevier Publisher

ELSEVIER LICENSE
TERMS AND CONDITIONS

May 11, 2016

This is a License Agreement between Wael Al ("You") and Elsevier ("Elsevier") provided by Copyright Clearance Center ("CCC"). The license consists of your order details, the terms and conditions provided by Elsevier, and the payment terms and conditions.

All payments must be made in full to CCC. For payment instructions, please see information listed at the bottom of this form.

Supplier	Elsevier Limited The Boulevard,Langford Lane Kidlington,Oxford,OX5 1GB,UK
Registered Company Number	1982084
Customer name	Wael Al-Zoughbi
Customer address	Auenbruggerplatz 25 Graz, 8036
License number	3865831460055
License date	May 11, 2016
Licensed content publisher	Elsevier
Licensed content publication	Seminars in Oncology
Licensed content title	Corrigendum to "Tumor Macroenvironment and Metabolism" [Seminars in Oncology, Vol 41, No 2, April 2014, pp 281–295]
Licensed content author	Wael Al-Zoughbi,Jianfeng Huang,Ganapathy S. Paramasivan,Holger Till,Martin Pichler,Barbara Guertl-Lackner,Gerald Hoefler
Licensed content date	August 2014
Licensed content volume number	41
Licensed content issue number	4
Number of pages	1
Start Page	e31
End Page	0
Type of Use	reuse in a thesis/dissertation
Portion	figures/tables/illustrations
Number of figures/tables/illustrations	1
Format	electronic
Are you the author of this Elsevier article?	Yes
Will you be translating?	No

Original figure numbers	Figure 1
Title of your thesis/dissertation	ATGL downregulation enhances tumor growth suggesting a function as metabolic tumor suppressor protein
Expected completion date	Jun 2016
Estimated size (number of pages)	80
Elsevier VAT number	GB 494 6272 12
Permissions price	0.00 EUR
VAT/Local Sales Tax	0.00 EUR / 0.00 GBP
Total	0.00 EUR
Terms and Conditions	

INTRODUCTION

1. The publisher for this copyrighted material is Elsevier. By clicking "accept" in connection with completing this licensing transaction, you agree that the following terms and conditions apply to this transaction (along with the Billing and Payment terms and conditions established by Copyright Clearance Center, Inc. ("CCC"), at the time that you opened your Rightslink account and that are available at any time at http://myaccount.copyright.com).

GENERAL TERMS

2. Elsevier hereby grants you permission to reproduce the aforementioned material subject to the terms and conditions indicated.

3. Acknowledgement: If any part of the material to be used (for example, figures) has appeared in our publication with credit or acknowledgement to another source, permission must also be sought from that source. If such permission is not obtained then that material may not be included in your publication/copies. Suitable acknowledgement to the source must be made, either as a footnote or in a reference list at the end of your publication, as follows:

"Reprinted from Publication title, Vol /edition number, Author(s), Title of article / title of chapter, Pages No., Copyright (Year), with permission from Elsevier [OR APPLICABLE SOCIETY COPYRIGHT OWNER]." Also Lancet special credit - "Reprinted from The Lancet, Vol. number, Author(s), Title of article, Pages No., Copyright (Year), with permission from Elsevier."

4. Reproduction of this material is confined to the purpose and/or media for which permission is hereby given.

5. Altering/Modifying Material: Not Permitted. However figures and illustrations may be altered/adapted minimally to serve your work. Any other abbreviations, additions, deletions and/or any other alterations shall be made only with prior written authorization of Elsevier Ltd. (Please contact Elsevier at permissions@elsevier.com)

6. If the permission fee for the requested use of our material is waived in this instance, please be advised that your future requests for Elsevier materials may attract a fee.

7. Reservation of Rights: Publisher reserves all rights not specifically granted in the combination of (i) the license details provided by you and accepted in the course of this licensing transaction, (ii) these terms and conditions and (iii) CCC's Billing and Payment terms and conditions.

8. License Contingent Upon Payment: While you may exercise the rights licensed immediately upon issuance of the license at the end of the licensing process for the transaction, provided that you have disclosed complete and accurate details of your proposed use, no license is finally effective unless and until full payment is received from

you (either by publisher or by CCC) as provided in CCC's Billing and Payment terms and conditions. If full payment is not received on a timely basis, then any license preliminarily granted shall be deemed automatically revoked and shall be void as if never granted. Further, in the event that you breach any of these terms and conditions or any of CCC's Billing and Payment terms and conditions, the license is automatically revoked and shall be void as if never granted. Use of materials as described in a revoked license, as well as any use of the materials beyond the scope of an unrevoked license, may constitute copyright infringement and publisher reserves the right to take any and all action to protect its copyright in the materials.
9. Warranties: Publisher makes no representations or warranties with respect to the licensed material.
10. Indemnity: You hereby indemnify and agree to hold harmless publisher and CCC, and their respective officers, directors, employees and agents, from and against any and all claims arising out of your use of the licensed material other than as specifically authorized pursuant to this license.
11. No Transfer of License: This license is personal to you and may not be sublicensed, assigned, or transferred by you to any other person without publisher's written permission.
12. No Amendment Except in Writing: This license may not be amended except in a writing signed by both parties (or, in the case of publisher, by CCC on publisher's behalf).
13. Objection to Contrary Terms: Publisher hereby objects to any terms contained in any purchase order, acknowledgment, check endorsement or other writing prepared by you, which terms are inconsistent with these terms and conditions or CCC's Billing and Payment terms and conditions. These terms and conditions, together with CCC's Billing and Payment terms and conditions (which are incorporated herein), comprise the entire agreement between you and publisher (and CCC) concerning this licensing transaction. In the event of any conflict between your obligations established by these terms and conditions and those established by CCC's Billing and Payment terms and conditions, these terms and conditions shall control.
14. Revocation: Elsevier or Copyright Clearance Center may deny the permissions described in this License at their sole discretion, for any reason or no reason, with a full refund payable to you. Notice of such denial will be made using the contact information provided by you. Failure to receive such notice will not alter or invalidate the denial. In no event will Elsevier or Copyright Clearance Center be responsible or liable for any costs, expenses or damage incurred by you as a result of a denial of your permission request, other than a refund of the amount(s) paid by you to Elsevier and/or Copyright Clearance Center for denied permissions.

LIMITED LICENSE

The following terms and conditions apply only to specific license types:
15. **Translation**: This permission is granted for non-exclusive world **English** rights only unless your license was granted for translation rights. If you licensed translation rights you may only translate this content into the languages you requested. A professional translator must perform all translations and reproduce the content word for word preserving the integrity of the article.
16. **Posting licensed content on any Website**: The following terms and conditions apply as follows: Licensing material from an Elsevier journal: All content posted to the web site must maintain the copyright information line on the bottom of each image; A hyper-text must be included to the Homepage of the journal from which you are licensing athttp://www.sciencedirect.com/science/journal/xxxxx or the Elsevier homepage for books athttp://www.elsevier.com; Central Storage: This license does not include permission for a scanned version of the material to be stored in a central repository such

as that provided by Heron/XanEdu.
Licensing material from an Elsevier book: A hyper-text link must be included to the Elsevier homepage at http://www.elsevier.com . All content posted to the web site must maintain the copyright information line on the bottom of each image.

Posting licensed content on Electronic reserve: In addition to the above the following clauses are applicable: The web site must be password-protected and made available only to bona fide students registered on a relevant course. This permission is granted for 1 year only. You may obtain a new license for future website posting.
17. **For journal authors:** the following clauses are applicable in addition to the above:
Preprints:
A preprint is an author's own write-up of research results and analysis, it has not been peer-reviewed, nor has it had any other value added to it by a publisher (such as formatting, copyright, technical enhancement etc.).
Authors can share their preprints anywhere at any time. Preprints should not be added to or enhanced in any way in order to appear more like, or to substitute for, the final versions of articles however authors can update their preprints on arXiv or RePEc with their Accepted Author Manuscript (see below).
If accepted for publication, we encourage authors to link from the preprint to their formal publication via its DOI. Millions of researchers have access to the formal publications on ScienceDirect, and so links will help users to find, access, cite and use the best available version. Please note that Cell Press, The Lancet and some society-owned have different preprint policies. Information on these policies is available on the journal homepage.
Accepted Author Manuscripts: An accepted author manuscript is the manuscript of an article that has been accepted for publication and which typically includes author-incorporated changes suggested during submission, peer review and editor-author communications.
Authors can share their accepted author manuscript:

- – immediately
    - via their non-commercial person homepage or blog
    - by updating a preprint in arXiv or RePEc with the accepted manuscript
    - via their research institute or institutional repository for internal institutional uses or as part of an invitation-only research collaboration work-group
    - directly by providing copies to their students or to research collaborators for their personal use
    - for private scholarly sharing as part of an invitation-only work group on commercial sites with which Elsevier has an agreement
- – after the embargo period
    - via non-commercial hosting platforms such as their institutional repository
    - via commercial sites with which Elsevier has an agreement

In all cases accepted manuscripts should:

- – link to the formal publication via its DOI
- – bear a CC-BY-NC-ND license - this is easy to do
- – if aggregated with other manuscripts, for example in a repository or other site, be shared in alignment with our hosting policy not be added to or enhanced in any way to appear more like, or to substitute for, the published journal article.

Published journal article (JPA): A published journal article (PJA) is the definitive final record of published research that appears or will appear in the journal and embodies all value-adding publishing activities including peer review co-ordination, copy-editing, formatting, (if relevant) pagination and online enrichment.
Policies for sharing publishing journal articles differ for subscription and gold open access articles:
Subscription Articles: If you are an author, please share a link to your article rather than the full-text. Millions of researchers have access to the formal publications on ScienceDirect, and so links will help your users to find, access, cite, and use the best available version.
Theses and dissertations which contain embedded PJAs as part of the formal submission can be posted publicly by the awarding institution with DOI links back to the formal publications on ScienceDirect.
If you are affiliated with a library that subscribes to ScienceDirect you have additional private sharing rights for others' research accessed under that agreement. This includes use for classroom teaching and internal training at the institution (including use in course packs and courseware programs), and inclusion of the article for grant funding purposes.
Gold Open Access Articles: May be shared according to the author-selected end-user license and should contain a CrossMark logo, the end user license, and a DOI link to the formal publication on ScienceDirect.
Please refer to Elsevier's posting policy for further information.
18. **For book authors** the following clauses are applicable in addition to the above: Authors are permitted to place a brief summary of their work online only. You are not allowed to download and post the published electronic version of your chapter, nor may you scan the printed edition to create an electronic version. **Posting to a repository:** Authors are permitted to post a summary of their chapter only in their institution's repository.
19. **Thesis/Dissertation**: If your license is for use in a thesis/dissertation your thesis may be submitted to your institution in either print or electronic form. Should your thesis be published commercially, please reapply for permission. These requirements include permission for the Library and Archives of Canada to supply single copies, on demand, of the complete thesis and include permission for Proquest/UMI to supply single copies, on demand, of the complete thesis. Should your thesis be published commercially, please reapply for permission. Theses and dissertations which contain embedded PJAs as part of the formal submission can be posted publicly by the awarding institution with DOI links back to the formal publications on ScienceDirect.

Elsevier Open Access Terms and Conditions
You can publish open access with Elsevier in hundreds of open access journals or in nearly 2000 established subscription journals that support open access publishing. Permitted third party re-use of these open access articles is defined by the author's choice of Creative Commons user license. See our open access license policy for more information.
Terms & Conditions applicable to all Open Access articles published with Elsevier:
Any reuse of the article must not represent the author as endorsing the adaptation of the article nor should the article be modified in such a way as to damage the author's honour or reputation. If any changes have been made, such changes must be clearly indicated.
The author(s) must be appropriately credited and we ask that you include the end user license and a DOI link to the formal publication on ScienceDirect.
If any part of the material to be used (for example, figures) has appeared in our